

**A GEOGRAPHIC BASED INFORMATION MANAGEMENT
SYSTEM FOR PERMAFROST PREDICTION IN THE
BEAUFORT AND CHUKCHI SEAS**

**PART I.
SUBMARINE PERMAFROST ON THE ALASKAN SHELF**

by

Michael Vigdorchik

Institute of Arctic and Alpine Research
University of Colorado
Boulder, Colorado 80309

Final Report
Outer Continental Shelf Environmental Assessment Program
Research Unit 516

September 1978

ACKNOWLEDGMENTS

This is the first work done by this Russian-born author, on American soil, in the American scientific environment; and for a part of America that, in a geological sense, could be considered to be a part of the Asian plate and physiographically indistinguishable from Siberia.

For their help from beginning to end we would like to thank Professors Jack D. Ives, R. Berry, our colleagues in INSTAAR and the World Data Center in Glaciology, and Mr. J. Fletcher (NOAA). For having provided the data we would like to thank Dr. M. Loughridge, H. Hittelman, K. Potter (NGSDC, NOAA) and World Data Center-A, Oceanography.

For encouragement, helpful advice and stimulating discussion, we would like to thank Dr. D. Hopkins and Professor T. Péwé, and also Professors A. J. Washburn, U. Radok, A. K. Lachenbruch, and Dr. J. Brown.

Extremely helpful were the data and the periodic exchange of opinions with Doctors N. Biswas, W. Harrison, T. Osterkamp, A. S. Naidu, K. Aagaard, H. O. Lahn, P. W. Barnes, E. Reimnitz, J. C. Rogers, P. W. Sellman, and W. Sackinger, and we would like to thank them all. We want to express our thanks to Professor G. Weller, T. Johnson, and Dr. W. Stringer for constant help in this work as part of the OSCEA Program. We thank also N. Hardin, Doctors D. Wolfe, W. Fisher, J. Murphy, and B. Farentinos for consultations and administrative help, and Dr. K. MacDonald (SAI) for the good base map used in our "Atlas." We would also like to thank the NCAR computing center where the computerized maps were plotted.

The author may only hope that the experience from the Eurasian Arctic, that was used in this work, will be as useful for the study of the American Arctic as the friendship, support, and new knowledge he has received here.

TABLE OF CONTENTS

	<i>Page</i>
ACKNOWLEDGMENTS	91
LIST OF FIGURES	95
LIST OF TABLES	97
LIST OF MAPS	99
INTRODUCTION	101
TASK OBJECTIVES	101
SUMMARY OF RESULTS	102
GENERAL STRATEGY AND APPROACH	102
DISCUSSION OF PALEOENVIRONMENTAL ASPECTS OF ALASKAN SUBMARINE PERMAFROST DEVELOPMENT	105
Indicators of Vertical Movement at Different Parts of the Beaufort Sea coast	106
Morphostructural Peculiarities of the Coastal Areas Related to Vertical Movements	110
Exposure of the Shelf During the Last Glaciation	118
Lack of Data on Thermokarst and Polygonal Forms at the Shelf	125
Role of the Meridional Lineaments of the North Alaskan Plains and Shelf	128
Possible Thickness of the Relic Submarine Permafrost	133
ENVIRONMENTAL DATA ON ALASKAN SUBMARINE PERMAFROST DISTRIBUTION	134
Data and Their Reliability; Defining the Gaps	135
Interpolation Scheme	147
Data Structuring	153
COMPUTERIZED MAPPING	153
Source Data Maps	155
Compilation of Derived Maps	168
Composite Mapping Algorithm	177
Candidate Areas for Submarine Permafrost Related to BLM Lease Nomination	178
APPLICATION OF THE SYSTEM TO BEAUFORT SEA AREAS WITH KNOWN SUBMARINE PERMAFROST-COMPARISON TO THE CANADIAN RESULTS	183
CONCLUSION	193
BIBLIOGRAPHY	197

LIST OF FIGURES

	<i>Page</i>
Figure 1. Spatial variation in the rate of present-day vertical movements in Arctic seas.	109
Figure 2. Average rate of coastal retreat	111
Figure 3. Possible rate of the Beaufort Sea recent coastal uplift proportionally to the average coastal retreat . . . ,	111
Figure 4. Relative rate of the recent uplift of the three major morphostructures of the Beaufort coast	112
Figure 5. Epicenters of earthquakes in northern Alaska	114
Figure 6. Earthquakes in and near Alaska	115
Figure 7. Generalized surficial deposits map of Arctic coastal plain.	116
Figure 8. Linear elements in the Alaskan geomorphological structure	117
Figure 9. Areas of the Beaufort Sea coastal plain and shelf with different rates of vertical movement	119
Figure 10. Reconstruction of sea level history on the continental shelves of western and northern Alaska with our additions on recent tectonics	120
Figure 11. Possible exposure of the shelf during the last glaciation	124
Figure 12. Polygonal profile with the ice wedge in the process of thawing at the Arctic shelf, Laptev Sea	126
Figure 13. Profiles of the thermokarst forms on the shelf after thawing	126
Figure 14. Submarine thermokarst profiles on the shelf	127
Figure 15. Location of some of the most prominent lineaments in the Alaskan Arctic	129
Figure 16. Scheme of the tangential stress orientation along the major lineament system of the earth	130
Figure 17. Rose diagram of lineaments from various areas	130
Figure 18. Direction of drainage patterns and major lineaments in the Bering Strait area.	130
Figure 19. Major meridional lineaments of the Beaufort Sea coastal plain and their possible continuation on the shelf	131

LIST OF FIGURES (Continued)

	<i>Page</i>
Figure 20. Physiographic provinces and location of submarine terrains susceptible to sliding..	132
Figure 21. Illustration for the reliability of data evaluation	136
Figure 22. Structure diagram of the data management system for submarine permafrost prediction in the Beaufort and Chukchi seas	154
Figure 23. Graph of unfrozen water content in frozen soils	156
Figure 24. Temperature deviation from the freezing point at 5-25 m	175
Figure 25. Bathymetry of the southern Beaufort Sea	184
Figure 26. Summer and winter bottom water temperature in the southern Chukchi Sea....	185
Figure 27. Summer and winter bottom water salinities in the southern Beaufort Sea....	186
Figure 28. An interpretation of the occurrence of subsea bottom ice-bonded permafrost	187
Figure 29. Summer temperature of seawater at the maximal sampling depth in the southern Beaufort Sea	188
Figure 30. Summer salinity of seawater at the maximal sampling depth in the southern Beaufort Sea	189
Figure 31. Freezing temperatures of seawater according to summer salinity in the southern Beaufort Sea	190
Figure 32. Seawater supercooling during the summer at the maximal sampling depth in the southern Beaufort Sea	191
Figure 33. Probability of seasonal supercooling at the maximal sampling depth in the southern Chukchi Sea	192

LIST OF TABLES

	<i>Page</i>
Table 1. Relative rate of present-day vertical coastal movements in Arctic seas in 1951-65..	108
Table 2. Variations of absolute elevations of the southeastern Alaskan seaboard	108
Table 3. Possible position of the Beaufort Sea shoreline in the past	118
Table 4. Distribution of observations by month, Beaufort Sea	146
Table 5. Distribution of observations by month, Chukchi Sea	146
Table 6. Unfrozen contents of salt-free soils vs. degrees of negative temperature	157
Table 7. Probability of submarine permafrost in the lease areas	181
Table 8. Division of the Beaufort Sea shelf according to the specifics of submarine permafrost origin and distribution	194

LIST OF MAPS

	<i>Page</i>
Map 1.	Points of observation for bottom deposit grain size, Chukchi Sea 138
Map 2.	Points of observation for bottom deposit grain size, Beaufort Sea 139
Map 3.	Reliability of the grain size data, Chukchi Sea140
Map 4.	Reliability of the grain size data, Beaufort Sea 141
Map 5.	Data distribution for temperature and salinity of seawater at the maximal sampling depth, Chukchi Sea142
Map 6.	Data distribution for temperature and salinity of seawater at the maximal sampling depth, Beaufort Sea 143
Map 7.	Data reliability for temperature and salinity of seawater at the maximal sampling depth, Chukchi Sea144
Map 8.	Data reliability for temperature and salinity of seawater at the maximal sampling depth, Beaufort Sea 145
Map 9.	Proximity of the maximal sampling depth to the bottom, Chukchi Sea148
Map 10.	Proximity of the maximal sampling depth to the bottom, Beaufort Sea149
Map 11.	General reliability of the data, Chukchi Sea150
Map 12.	General reliability of the data, Beaufort Sea151
Map 13.	Sand and silt distribution, Chukchi Sea158
Map 14.	Sand and silt distribution, Beaufort Sea159
Map 15.	Silt distribution, Chukchi Sea.160
Map 16.	Silt distribution, Beaufort Sea.161
Map 17.	Clay distribution, Chukchi Sea.. . . .162
Map 18.	Clay distribution, Beaufort Sea.163
Map 19.	Temperature of seawater in summer at the maximal sampling depth, Chukchi Sea164
Map 20.	Temperature of seawater in summer at the maximal sampling depth, Beaufort Sea.165

LIST OF MAPS (Continued)

	<i>Page</i>
Map 21. Salinity of seawater in summer at the maximal sampling depth, Chukchi Sea	166
Map 22. Salinity of seawater in summer at the maximal sampling depth, Beaufort Sea.	167
Map 23. Freezing temperatures of seawater at summer salinities, Chukchi Sea . . .	169
Map 24. Freezing temperatures of seawater at summer salinities, Beaufort Sea . . .	170
Map 25. Supercooling of seawater in summer, Chukchi Sea.	171
Map 26. Supercooling of seawater in summer, Beaufort Sea	172
Map 27. Probability of seasonal supercooling of seawater, Chukchi Sea	173
Map 28. Probability of seasonal supercooling of seawater, Beaufort Sea	174
Map 29. Suitability for ice-bonded permafrost at the upper layers of the seabed, Chukchi Sea	179
Map 30. Suitability for ice-bonded permafrost at the upper layers of theseabed, Beaufort Sea	180
Map 31. Division of the Beaufort Sea shelf according to the specifics of submarine permafrost origin and distribution	182

NOTE: It is difficult to use the reduced copies of the computerized environmental maps which are included in the text of Part I for BLM needs. Therefore, an atlas of these maps has been prepared and submitted separately from this document. The Atlas includes the 31 maps, which were made on a base map especially prepared by Science Applications, Inc., in a scale directly appropriate for practical use by BLM.

INTRODUCTION

According to the Program Development Plan (NOAA, BLM, 1976), this work is a part of the investigations related to the identification and estimation of the potential hazards posed by the environment to petroleum exploration and development (p. 3-3). This study involves quantitative assessments of information that can be used to assess future alterations resulting from various phases of lease site development. This study uses a computerized approach and analytical design which allows conclusions to be stated in terms of probability. The main products are computerized source, derived, and composite maps of several physical fields—oceanographic, geologic, topographic. The maps delineate environmentally sensitive areas; i.e., those conducive to formation of submarine permafrost. These areas are potentially dangerous for exploration and development of oil and gas in the Beaufort and Chukchi seas as a whole, and specifically in the limits of the lease areas. The maps are in scales directly applicable to BLM needs for prediction, assessment, and regulation.

TASK OBJECTIVES

This final report includes two parts which correspond to the two principal objectives of the work.

The *first objective* was to develop a computerized system to aid in the prediction of the distribution and characteristics of offshore permafrost. Development of this system involves (1) the gathering and study of all source data about direct and indirect indicators of permafrost in the given area (depth, temperature and salinity of water, topography, bottom deposits, ice, etc.); and (2) the generation of source and derived maps and construction of a candidate area map for submarine permafrost in the Beaufort and Chukchi seas. The decisive factor in this work was the close relationship with the NOAA Environmental Data and Information Service, especially the National Geophysical and Solar-Terrestrial Data Center (NGSDC) in Boulder, that also operates World Data Center-A for Solid Earth Geophysics and for Solar-Terrestrial Physics. We also used data from World Data Center-A, Oceanography, in Washington, D.C., and Glaciology in Boulder (INSTAAR). A description of the system and results is given in Part I of this report.

The second *objective* was to undertake a comprehensive review and analysis of past and current Soviet literature on subsea permafrost and related natural processes. The data and concept analysis on subsea permafrost of the Eurasian part of the Arctic in its relationship with the Arctic development in the Pleistocene, is given in Part II of this report as a monograph with bibliography related to the problem.

The work was done by M. Vigdorichik (Principal Investigator), B. Skholer (Computer Programmer), and J. Adams (Senior Graphic Artist) during the period of October 1976-September 1978.

SUMMARY OF RESULTS

1. An evaluation of existing environmental data on submarine permafrost of the Alaskan Shelf has been made. The reliability of the data and the gaps have been defined.
2. The paleoenvironmental aspects of the submarine permafrost of the Beaufort and Chukchi seas have been discussed. According to the specifics of the origin and development of the permafrost, the Beaufort Sea shelf has been divided into three parts: (a) the shelf area suitable for submarine relic permafrost-western part; (b) the area with low suitability for relic permafrost-central part; (c) the area without relic permafrost-eastern part. Estimations of thickness and other specifics of submarine permafrost in each area have also been made.
3. A computer system has been developed for the evaluation of all existing environmental data on recent subsea permafrost development. Thirty computerized maps of different oceanographic, geologic, glaciologic, and other parameters have been generated: source data maps, derived maps (three generations), and a composite map specifying the candidate area for submarine permafrost development. To develop the system a composite mapping algorithm for submarine permafrost prediction has been made.
4. The system has been checked in the Beaufort Sea areas with known permafrost. A comparison with Canadian data on submarine permafrost has shown positive results and high correlation.
5. The system can be readily updated according to new data and in this way the results can be enhanced.
6. The shelf maps showing suitability for submarine permafrost have been compared with the BLM lease nomination map. The extension of the suitable areas for permafrost at each nomination site has also been calculated.
7. The same work was done for the Chukchi Sea. It was found that there is a limited distribution of areas suitable for ice-bonded submarine permafrost. The areas were to the northwest from the Barrow Canyon and at some sites along the coast line.

GENERAL STRATEGY AND APPROACH

The study of submarine permafrost distribution and offshore ice content in the perennially frozen rocks is a part of the interdependent biological, physical, oceanographic, and geological investigations intended to minimize the environmental damage during future exploitation of oil and gas resources. The experience obtained in the terrestrial and shelf environments of northern Eurasia and America, along with the scenario worked out during the Barrow synthesis meetings (1977, 1978), clearly shows the danger of subsea permafrost, first for the

production structures themselves, and then for biota and populations. Such peculiarities of the offshore permafrost as the high variability of its surface position in vertical and horizontal directions, sporadic distribution, and multi-layer character (two or more) could pose a threat to pipelines and the foundations of offshore structures because of possible differential subsidence through changes in the thermal regime. The buried thick ice lenses in the 'ancient canyons' which cross the Arctic shelf usually in a meridional direction (see below and Part II) along with the thawing ice wedges in the thermokarst zones of the shelf areas formed in the case of their exposure during the last glaciation need to be taken into account.

We will discuss more of this problem later, but in the sense of the potential danger, it is useful to know that in the "ancient buried canyons" ice lenses 5-15 m thick were met in the Eurasiatic Arctic shelf in the first hundred meters from the sea floor in the narrow, usually meridionally oriented strips about several hundred meters in width. Ice wedges, in different stages of thawing under seawater influence, usually form the polygonal-tetragonal network straight from the seabed. These have an average size of about 100-150 m at a distance of 400-500 m one from another and may give the subsidence about 10 m. These figures might be kept in mind when assessing the potential difficulties for pipeline or foundations during the first phases of exploration and later when hot oil starts to flow from offshore wells.

The development and main features of the submarine permafrost on any part of the Arctic shelf depend on many factors and conditions:

- 1) Geologic structure of the shelf.
- 2) Hydrogeological structure of the shelf, specifically the formation, dynamics, and chemical composition of the underground water.
- 3) Morphostructural features of the shelf, the peculiarities of its relief.
- 4) History of the geological development of the shelf and adjacent coastal areas in Pleistocene and Holocene.
- 5) Recent tectonic activity.
- 6) Peculiarities of the modern marine basin, including bathymetry, salinity, and temperature regime of the seawater.
- 7) The specifics of the hydrological regime on the shelf close to the coast connected with the river activity.
- 8) Role of ice in the zone of ice/sea bottom development.

In a broad sense the specifics of subsea permafrost interaction, distribution, and local peculiarities are always related to the paleoenvironmental and modern environmental conditions. Knowledge of these eight factors is necessary to give a more or less comprehensive picture of the distribution and thickness of permafrost on the Alaskan shelf. Today, not all of these factors are represented by a sufficient data base for a comprehensive analysis. Pieces

of information have been collected at various times and places and the coordinated programs to synthesize the existing data are now in a developmental stage.

The most comprehensive evaluation of current knowledge on Alaskan subsea permafrost has been done by T. Osterkamp and W. Harrison in their annual report of 1977-78. This report also summarized all existing direct data about submarine permafrost in the Beaufort and Chukchi seas, its probing, thermal regime models and data analysis. The study of Lachenbruch et al. (1962), Lachenbruch and Marshall (1977), Lewellen (1973, 1976), Osterkamp and Harrison (1976, 1977, 1978), Rogers et al. (1975), Rogers and Morack (1976), Chamberlain et al. (1977), and Sellman et al. (1976) took place only at two sites in the Chukchi Sea (near Kotzebue, Rabbit Creek, and near Barrow) and at two sites in the western Beaufort Sea (Elson Lagoon, Prudhoe Bay). In the Canadian Beaufort Sea the submarine permafrost was studied by Hunter et al. (1976) in the Mackenzie Delta.

Drilling, probing, seismic study and modelling were the major methods used at these sites. The results of these investigations are the following:

- 1) A negative temperature is typical for the shelf deposits at a depth of at least 80 m from the seabed.
- 2) The maximum distance from the shore where subsea permafrost was met by drilling was 17 km at Prudhoe Bay and about 25 km at the eastern Beaufort Sea (MacKay 1972).
- 3) The upper surface of ice-bonded permafrost maybe quite variable with relief changes of several tens of meters over short distances and may be near the seabed at sites far offshore (according to the seismic studies).
- 4) Data on lower surfaces of permafrost are not sufficient at any site investigated.
- 5) Some data indicate the two bonded permafrost layers under some islands (Prudhoe Bay, Reindeer Island).
- 6) The grain size, pore water salt concentration, and temperature of the deposits play an important role in the distribution of ice-bonded permafrost in the shelf deposits zone of negative temperature.

The site-specific study of submarine permafrost and modelling are of great value for a better understanding of the nature, peculiarities, and thermal regime. Perhaps the site-specific character of the investigations limits their application to definition of areas of submarine extension because of the highly variable environmental conditions of the Alaskan shelf. It is understandable that site-specific information on offshore permafrost from the seismic or drilling methods cannot be obtained for all locations on the continental shelf. In order to meet the need for predictive information on the potential distribution and characteristics of offshore permafrost, a different kind of modelling approach has to be used, drawing on all existing

data. This work is an attempt to use all available environmental data to produce the series of computerized maps of different "generations" to predict areas suitable for subsea permafrost. In addition to providing a tool for storing and retrieving geographically based data, the system is used to produce derived maps showing the important aspects of the conditions for the extension of submarine permafrost and its possible character.

Use of the data management system provides a comprehensive framework for recording, storing, manipulating, and displaying mappable information used in preparing planning studies. This program entails the use of electronic data processing and computer graphics to organize and present a variety of complex data in an orderly and systematic manner. Data are stored on magnetic discs allowing retrieval, analysis, and display of the data in the form of computer-generated maps. The program gives a dynamic base that can be readily updated, and it allows the evaluation of many alternatives. The system can automatically generate a great deal of secondary data, saving time and money during the collection phase of the project. During the data analysis phase, it was possible to aggregate a number of subjective judgments into an integrated set of evaluations. These evaluations identify the most suitable offshore candidate areas for permafrost, based on a multiplicity of geomorphological, geological, cartometrical, geophysical, and oceanographic factors. The system provides a complete trace of the decision-making process as well as an up-to-date base which can be used for siting and routing and environmental studies of this territory. This computer-oriented approach allows the coordination of information for project analysis, to control the selection and format of the data used, and to establish their value.

In this study we tried to analyze both the paleoenvironmental and modern environmental data to trace the area suitable for submarine permafrost. Of course, our attempts are restricted by the distribution and quality of the existing materials. New data might help answer the remaining questions.

DISCUSSION OF PALEOENVIRONMENTAL ASPECTS OF ALASKAN SUBSEA PERMAFROST DEVELOPMENT

Usually the paleoenvironmental aspects of the submarine permafrost are the most talked-about. One basic concept for subsea permafrost origin is that of a shelf exposure, but this is only one idea. In Part II we describe the types of the submarine permafrost on the shelf with undersea deposits saturated in saline cold water, supplied from the continent, or the perennially frozen rocks of the shelf which were formed under coastal conditions, often beneath a layer of low-temperature saline water. The long term role of cooling effects of the thick (250-600 m) body of the continental permafrost has not yet been the subject of adequate investigation.

Following the popular “shelf exposure” concept that helps to assume the shelf submergence-emergence history, taken into consideration in the models of the thermal conditions in submarine permafrost and its configuration (Lachenbruch 1957; Osterkamp 1975; Harrison and Osterkamp 1976; Lachenbruch and Marshall 1977), we will discuss the different possibilities for such exposure. For this purpose we will use the glacioeustatic sea level history of Hopkins (1973, 1977) for the time of the Last Glaciation, direct and indirect information on differential vertical movements at Arctic coastal areas, and some form of a morphostructural analysis.

Indicators of Vertical Movement at Different Parts of the Beaufort Sea Coast

Let us first discuss the role of the coastal retreat data for evaluation of vertical movement in the coastal area. As noted in the “Interim Synthesis: Beaufort/Chukchi, August 1978” (pages 122-126), the rates of coastal retreat differ depending on variations in the coastal bluff composition (including content of ice), exposure, morphology of the coast, and adjoining sea bottom. This rate also changes from year to year. The special investigations in the Laptev and eastern Siberian seas made by F. Are (1967, 1972) and P. Sisco (1970) show that this exposure rate in the Arctic does not depend on coastal exposure or steepness, that the snow cover reduces this rate by 30-40% in comparison with the uncovered coastal slopes, and that solar radiation and the temperature of air (in the case of thermodenudation) and seawater (thermoabrasion) are the key factors influencing this rate. At the same time, the average rate of coastal retreat in the limits of the different geological and geomorphological structures usually reflects the neotectonic recent vertical movements of these morphostructures. Of course, the highest rates of coastal retreat in the Arctic are on promontories and points, but it is important that ‘many bays and estuaries have persistently cuspate outlines showing that thermal erosion and thermokarst collapse tend to cause parallel retreat of the shoreline regardless of coastal orientation” (Interim Synthesis, 1978, p. 1.26). Therefore, to use the coastal retreat data for approximation of the recent movements, we must consider only average rates in the areas with the different morphostructural conditions. The average figures help to exclude local factors and to specify the role of the seawater as a major agent of thermoabrasion, keeping in mind that the thermoabrasion processes are more intensive and consequently the coastal retreat more active at the areas of submergence or the low rate of the positive vertical movements. In evaluating vertical movements on the Beaufort Sea coast we have made a comparative analysis of the rates of coastal retreat and vertical movement according to data from the Laptev and East Siberian seas. The vertical uplift data of Baskakov and Shpaikher (1970) are based on the graphic method for the seaboard of the Kara, Laptev, and East Siberian seas and the Bering Strait. The method assumes that the year-to-year sea level variations are the same order of

magnitude in all regions of a given sea or adjacent seas (Mesheryakov 1964). The rate, V, of the present-day movements of the seaboard and the calculation errors were calculated by means of the following equations:

$$V = \frac{\sum Ht}{\sum t^2} \quad \delta_v = \pm \frac{\delta H}{\sum t^2} \quad \delta_H = \pm \sqrt{\frac{\sum H^2 - V\sum Ht - b\sum H}{n - 1}}$$

where:

V = the rate of present-day vertical movements of the seaboard;

H = the mean annual level;

b = the mean long-term annual level ($\sum H/n$);

n = the number of years of observations (length of the series);

t = the serial number of the year counted from the mid-point of the observation period;

δ_v = the RMS error involved in the calculation of the rate of present-day coastal movement; and

δ_H = the RMS error involved in the calculation of the sum total of annual levels ($\sum H$).

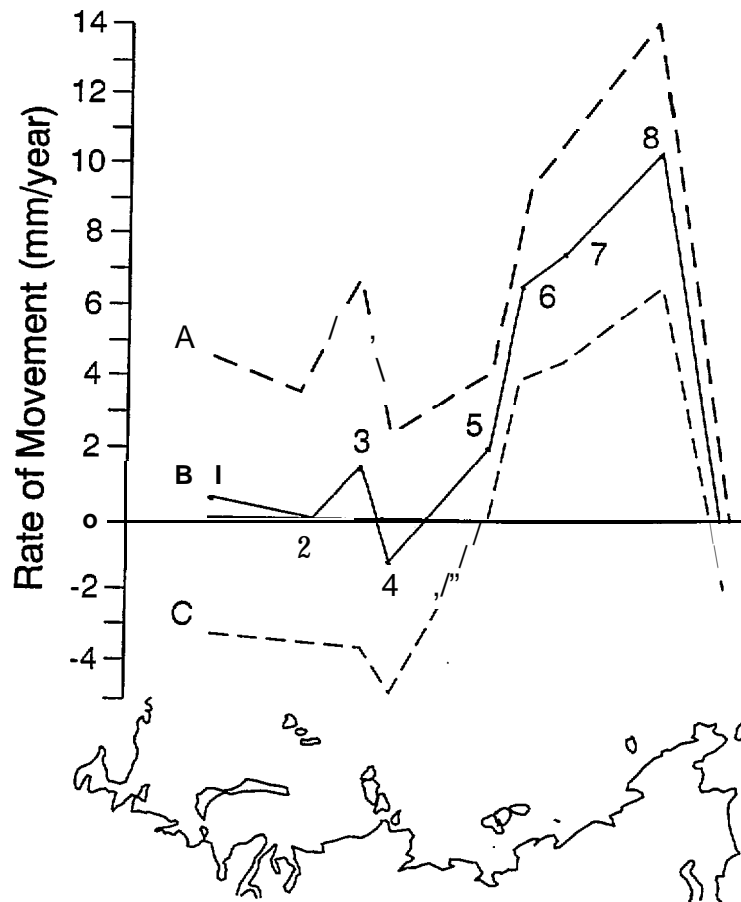
The rate of present-day coastal movements was calculated for nine polar stations, four of which are located in the Kara Sea, one in the Laptev Sea (Tiksi Bay), two in the East Siberian Sea (Cape Shalaurov and Ambarchik Bay), one in the Chukchi Sea (Cape Schmidt), and one in the Bering Strait (Providence Bay). The calculations were based on coastal observations of the sea level during the years 1951-65 (Table 1, Figure 1). The RMS errors make it possible to assess the present-day coastal movements more objectively by characterizing the possible variation range of the rate of these movements. We see that seaboards are currently rising, except for the regions of the Vilkitski and Bering straits (where the coasts are settling). The rate of uplift increases from west to east, from values not exceeding +1.5 mm/year in the Kara Sea to +10.5 mm/year in the Chukchi Sea. An especially high coastal uplift rate, ranging from +12.7' to +39.5 mm/year, was calculated by Pierce (1960) for the southeastern coast of Alaska (Table 2). Pierce's results were mostly confirmed by Bird and Barnett on the northern Canadian seaboard. From his sea level analysis at Churchill (1940-64), Barnett (1966) determined a coastal uplift rate of 7.3 mm/year. According to Bird (1954), coastal uplift of as much as 90 cm over a period of 100 years was registered in the region of Boothia Peninsula, and some 80 cm per 100 years between Chesterfield and Cape Eskimo. According to all this data on the Kara and Laptev sea coasts where the rate of uplift is very small and does not exceed the calculation error, the coast is relatively stable. The point of observation (Tiksi Bay,

Table 1.—Relative rate of present-day vertical coastal movements in Arctic seas in 1951-65, mm/year. After Baskakov and Shpaikher (1970).

Serial Number		Relative Rate of Movement	RMS Error of the Rate of Movement	Sea
1	Amderma	+0.7	*3.9	Kara
2	Dikson Island	+0.1	± 3.6	Kara
3	Pravda Island	+1.5	± 5.2	Kara
4	Cape Chelyuskin	-1.2	± 3.8	Kara
5	Tiksi Bay (Bulunkan Inlet)	-2.2	± 2.0	Laptev
6	Cape Shalaurov	+6.7	± 2.6	East Siberian
7	Ambarchik Bay	+7.5	± 3.0	East Siberian
8	Cape Schmidt	+ 10.5	± 3.8	Chukchi
9	Providence Bay	-1.0	± 1.0	Bering Strait

Table 2.—Variations of absolute elevations on the southeastern Alaskan seaboard. After Pierce (1960).

Observation Site	Observation Period	Change in Coastal Elevation over Observation Period (cm)	Rate of Vertical Coastal Movement (mm/year)
Skagway	1909-1959	89	+ 17.8
Haines	1922-1959	82	+ 22.2
Tepri Bay	1922-1959	82	+ 22.2
Muir Inlet	1940-1959	67	+ 35.3
Willoughby Inlet	1939-1959	53	+ 26.6
Bartlett Cove	1938-1959	83	+ 39.5
North Inian	1902-1959	135	+ 23.7
Lisianskii Bay	1917-1959	58	+ 13.8
Elfin Cove	1938-1959	40	+ 19.5
Hoopak	1932-1959	57	+ 15.8
Svenson Harbor	1901-1959	99	+ 17.0
Funter Bay	1922-1959	52	+ 14.0
Auke Bay	1937-1959	42	+ 19.3
Juneau	1911-1959	61	+ 12.7
Annexe Creek	1937-1959	30	+ 13.6
Greeley Point	1937-1959	30	+ 13.6



A = Rate of movement (mm/year); B, C = Rate of movement (mm/year) taking account of the RMS error; 1, 2, 3 . . . 9 = serial numbers of observation sites (See Table 1).

Figure 1.—Spatial variation in the rate of present-day vertical movements in Arctic seas.
After Baskakov and Shpaikher (1970).

Bulunkan Inlet) has a relative rate of movement of +2.2 mm/year. This is part of the Laptev Sea submarine permafrost and thermoabrasion study polygon. According to Are (1972, 1973) and others, the average rate of the coastal retreat here is about 4–5 m/year. The seaboard of the eastern part of the Laptev and East Siberian seas with a higher rate of recent uplift has proportionally lower rates of average coastal retreat.

The data of Stovas (1965) and Gutenberg (1941) indicate a possible settling of the Bering Strait western coast and uplift of the areas east of the strait. Pierce (1960), Barnett (1966), and Bird (1954) also emphasize the very high uplift rate of the eastern part of the Bering Strait, especially east of Cook Inlet and on the northern Canadian seaboard.

Figure 2 shows the average rate of coastal retreat in the Beaufort Sea. Data from the Interim Synthesis (1978, p. 125) shows three areas with three different rates of retreat:

- 1) Pt. Barrow-Harrison Bay—4.4 mm/year
- 2) Colville River (148 O?) to 1420 —1.6 mm/year
- 3) 142° to Mackenzie River—1 mm/year (in the “Synthesis”: Demarcation point-Mackenzie River delta).

Using the comparative data on coastal retreat and the vertical uplift equivalents from Siberian seas we consider that the recent uplift rate at the first area is about 2.2 ± 2.0 mm/yr, which identifies that territory as a relatively stable one (Figure 3).

The second area, with coastal retreat through time less than the first one, has a rate of vertical uplift of about 6.6 ± 2.6 mm/yr, and the third one, Canada, about 10.34 ± 3.7 mm/yr. This means that the first area is considerably late in the general uplift of the Arctic coasts, the second area is transitional, with a clear picture of the modest uplift, and the third one could be characterized as an area with a high rate of recent vertical uplift, comparable with the rates of southeastern Alaska, the territory situated to the east of Cook Inlet. It is possible to find the explanation of the differential vertical movements on the Beaufort Sea shelf in its geological and geomorphological peculiarities.

Morphostructural Peculiarities of the Coastal Areas Related to Vertical Movements

The differences in the rates of coastal retreat and the rate of vertical movement at the three named areas could be explained by their different morphostructural conditions. The first area (Point Barrow-Harrison Bay) is a low, flat plain with very high density of lakes generally oriented north. It is situated to the west from the major zone of seismic activity which has meridional orientation here. This zone is a continuation of the Aleutian Islands-Cook Inlet active zone. This gigantic transitional, tectonically active zone divides Alaska and its northern slope along 150°, 1480-1420 and includes Prudhoe Bay, the seismic zone around

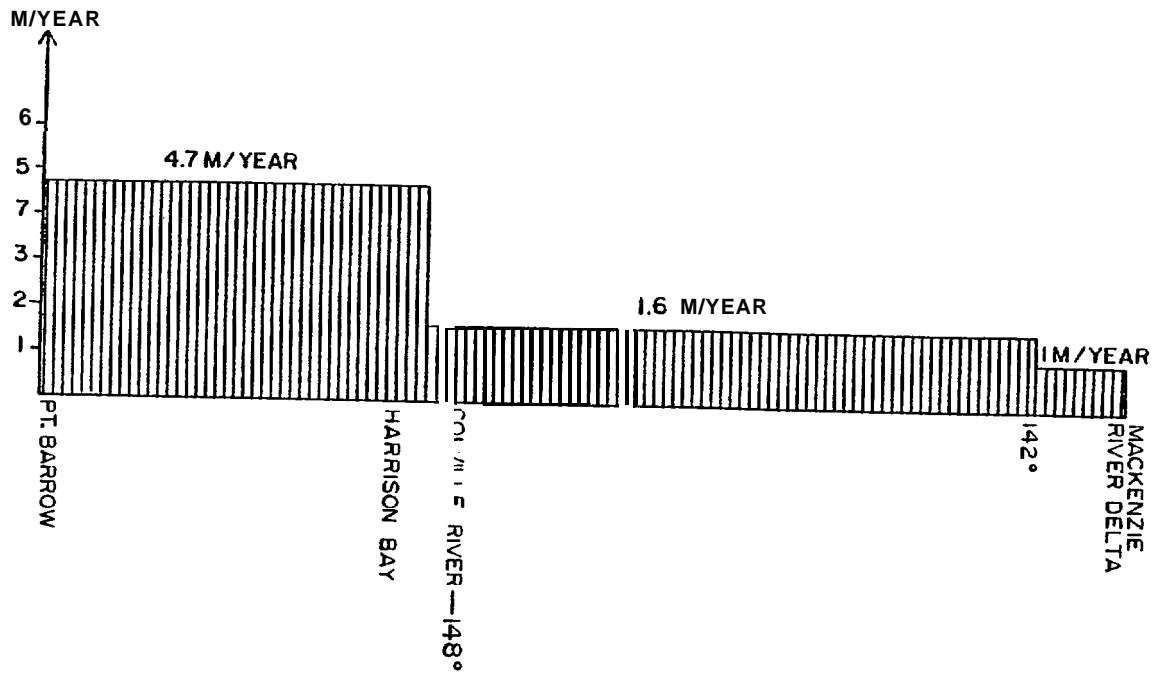


Figure 2.—Average rate of coastal retreat according to the Interim Synthesis, August 1978, Figure 3.13, pp. 125, 126.

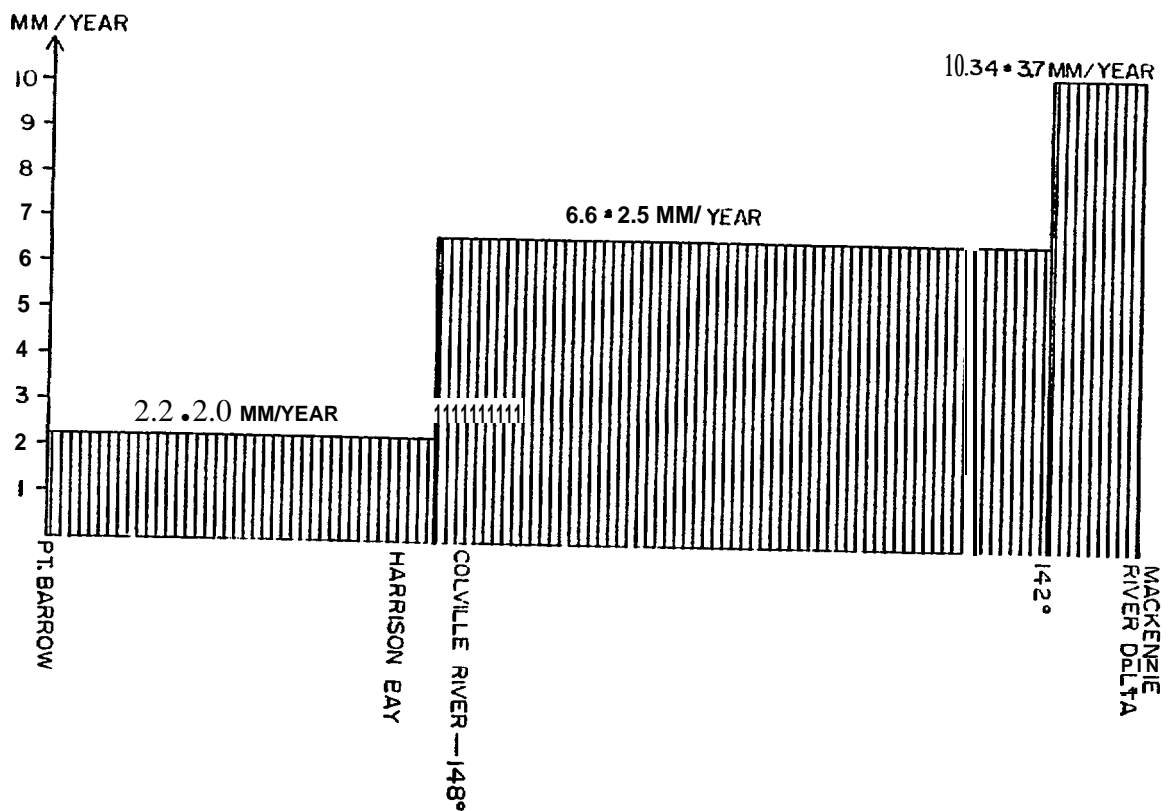


Figure 3.—Possible rate of the Beaufort Sea recent coastal uplift proportionally to the average coastal retreat.

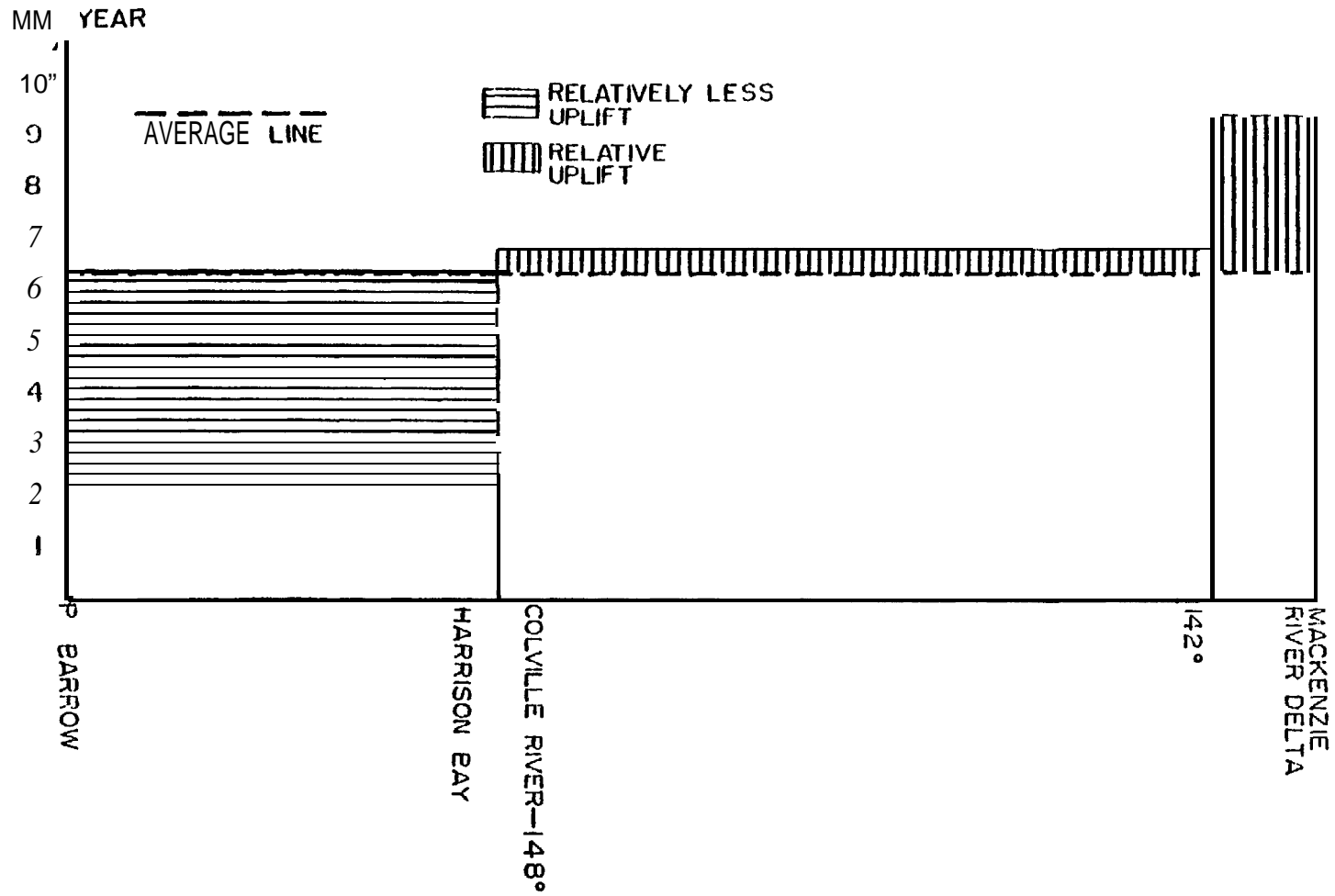


Figure 4.—Relative rate of the recent uplift of the three major morphostructures of the Beaufort coast.

Barrier Island and the point 30 km offshore (with the largest earthquake registered ($M_L = 5.3$) and a series of aftershocks) showing an ENE-WSW seismic trend along the axial traces of the offshore folded structures. The study made by Biswas (1977) traced this zone in northeast Alaska, as shown in Figure 5. Figure 6 shows the major transitional active zone of Alaska through distribution of the earthquakes. Both pictures are reproduced here from the 'Interim Synthesis:' (1978, pp. 103-104). If our first area is situated to the west of the tectonically active zone and it is not included in this zone, the second area is part of it. We might also suggest that the boundary between our first and second areas could be traced, not along the Colville River and its delta, but following the western limit of the named seismically active zone. At latitudes $70^{\circ}30' - 71^{\circ}$, the tectonic boundary corresponds more to 1480 and this meridian looks more appropriate as a divide between the two morphostructures of our first and second areas. Thus, the second area fully corresponds to the tectonically active transitional zone ($148^{\circ} - 142^{\circ}$). The third area is mostly situated to the east from Barter Island/1420 and extends possibly towards the Mackenzie Delta, or east from the major seismic zone, and it is an area with low density of lakes, with domination of the higher absolute altitudes and more steep and narrow part of the Beaufort Sea shelf.

According to Bulard's suggestion (1971) the Anchorage-Prudhoe Bay transitional active zone could be considered as the boundary of the American and Asian plates. During the Paleozoic stage of the Alaskan Cordillera geosyncline development, this zone was one of the zones of relative uplift. The thickness of the Paleozoic system reached only 500 m. In the western and southeastern parts of Alaska this thickness reached several thousands of kilometers. During the Mesozoic stage this structure played the role of a barrier. Then and now the tectonic movements in this zone and to the east and west from it had, and have, different character and magnitudes. In the late Cenozoic the eastern part of the northern Alaska plain (White Hills Province) was under relative uplift. The fact that one can see dislocated tertiary rocks in the centers of the dome-structures here shows a result of the positive movement. On the other hand, the basin of Teshekpuk Lake in the west could be characterized by the great thickness of the unconsolidated Quaternary deposits (see Williams et al. 1977) on top of the Cretaceous Colville formation. The distribution of the surficial deposits of this part of the coastal plain is shown in Figure 7. This means that the western part of the Alaskan Arctic plain, or our "first area," was significantly late in the uplift of the coast and shelf in comparison with the more eastern parts of the plain, or our 'second area,' and 'third area.' Both the Tertiary and Quaternary periods at Alaska were the periods of relative positive movements of the eastern part of Alaska. At the same time the western plate was involved in relative submergence related to the development of the marine basins of the Arctic and North Pacific. Figure 8 represents the scheme of the major linear morphostructures of Alaska

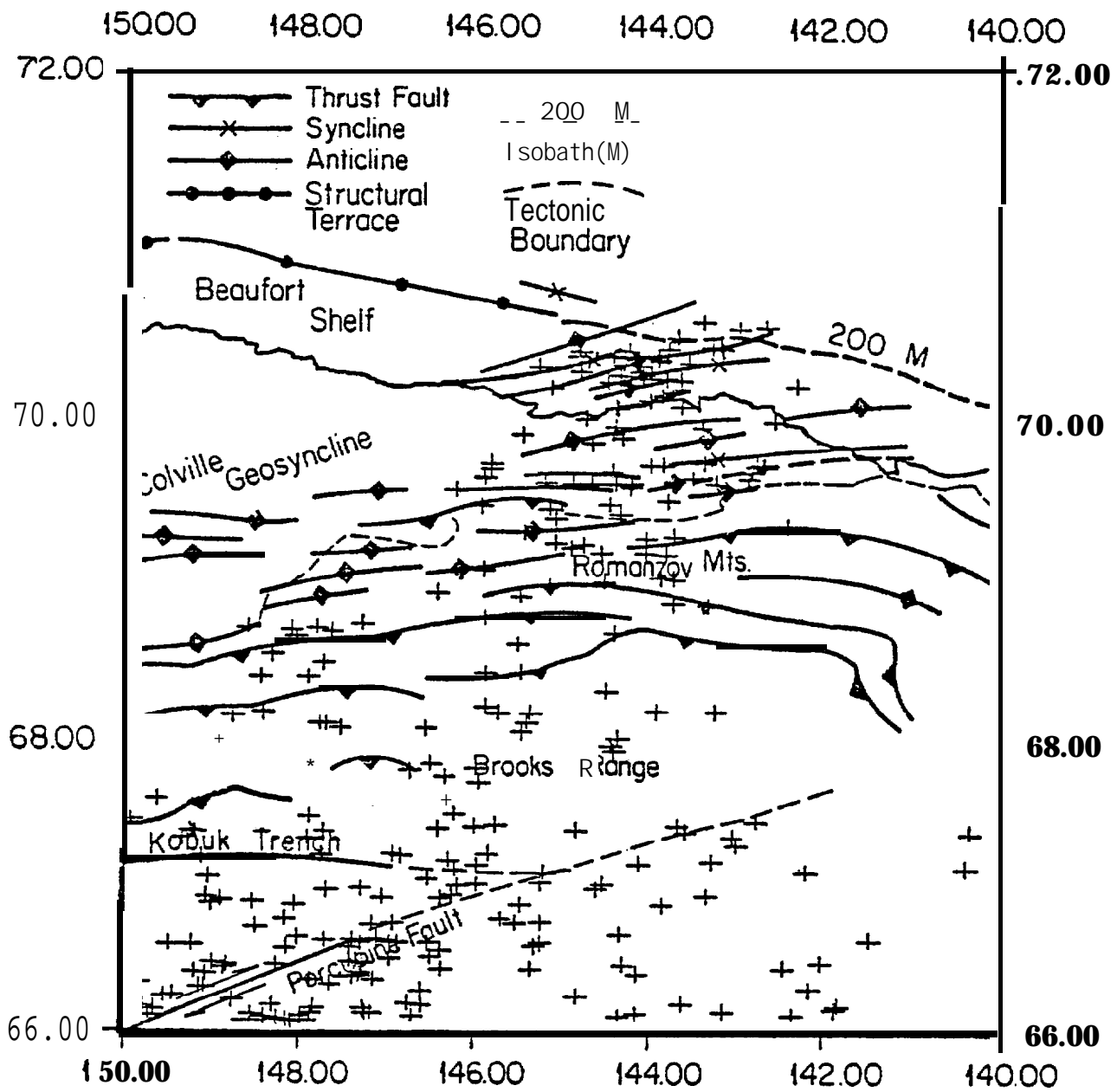


Figure 5.—Epicenters of earthquakes in northern Alaska according to Biswas (1977).

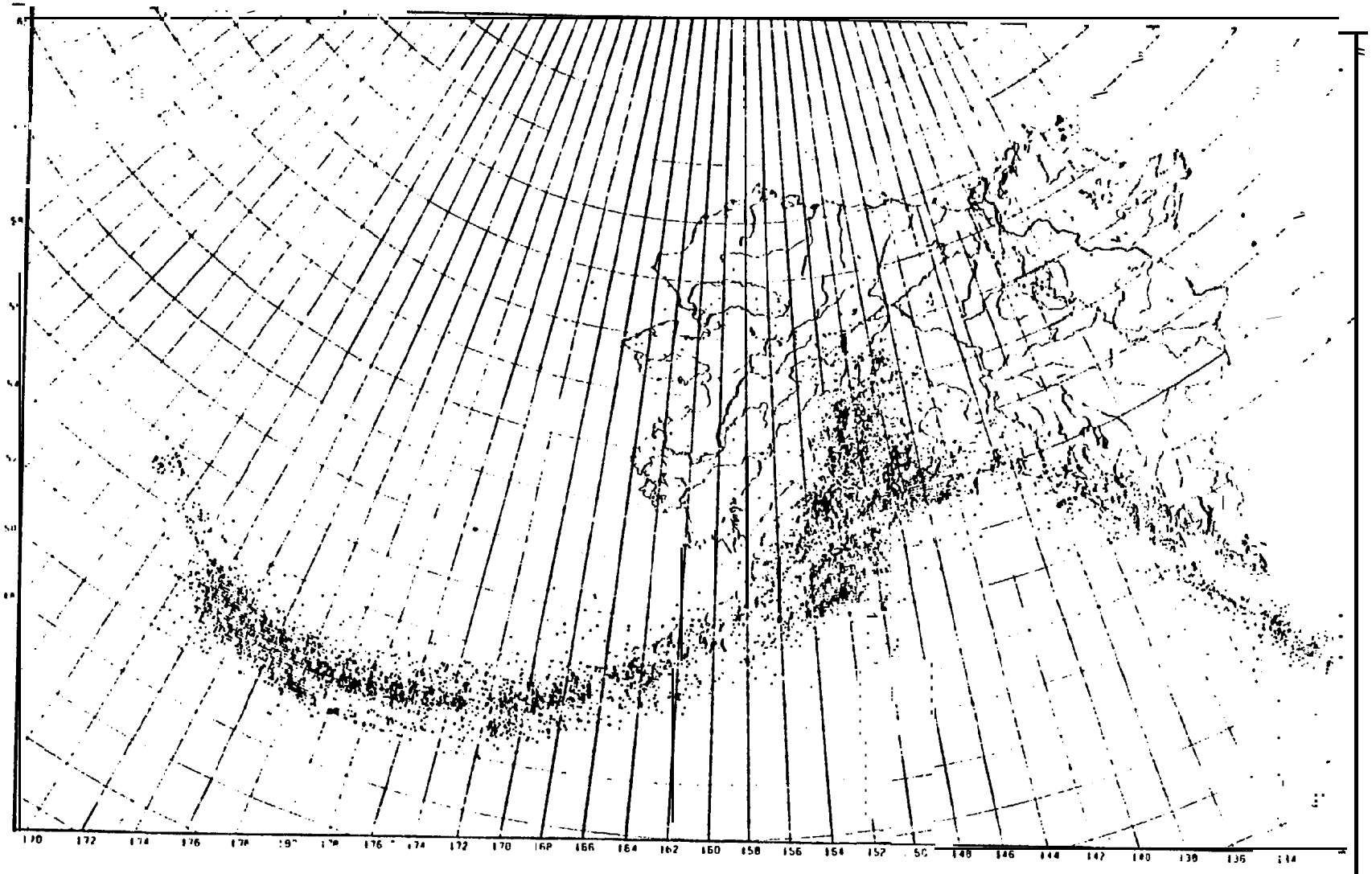


Figure 6.—Earthquakes in and near Alaska (Interim Synthesis 1978).

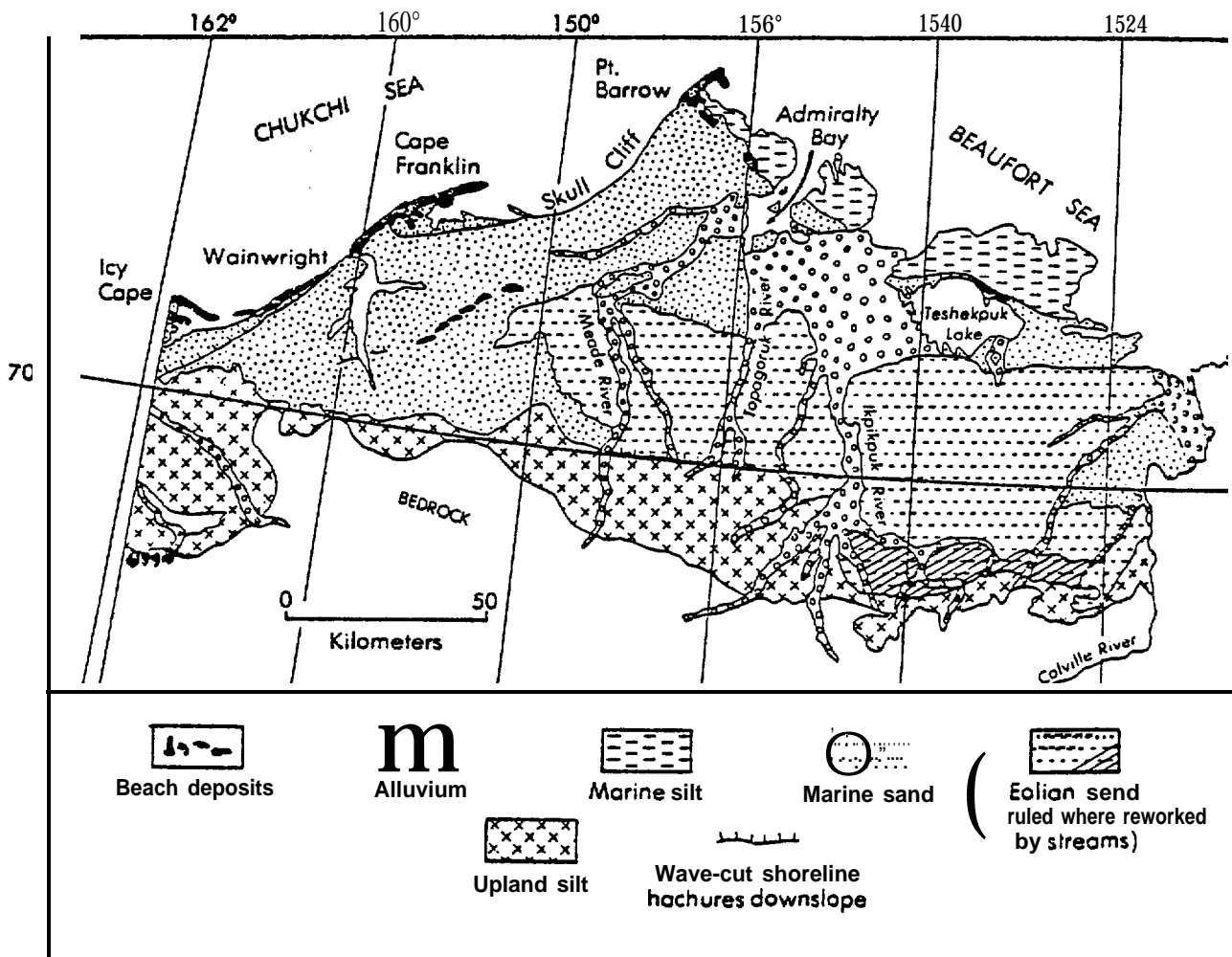
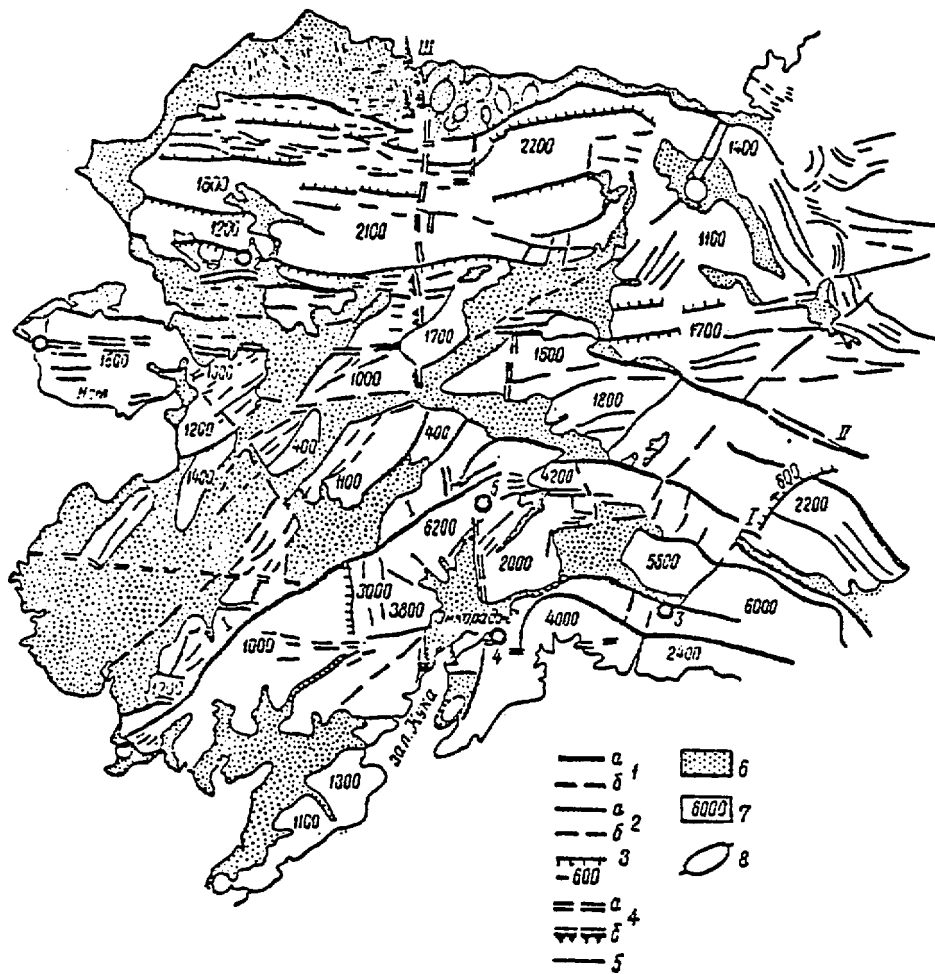


Figure 7.—Generalized surficial deposits map of Arctic coastal plain. After Williams et al. (1977).

made by I. Volochanskaya (1971) with use of satellite and topographical data, the scheme that could be used for better understanding of the nature of the differences in the recent vertical movement rate. It should be noted that these rates for northeastern and southeastern parts of Alaska are comparable (Table 2, Figure 3). Of course, the *glaciostatic* component of the eastern parts of Alaska close to the Laurentide Ice Sheet development increases the rates of vertical uplift because of the postglacial rebound. For the Mackenzie River basin such rebound looks appropriate.



1. Major lineaments: a) well seen, b) fragments(I-Denali system, II-Tintin fault)
2. Other lineaments: a) well seen, b) fragments
3. Topographical levels along the lineaments and their relative height
4. Transitional zones (a) and levels of regional basic heighte (b) (III Anchorage-Prudhoe Bay Zone).
5. Boundaries of the morphostructures
6. Plains
7. Mountain relief and altitude of divides
8. Dome structures

Figure 8.—Linear elements in the Alaskan geomorphological structure. After Volochanskaya (19'73).

We see that the major trends and differences in vertical movement rates in the western (Point Barrow-Harrison Bay), central (Colville River-1420), and eastern (1420-Mackenzie River Delta) parts of the Alaskan coastal plain (Figure 9) have a long term and genuine character explainable on the basis of plate tectonics, morphostructural specifics, and the role of glaciostatics.

Exposure of the Shelf During the Last Glaciation

If our considerations are right and the rates of vertical movement were constant during Late Glacial and Holocene times, we may evaluate the possible position of the Beaufort Sea shoreline in the past (Table 3). Then following Hopkins' curve (Interim Synthesis, 1978, p. 105) we will try to specify the areas of exposure suitable for permafrost development and then for the thermal influence of the seawater. In Figures 10 and 11, we can see that only the western part of the Beaufort shelf could have been exposed and only from 25,000 to 10,000 years ago, and isobath 60 ± 20 m is the best candidate to limit the exposed part of the shelf. Evidence of exposure, such as thermokarst and polygonal forms of relief, could be of great help to prove the exposure version.

Table 3.—Possible position of the Beaufort Sea shoreline in the past.

Thousands of Years Ago	Point Barrow- Harrison Bay (m)	Colville River- 1420 (m)	142 °- Mackenzie Delta (m)
0	0	0	0
5	-11	-33	-51
10	-22	-66	-103
15	-33	-79	-154
20	-44	-111	-205
25	-55		

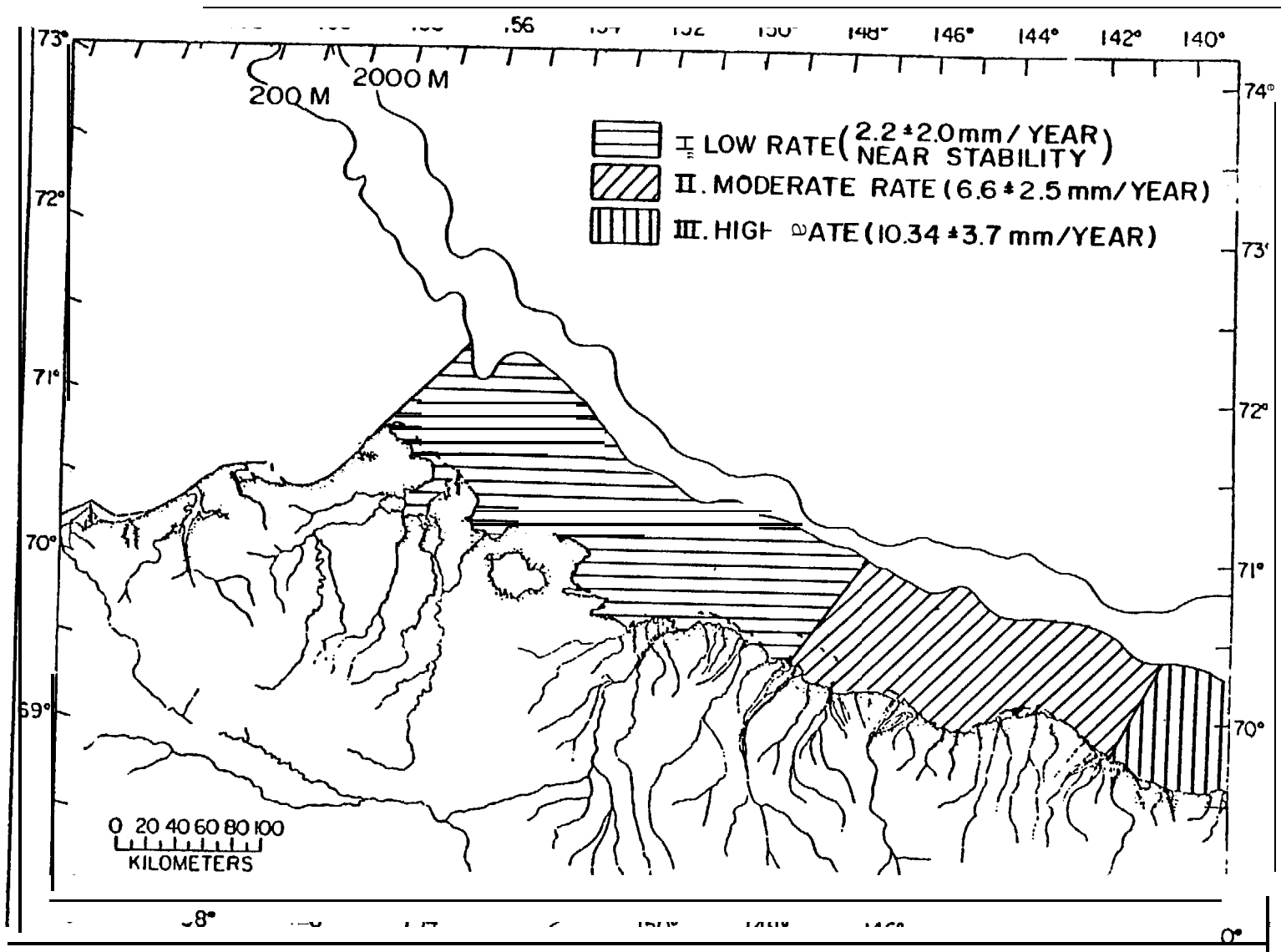
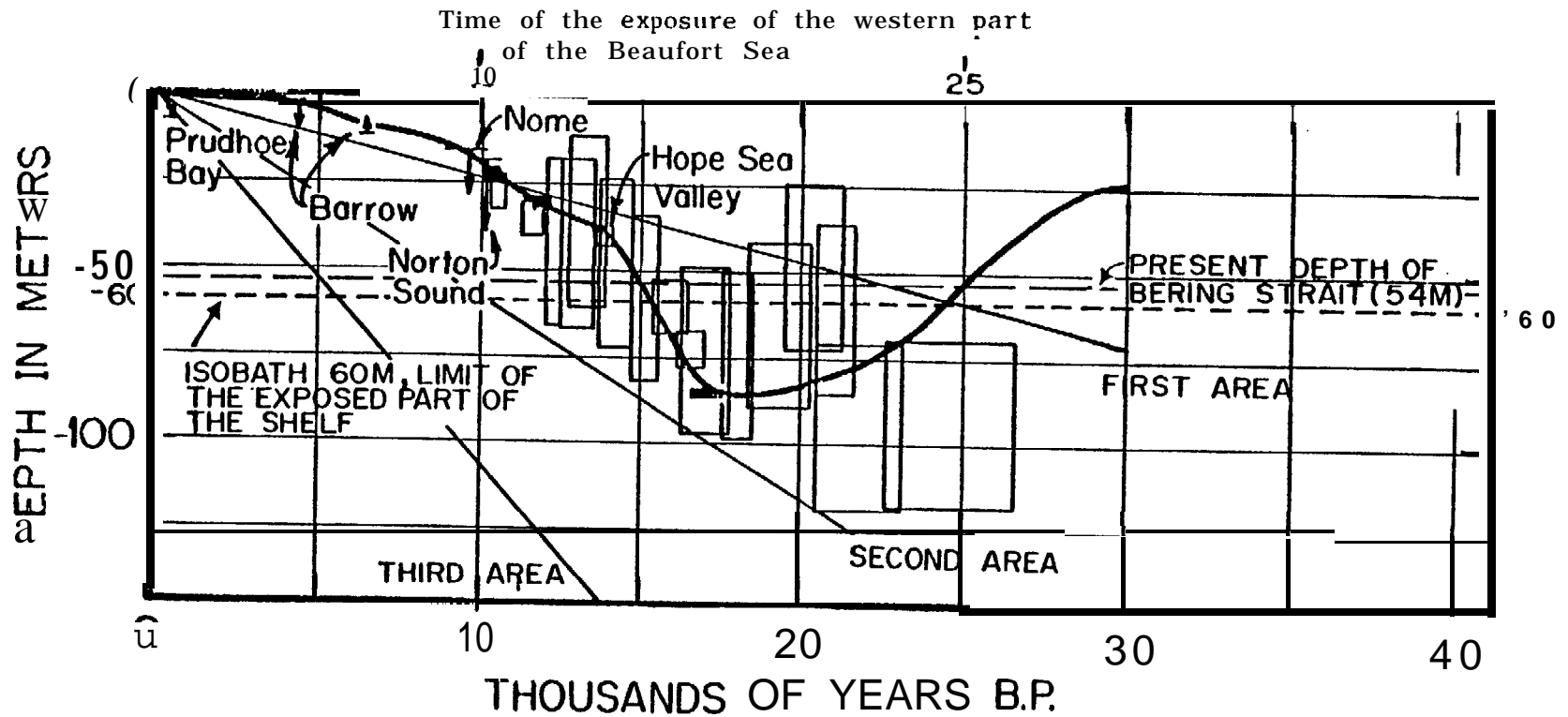
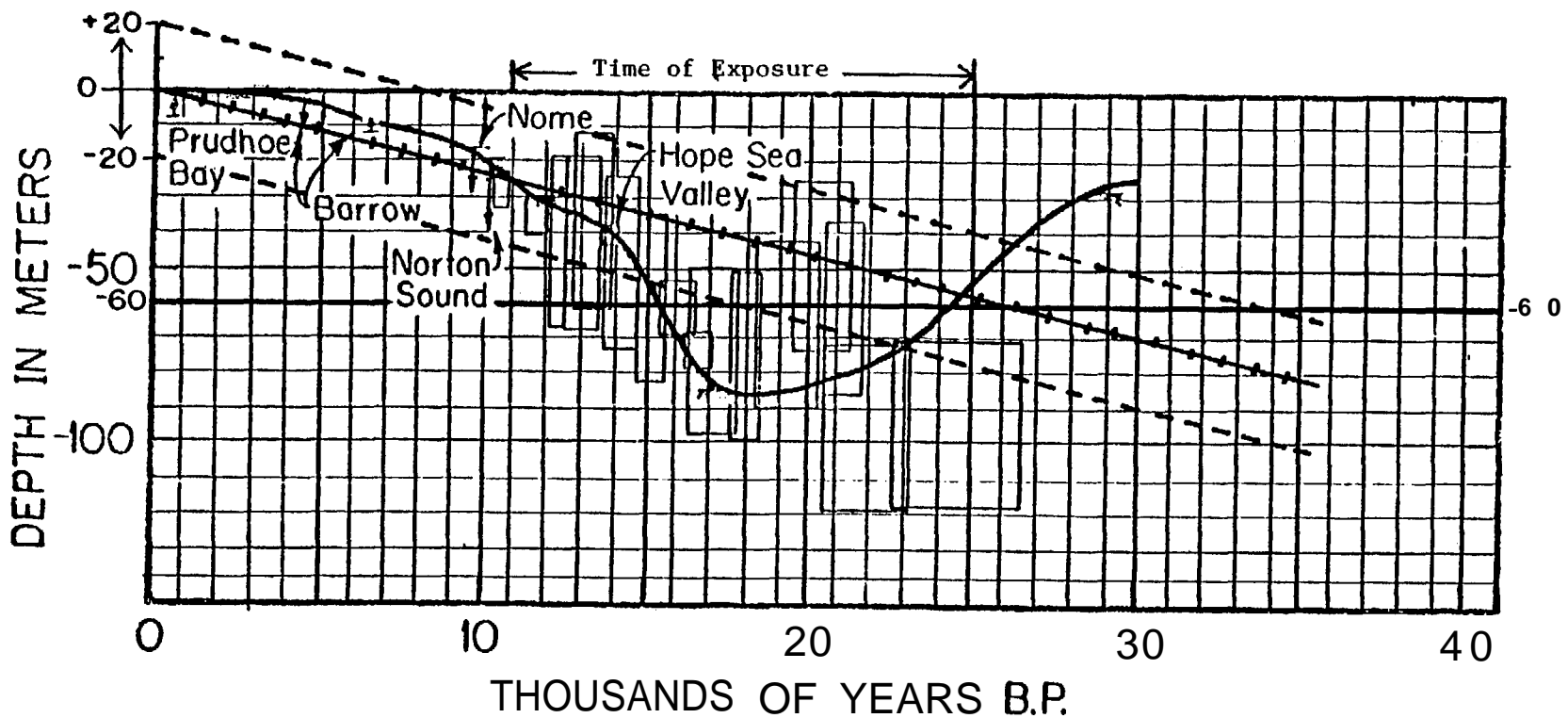


Figure 9.—Areas of the Beaufort Sea coastal plain and shelf with different rates of vertical movement.



First area: Barrow to Harrison Bay
 Second area: Colville River (148°) to 142°
 Third area: Mackenzie River to 142°

Figure 10a.—Reconstruction of sea level history on the continental shelves of western and northern Alaska. Possible position of the Beaufort Sea shoreline in the past, according to the Hopkins (1977) curve of the sea level reconstruction with our additions on differential recent tectonics.



ISOBATH 60*20M —LIMIT OF THE
EXPOSED PART OF THE SHELF (AREA 1)

Figure 10b.—Reconstruction of sea level history on the continental shelves of western and northern Alaska, After Hopkins (1977) with our additions related to the differential recent tectonics. Possible position of the Beaufort sea shoreline in the past at the northwestern part of the shelf (first area) with correction on RMS error of the rate movement.

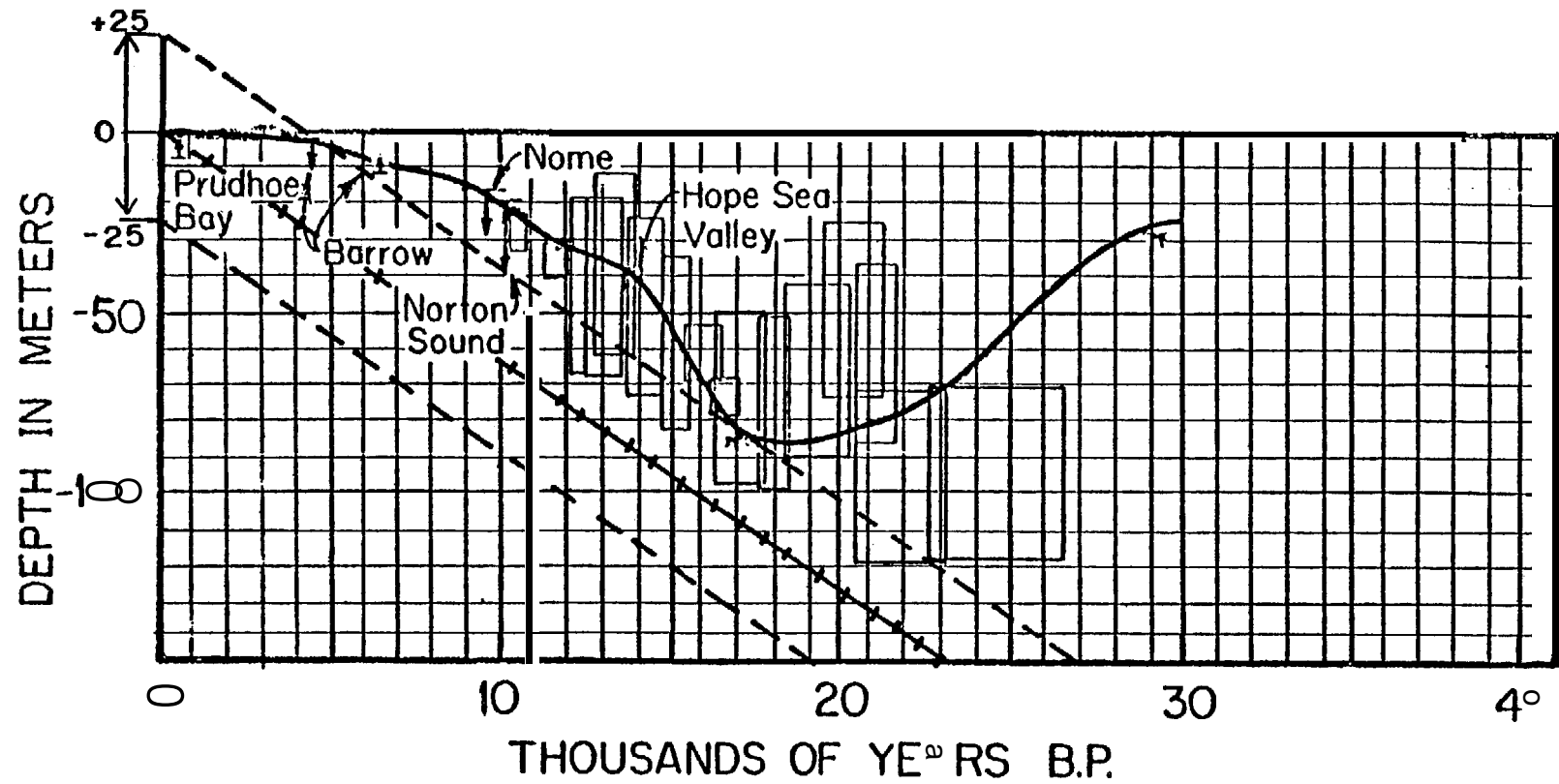


Figure 10c.—Reconstruction of sea level history on the continental shelves of western and northern Alaska. After Hopkins (1977) with our additions related to the differential recent tectonics. Possible position of the Beaufort Sea shoreline in the past at the central part of the American Beaufort Sea shelf (second area) with correction on RMS error of the rate movement.

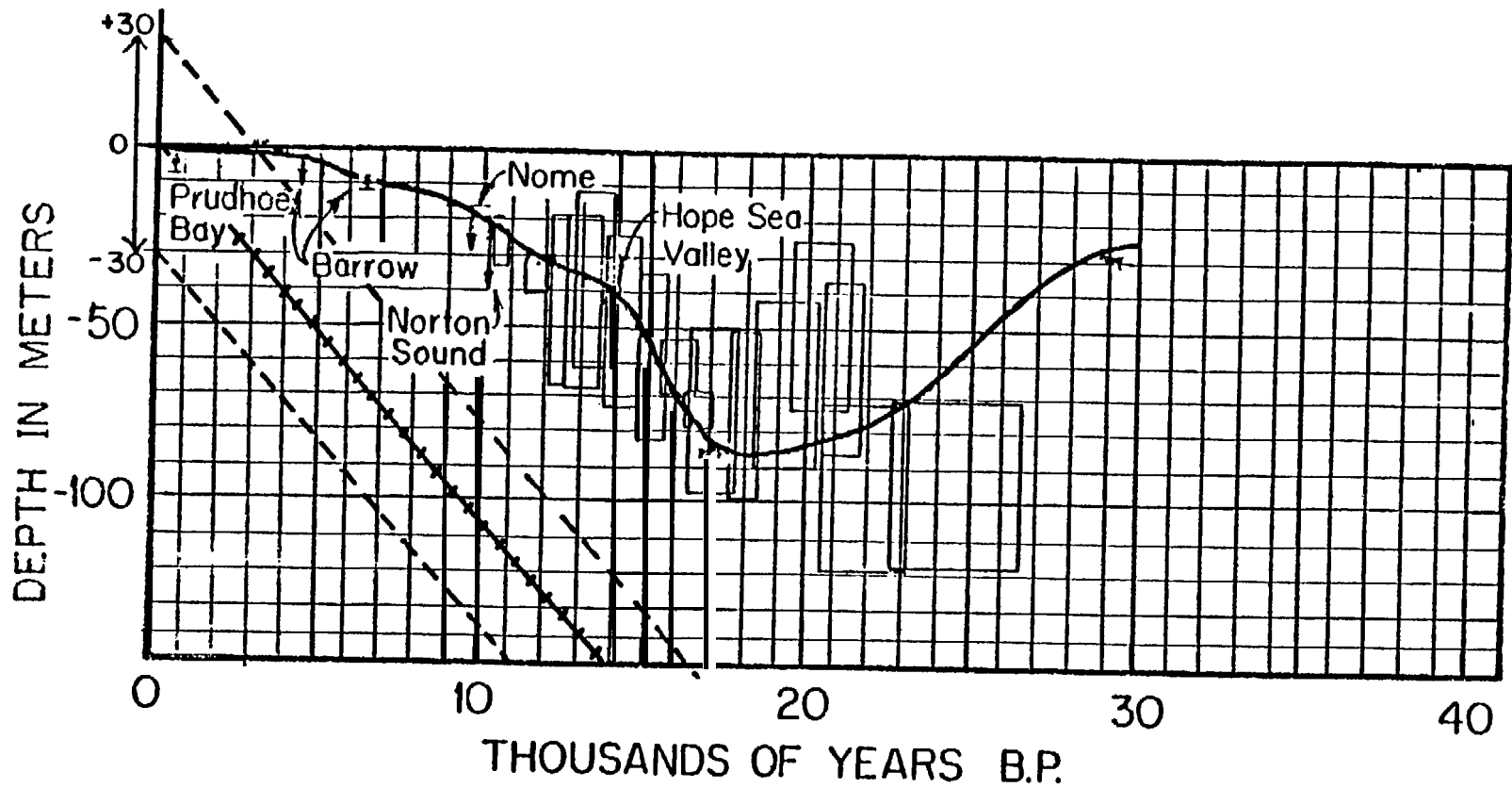


Figure 10d.—Reconstruction of sea level history on the continental shelves of western and northern Alaska. After Hopkins (1977) with our additions related to the differential recent tectonics. Possible position of the Beaufort Sea shoreline in the past at the eastern part of the American Beaufort Sea shelf (third area) with correction on RMS error of the rate movement.

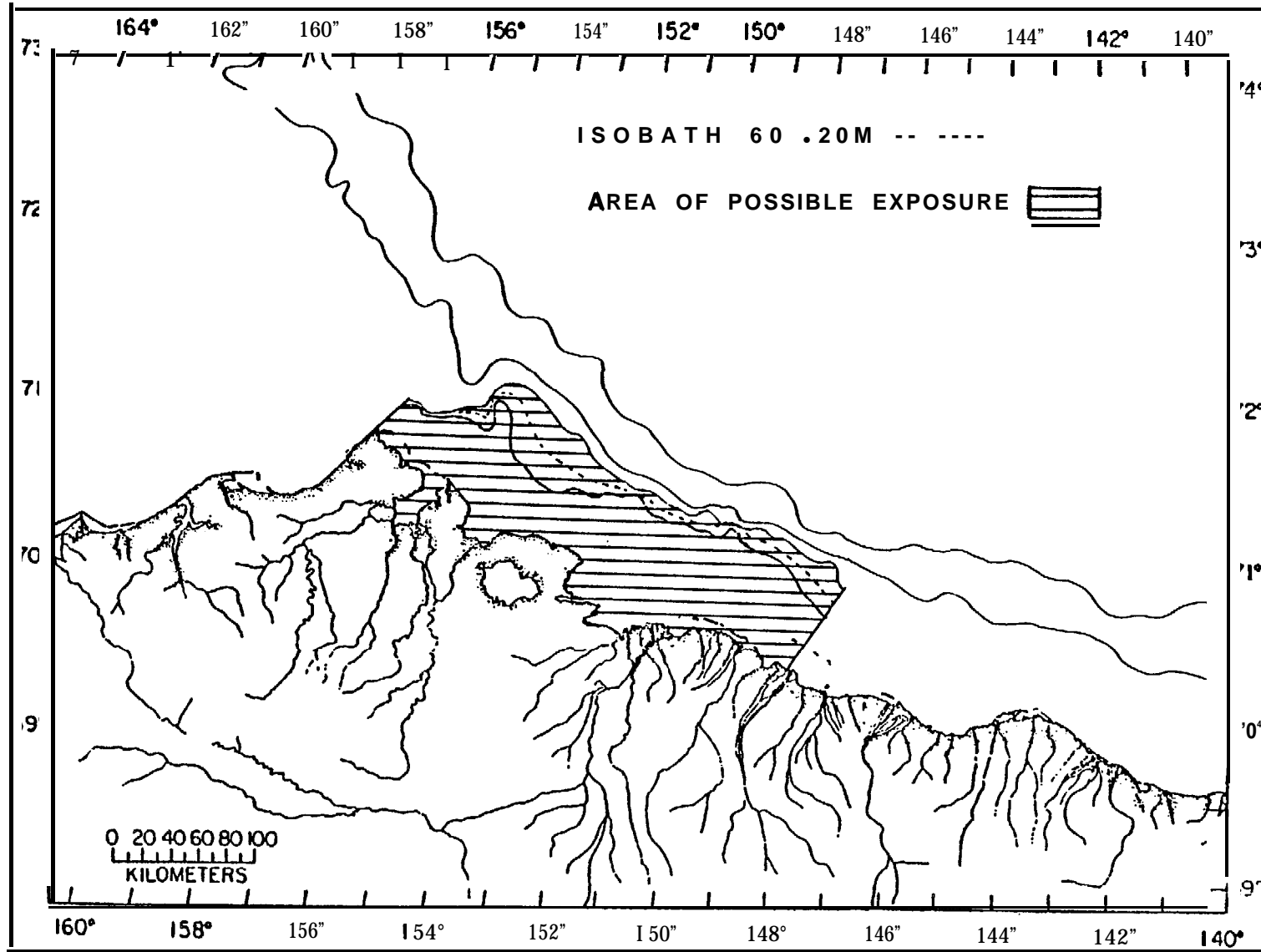


Figure II.-Possible exposure of the shelf during the last glaciation.

Lack of Data on Thermokarst and Polygonal Forms at the Shelf

Hopkins' curve and the data on coastal retreat and morphostructural specifics today are the only base for the Beaufort Sea shelf exposure evaluation during the last 25,000 years. At the **Eurasian** part of the Arctic shelf the conclusions about the exposure of one or another area of the shelf are usually supported by such evidences as thermokarst or **polygonal-tetragonal** forms. **Hydroacoustic** investigations, for example, have been used by Klyev (1966) in the Laptev Sea for the detection of submarine **thermokarst** relief. Figure 12 shows the polygonal profiles and the sizes of the forms according to the acoustical diagrams. The author described wedge-like forms in the different stages of the ice thawing. The silty mud typical for this part of the Laptev Sea shelf has not filled in these forms yet. The later stages of thermokarst form development are shown in Figure 13. The space left by the thawed ice wedges are here in the process of being filled in. These forms are most typical for depths of 10-15 m where gravel and coarse sand dominate. The deeper part of the shelf is characterized by smoother **microrelief** of such forms. Some of the negative forms of relief, considered by Klyev as the thermokarst, are oriented along the **isobaths** and have a length of about 3-4 km (sometimes 7 km), an average width of about 135 m, and depth of 4-6 m. In this sense they look very similar to the ice gouging features described by Reimnitz and Barnes (1976, 1977). But such forms in the Laptev Sea are usually connected with the same kind of depressions forming polygons, tetragons, or "chess board" patterns. At some places these patterns of submarine thermokarst have a very clear expression. **As** a rule the subsea thermokarst forms are comparable with their analogs in the adjacent coastal areas. At some areas of the **Eurasian** shelf exposed during the late Pleistocene the thermokarst forms were found at a depth of 35-40 m. Often these formations have been found near areas of river-water influence. This shows the continuation of the submarine permafrost and its forms degradation in present time. It is possible that some of the depressions described on the **Eurasian** shelf are not **thermokarst** but are of ice gouging origin. As for the Beaufort Sea shelf, all the depressions of similar size and position are described here as the result of ice gouging processes (Reimnitz and Barnes 1976, 1977). The possible future finding of thermokarst and **polygonal-tetragonal** forms in the western part of the shelf (to isobath 60 ± 20 m) could give direct evidence for a shelf exposure. The sizes and distribution of these forms have to correspond to the parameters of their analogs on the western part of the Beaufort coastal plain. If such direct evidence were found, it would be a great support for the shelf exposure concept related to the origin of the submarine permafrost now considered as a relic.

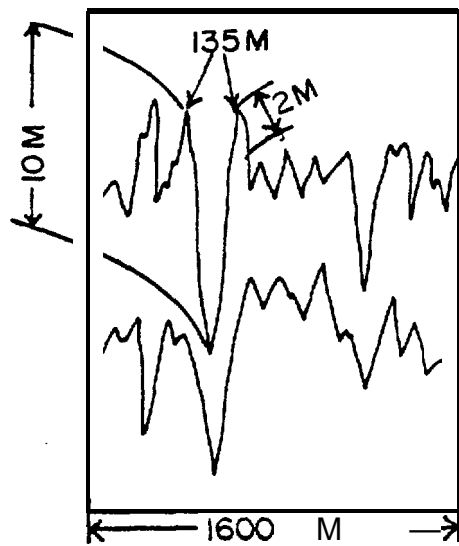


Figure 12.—Polygonal profile with the ice wedge in the process of thawing at the Arctic shelf, Laptev Sea. After Klyev (1964).

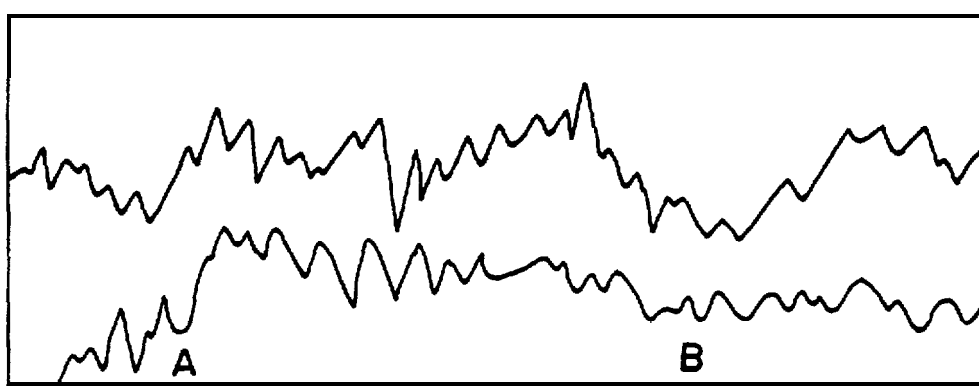
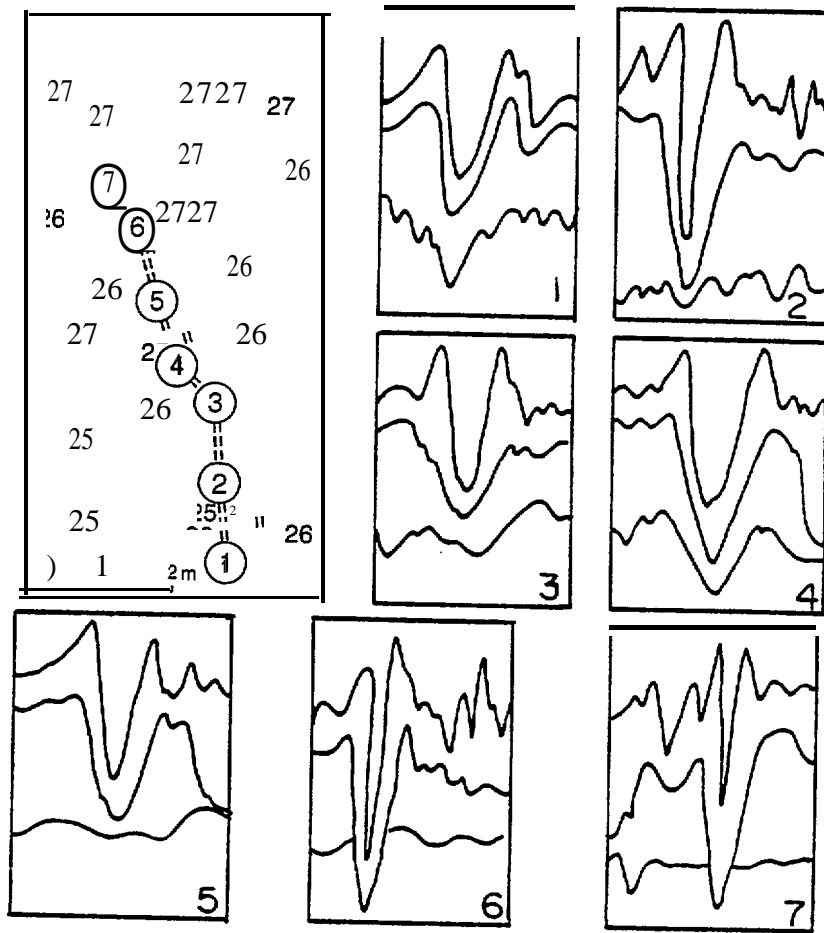


Figure 13.—Profiles of the thermokarst forms on the shelf after thawing, according to Klyev (1964).



vertical scale for 1,3,5 - 1mm = 1m
 for 2,6,7 - 5mm = 1m

Horizontal scale for 1,3,5 - 1mm = 12m
 for 2,6,7 - 1mm = 23m

Figure 14.-Submarine thermokarst profiles on the shelf. After Klyev (1964).

Role of the Meridional Lineaments of the North Alaskan Coastal Plains and Shelf

Short and Wright (1974) have identified two sets of lineaments on the Alaskan North Slope by inspection of map contour patterns and surficial geomorphic trends. They have noted that primary and secondary lineaments, with 40° and 3000 azimuths, have an effect on the coastal configuration and other physiographic features. Two systems of the lineaments of Short and Wright (Figure 15) fully correspond to the tangential stress orientation along the major lineament systems of the earth (Figures 16 and 17). These lineaments are a part of the global system and they do not specify some important regional morphostructural peculiarities of the Alaska Peninsula, including the northern slope. Usually, a comparison of maps which portray deep-seated faults with topographical maps of the corresponding areas gives an indication that the directions of the dominating faults are reflected in the general pattern of the drainage system (Kudryavtsev 1963; Chebanenko 1963). Close relationships between tectonic lines and the drainage patterns were noted on the Siberian platform (Vakat et al. 1958). The trend of the major faults is shown in the bends of the Lena River. Such Siberian rivers as Vilyui, Augara, and Aldan generally flow along the trend, which coincides with the primary structural pattern of the corresponding region. A rose diagram of lineaments from various areas in the different parts of the earth (Figure 17) gives some kind of summary in lineaments distribution and orientation made by Voronov et al. (1970). The same authors give the general picture of drainage patterns and direction of major lineaments in the Bering Strait area (Figure 18). This picture shows not only 'diagonal' lineaments but also meridional structural features, the major of which is the transitional highly seismic zone, Cook Inlet-Prudhoe Bay. We tried to specify these meridional lineaments according to the direction of several rivers on the Beaufort Sea coastal plain (Figure 19). It seems that these lineaments are the continuation and reflection of the same features that were discovered by Eittreim and Grantz (1977) as the "sea valleys" at the upper slope of the Beaufort-Chukchi shelf (Figure 20). In Part II of this work we have described the phenomena of the 'ancient valleys.' Their development is connected with a sharp ocean level drop at the time of Brunhes-Mathuyama paleomagnetic changes. They look usually as the canyons in the sedimentary rocks of the coastal plains and shelves, filled in mostly by silty sand and gravel, frozen in Arctic basin, and could represent a big danger in the case of the disturbance of the thermal regime during any operational activity on the shelf. At the same time these valleys could be traced easily by the different geophysical methods. The meridional lineaments of the Beaufort Sea shelf as the special combination of the tectonic structures with the 'ancient' erosional forms, filled in with Quaternary deposits, or partly reflected in the relief (half buried), or at the sites of crossing with the 'diagonal lineaments' could be responsible for anomalies in the parameters of the bottom deposits and seawater (temperature, salinity, etc.). These sites are convenient for discharge of the deep ground water

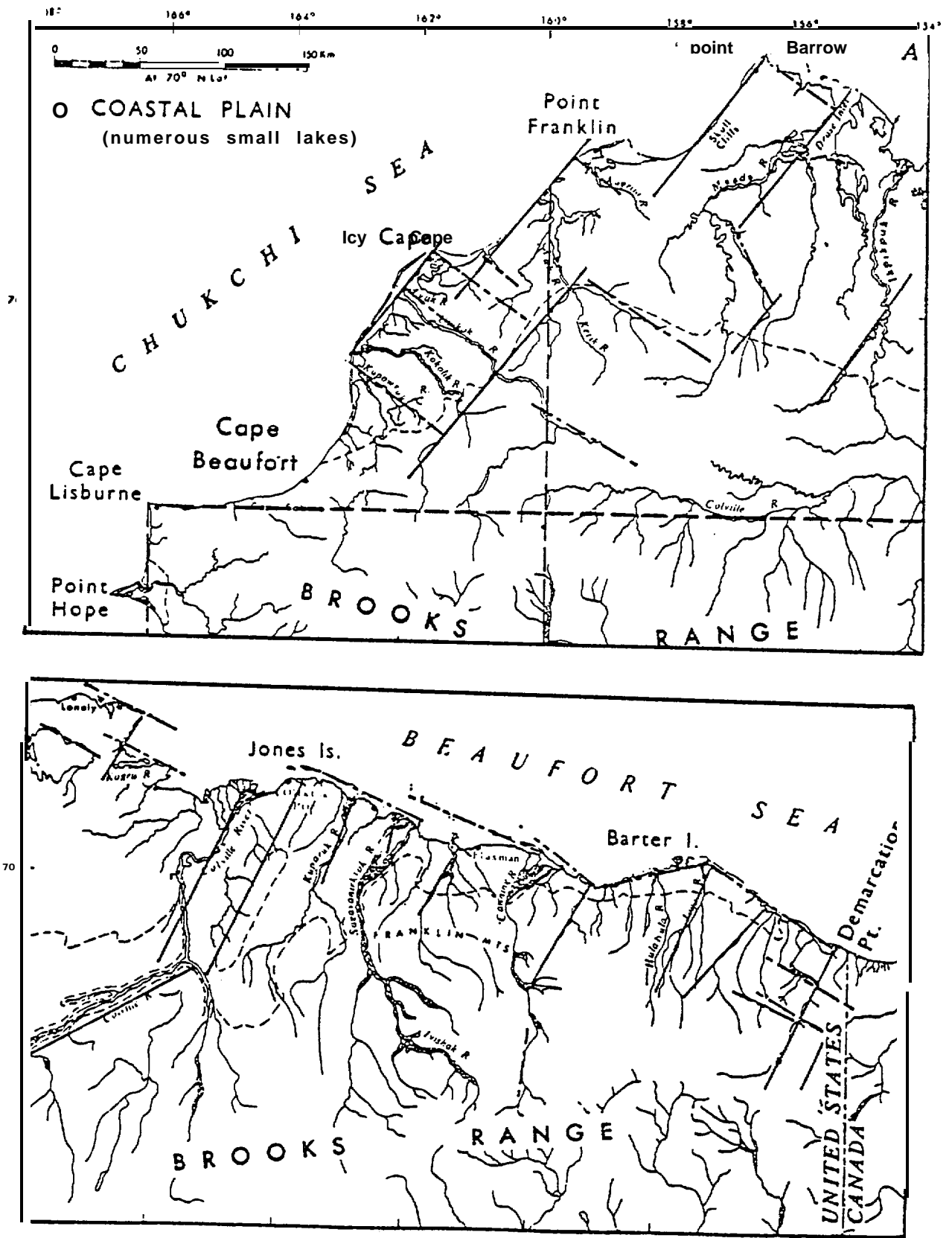


Figure 15.—Location of some of the most prominent lineaments in the Alaskan Arctic. After Short and Wright (1974).

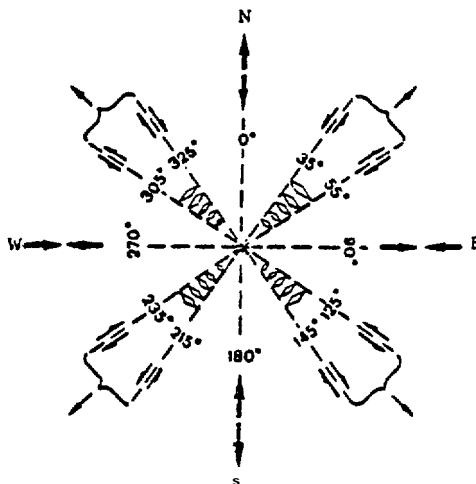


Figure 16.—Scheme of the tangential stress orientation along the major lineament system of the earth. After Voronov et al. (1970).

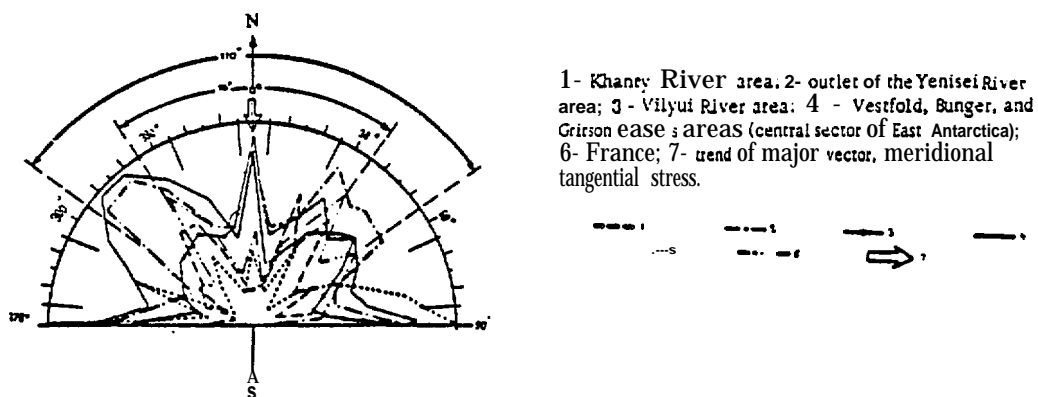


Figure 17.—Rose diagram of lineaments from various areas. After Voronov et al. (1970).

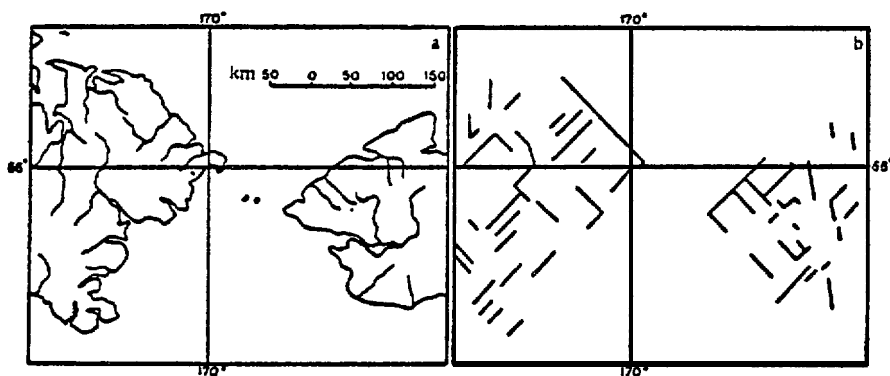


Figure 18.—Direction of drainage patterns (a) and major lineaments (b) in the Bering Strait area. After Voronov et al. (1970).

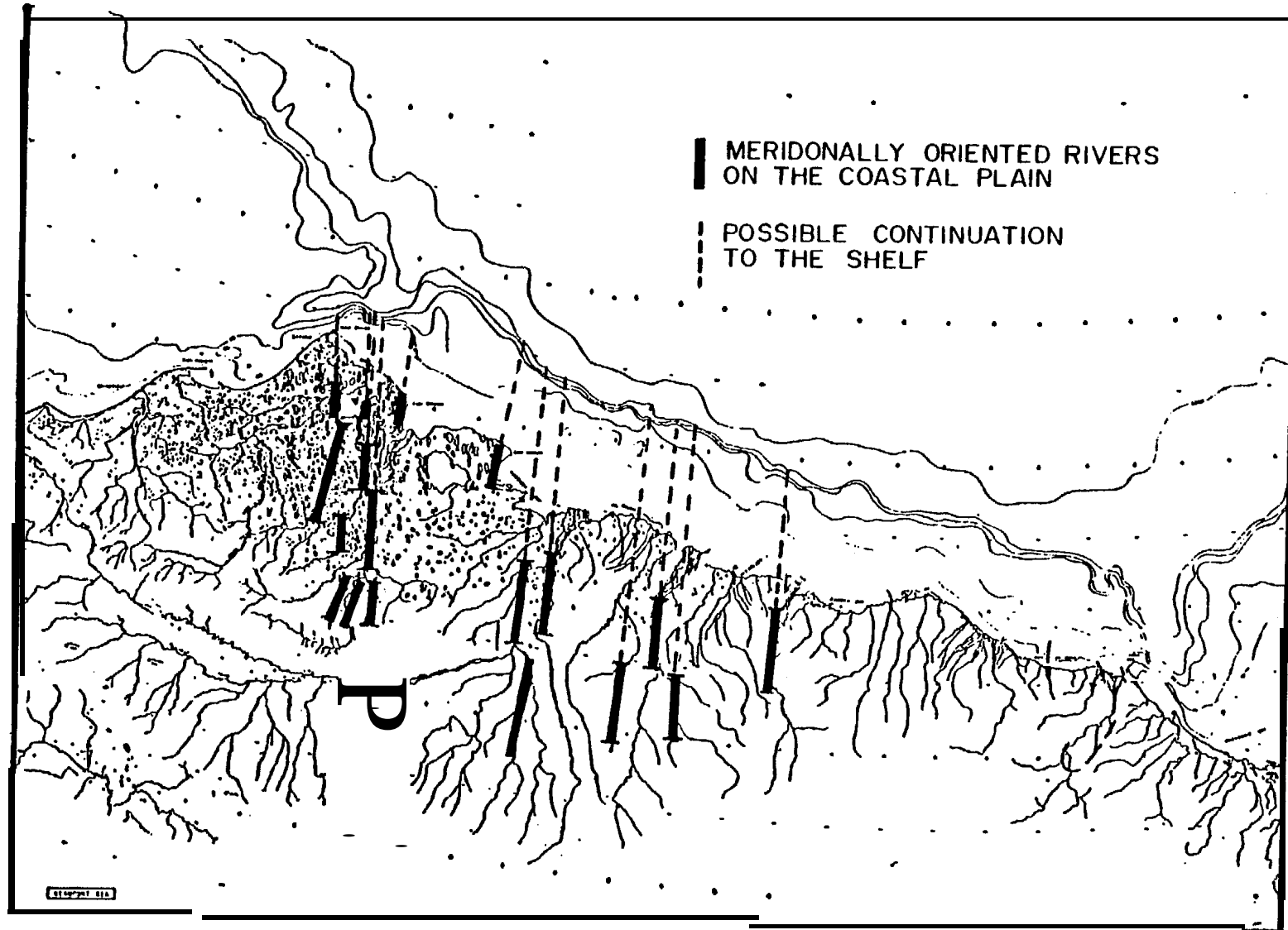


Figure 19.—Major meridional lineaments of the Beaufort Sea coastal plain (rivers) and their possible continuation on the shelf.

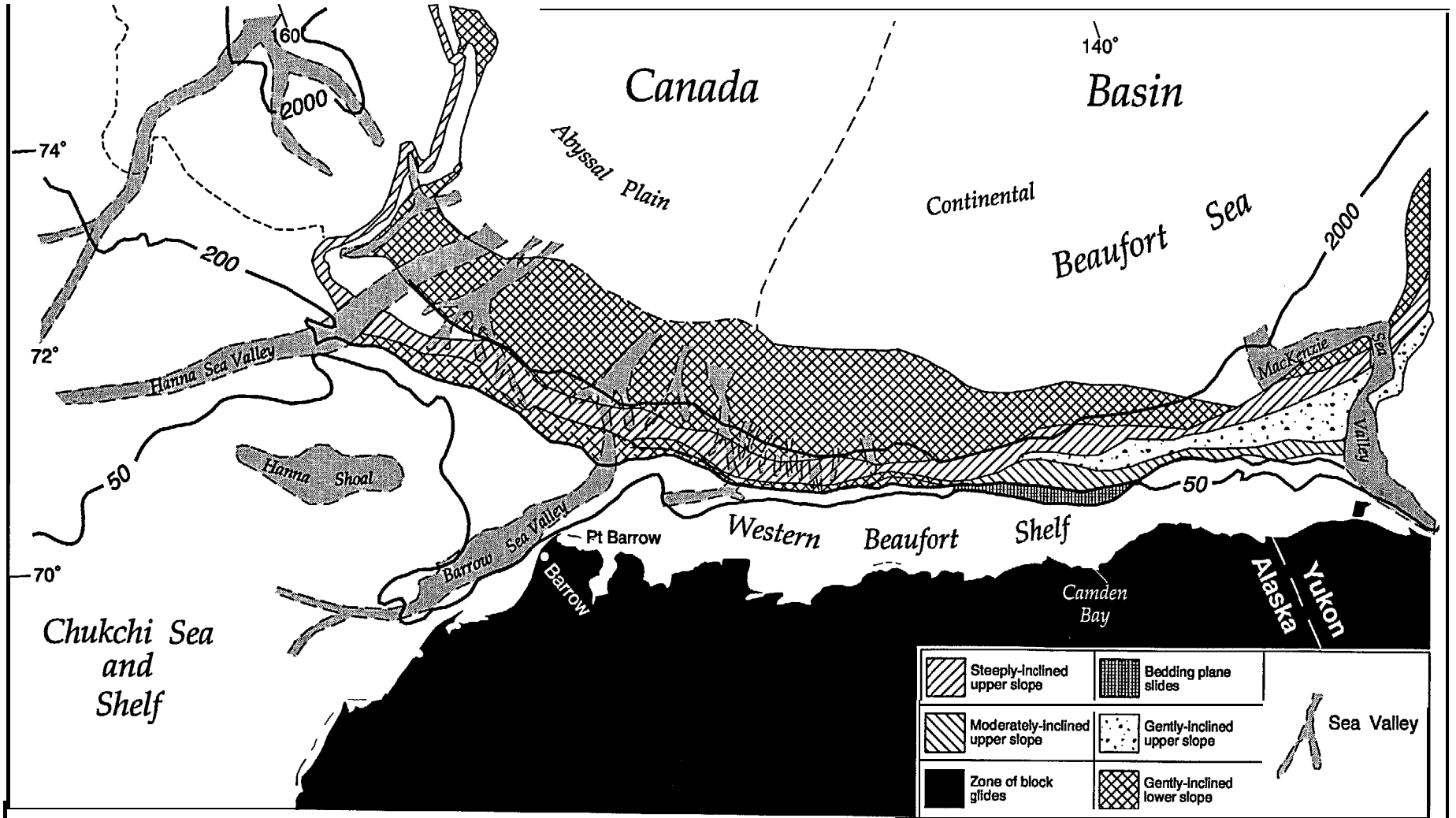
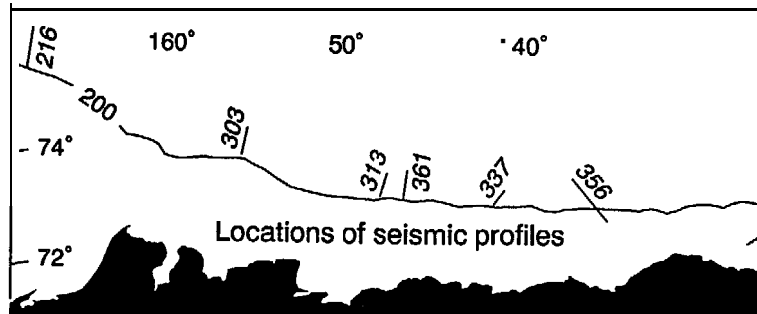


Figure 1. Geological map of the Beaufort Sea and Western Beaufort Shelf.



with different ranges of temperature from warm to the ‘ ‘Crioepgi” type (saline, cold, supercooled water; see Part II).

Possible Thickness of the Relic Submarine Permafrost

On the north coast of Alaska, the geothermal heat flux is equal to 0.050 Kcal/(hr m') (Gold, Lachenbruch 1973). Consideration of modern concepts about geological structure and the developmental history of the western part of the Beaufort Sea shelf shows that the value of the flux of geothermal heat within limits of the shelf is probably similar to the value on the coast; i.e., if is approximately 0.050 Kcal/(hr m²) with possible deviations of at least ±14% (Are 1978). We saw that the development of the western part of the Beaufort shelf in marine conditions took place during the last 10,000 years (in the limits of isobath 60 ± 20 m). This means that thawing of the shelf deposits from below because the thermal heat flux continued here about 10,000 years. Following the simple formula used by Chekovsky (1972) for the calculation of the submarine permafrost thickness in the Kara Sea, we tried to use this approach for the western Beaufort Sea subsea permafrost. The formula:

$$G_t \lambda_t = \frac{Q_p H}{T}, \text{ where}$$

G_t - Geothermal gradient of the thawing zone, in our case 0.030°C/m

λ - Coefficient of the thermoconductivity in the thawing zone, 1.1 (Kcal/M hour°C)

Q_p - Phase change heat, 24,000 (Kcal/M³)

T - Thawing time, 10,000yr

H - The value of thawing zone (from below) thickness (m)

$$\text{The solution is: } H = \frac{G_t \lambda + T}{Q_p}$$

The figures of the thawing zone from below thickness depend on the changes in the value of the geothermal gradient here. They could change in the limits of 130-175 m. Now according to these data, we can decrease the figures of the present coastal permafrost thickness at the northern **Chukchi** and western part of the Beaufort seas that are approximately 400 m (near Barrow), 300 m (near Cape Simpson), 350 m (near Cape Thompson). It means that the average figure of the western Beaufort Sea subsea permafrost would be: 350 m -150 m = 200 m (roughly), but these figures characterize the possible submarine permafrost thickness only with the decrease related to thawing from below. We need **also** to decrease the last figure because of thawing from above. In the works of Osterkamp and Harrison (1976) and Lachenbruch

and Marshall (1977) the several possibilities have been considered. Two of them are the most important: first, when the mean seabed temperature is greater than melting at the top of the permafrost; and second, when the mean seabed temperature is less than melting at the top of the permafrost. Today we cannot answer which part of the Beaufort or Chukchi seas could be related to the first or second cases, or for how long. During sea level changes in Late and Post-glacial times, seawater currents, their direction and thermal regime in the lower layers, as the factors influenced the temperature of the seabed could be changed often and drastically, especially in the sense of Bering and Chukchi water exchange. In our opinion, the parameters of the Bering Strait—its exclusively shallow depth and small width, high recent tectonic activity, and potential to be dammed by ice (Péwé 1976)—today give no clue for reconstructions that could help in calculating the decrease of the subsea permafrost from above.

According to some very approximate data from the different sites of study in the Eurasiatic and American shelves of the Arctic the decrease of the subsea permafrost thickness from above during 10,000 years might reach about 80-100 m. In our also approximate calculations the thickness of the relic permafrost in the western Beaufort Sea consequently could be about 100-120 m and permafrost might be met at the limits of the first 50-100 m from the seabed (in the limit of the water depth— 60 ± 20 m).

At the second, or the central, area of the Beaufort Sea a body of deep permafrost could be only a continuation of a thick (about 600 m) coastal cryogenic zone and limited to 18-22 km offshore. General thickness would be about 150-200 m; seaward this is less, 50-30 m. In the third, or eastern, part of the sea the continuation of coastal permafrost could not be extended farther than 2-5 km offshore. The depth of the permafrost here could be 50-100 m. There is not enough data on coastal permafrost thickness here to give an idea of the thickness of the permafrost offshore. According to comparable data from the Eurasiatic shelf it could be 2-3 times less than coastal permafrost here. Seasonally frozen layers might be met on any part of the Beaufort Sea and Chukchi Sea coasts within the limits of the sea ice-sea bottom interaction (2-m isobath). In the Chukchi Sea the permafrost could exist only extremely close to the coast (usually less than 1.5-2.0 km) and might be connected with the coastal permafrost body or disconnected (lenses). In both cases the thickness of the submarine permafrost could reach nearly 20-30 m.

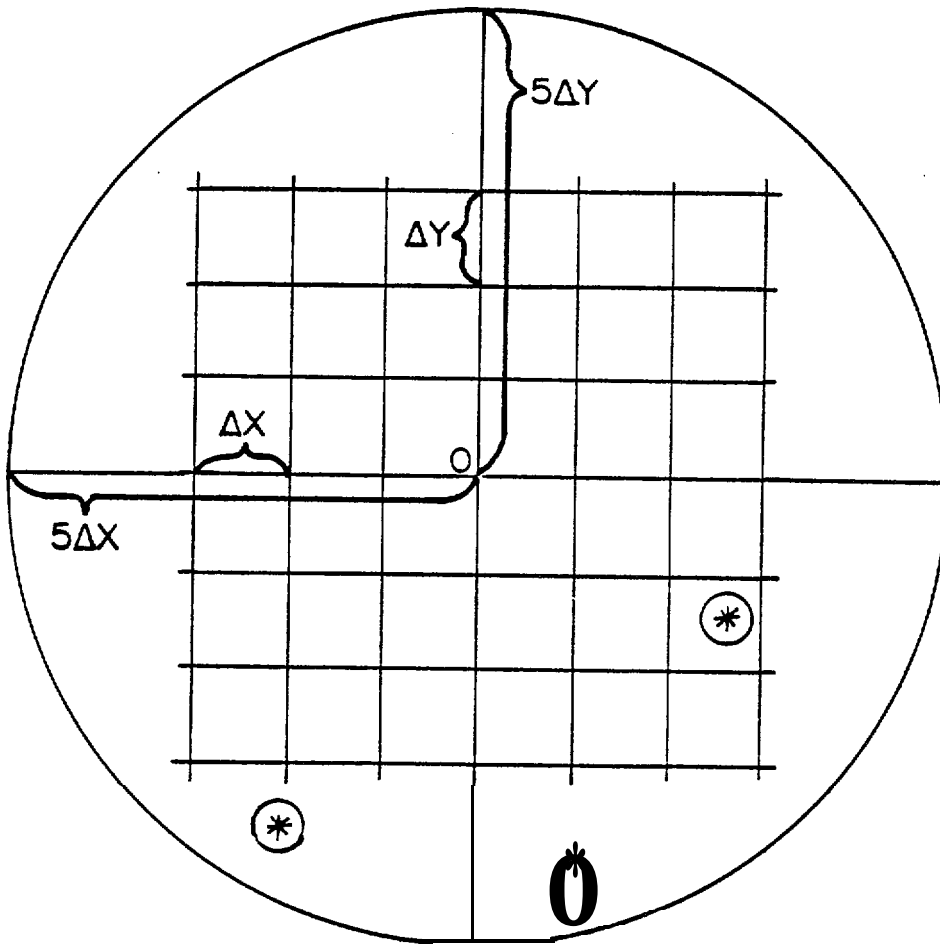
ENVIRONMENTAL DATA ON ALASKAN SUBMARINE PERWROST DISTRIBUTION

The available geologic, oceanographic, topographic and glaciologic materials have been included in our system in an attempt to find the most suitable combination of interdisciplinary data for submarine permafrost prediction. The evaluation of all these data has been done in terms of probability.

Data and Their Reliability; Defining the Gaps

As was mentioned above, the direct data on submarine permafrost (drilling) in the Beaufort and Chukchi seas are restricted to a very few sites and in variable environmental conditions of the shelf they cannot characterize any significant part of it. The seismic methods for defining the upper surface of the subsea permafrost are exclusively prospective, but according to the latest publications, some of the methods do not give the necessary answers. According to Reimnitz et al., "High resolution seismic reflection records in the Arctic today have given no clue on the depth to ice-bonded sediments" and 'careful analysis of the seismic records provides no clues on the distribution of ice-bonded sediments" (Miscellaneous hydrologic and geologic observations in the inner Beaufort Sea shelf, Alaska, 1977, p. G-10). The only geological information available to use for our purposes is the bottom sediment grain size data. The topographical picture of the shelf is sufficient. The bathymetrical data provide knowledge of the bottom depth for any area of the Beaufort and Chukchi seas out to several hundreds of kilometers. The glaciological data, gathered mostly during the OCS program research, also sufficiently describe the processes of the sea ice-seabed interaction close to the coast and the barrier islands. The role of the sea ice as a cooling agent of the sea bottom in the stamukhi zone (Barnes and Reimnitz 1976, 1977) is not clear. Oceanographic data on temperature and salinity of the seawater close to the bottom in the shelf limits had been gathered during different years, different periods of the summer, and at different times of the day. This explains the necessity of designation of statistical reliability on source and derived products. This point was emphasized in the letter of D. A. Wolfe of July 17, 1978. The importance of the documentation of the statistical reliability of the data presented is obvious. Interval contouring of source and derived maps is based on multiple data points non-uniformly distributed over a broad geographic area. Because of this the confidence intervals vary in different parts of the field. The measure of the reliability or confidence level needs to be associated with the probabilities predicted and to be incorporated directly onto the product.

The reliability of contouring is connected with the distance between the grid points, or the size of the grid-cell chosen. The size of the cells is determined by several factors: the overall goals of the study, the character of the data, the size of the study area, the scale of mapping, and of course, the computer efficiency resources. Since the main objective of the study is to specify the lease areas with the different probability of subsea permafrost, special consideration is given to the elementary amount of land required for leasing. A grid-cell size of about 4 square miles, which approximated the size of an individual lease, was finally selected. At latitude 71° north the distance 1.8 miles corresponds to 5' The Beaufort Sea area which is under consideration lies between 1410-1570 west longitude and 69030 '-73030' north latitude. We need enough space in the computer memory for at least two different fields. For example,



- O - Point for which we want to find the reliability
- $5\Delta Y$ - Vertical distance between two nearest grid points
- ΔX - Horizontal distance between two points
- @ - Points of observation

Figure Z1.—Illustration for the reliability of data evaluation.

to compute the supercooling of the seawater close to the bottom, two parameters are used at the same time: seawater temperature and salinity. Coordinates of the shoreline are included in the computation too. The smallest step in longitudinal and latitudinal directions, which still allows only use of the main memory, is the same 4 square miles. This means a total of 9,457 words of computer memory.

Reliability of our maps at grid point is

$$R = 100 (1 - \zeta/\delta) \text{ in percents}$$

where $0 \leq \zeta \leq \delta$ is the distance between grid point and the nearest observational point and $\delta = 5 \max(\Delta x, \Delta y)$. Δx is horizontal distance between 2 adjacent grid points and Δy is vertical distance between grid points. We chose Δx and Δy to equal approximately 2 miles. This was done by the following procedure:

$$\Delta y = a \Delta \varphi, \Delta x = a \Delta \lambda \cos \varphi, \text{ where}$$

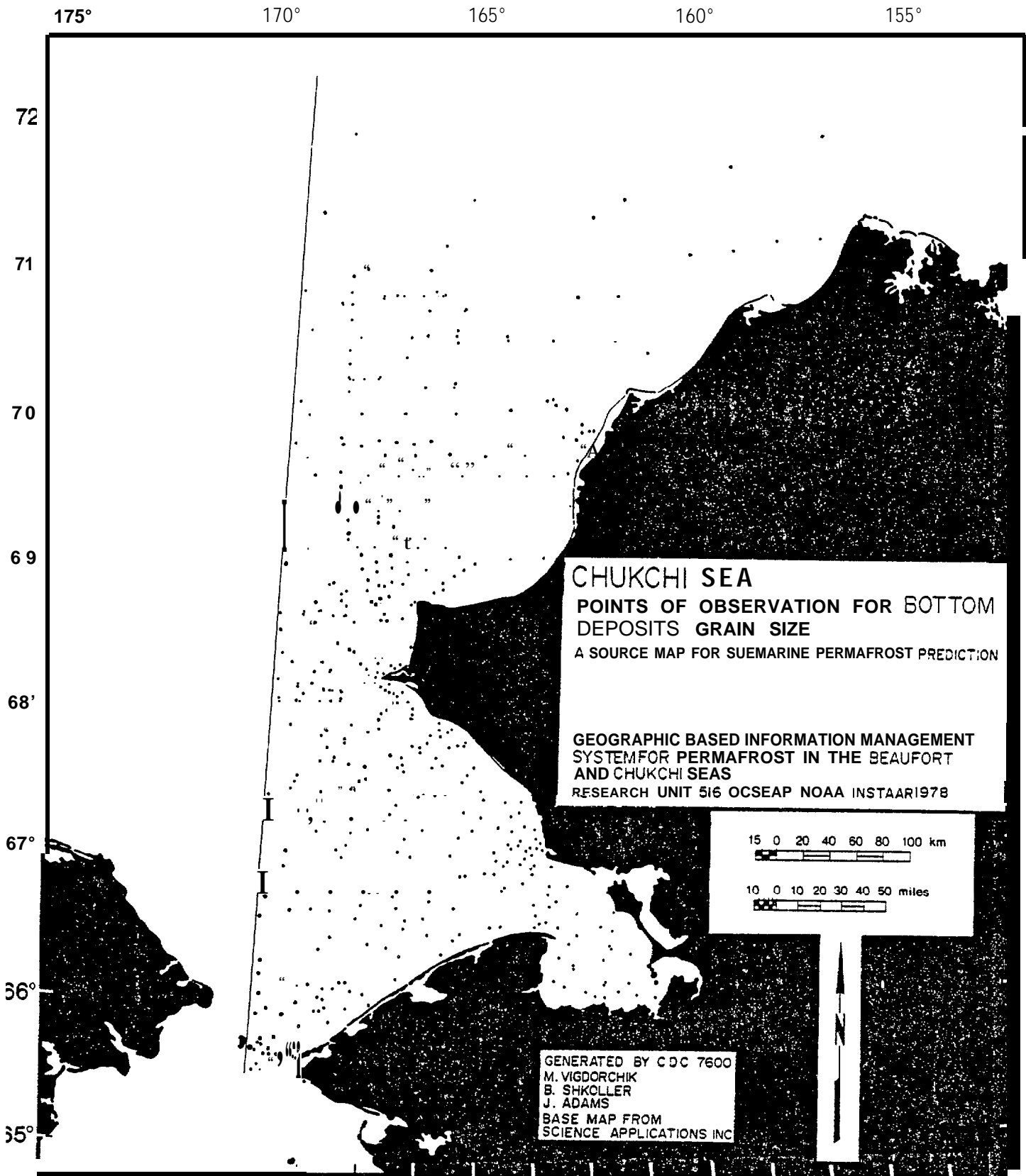
$$a \text{ (radius of earth)} = 6,371 \text{ km}$$

$$\Delta \varphi \text{ (latitudinal distance between 2 grid points)} = (1/35)^\circ$$

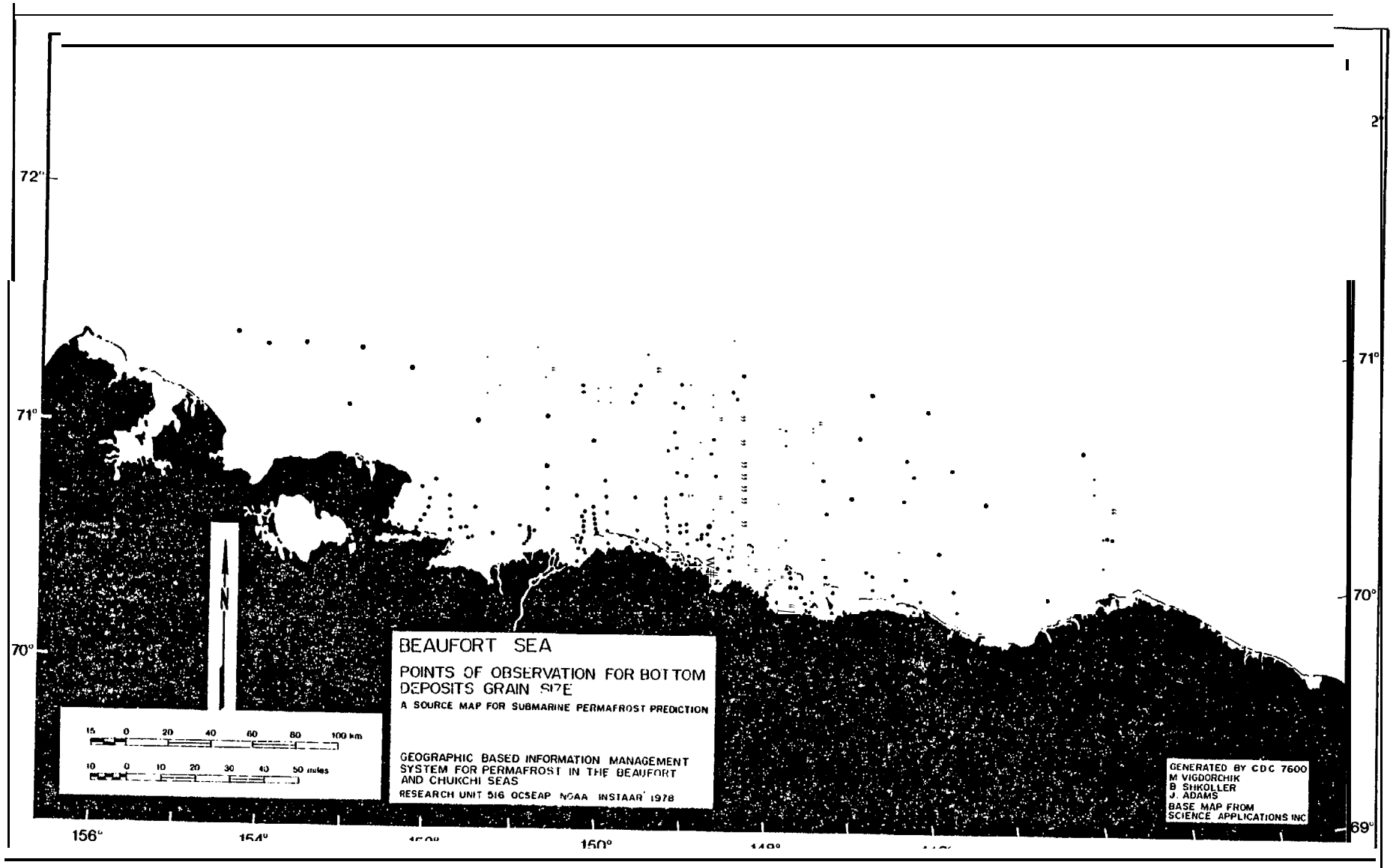
$$\Delta \lambda \text{ (longitudinal distance between 2 grid points)} = 1/120$$

Then $\Delta y = [a \cdot (1/35) \cdot 11/180 \cdot 1/16]$ miles = 1.99 \approx 2 miles, and Δx (at latitude 70°) = $a (1/120) \cdot 11/180 \cdot \cos(700) \cdot 1/16 = 1.98 \approx 2$ miles ($\Delta x = 1.92$ at latitude 71°).

We distinguish two levels of data reliability, one for each parameter separately, another to characterize the relative density of all data used in the different parts of the area. Maps of the "Points of observation for bottom deposits grain size" in the Chukchi (Map 1) and Beaufort (Map 2) seas and maps of "reliability for the grain size data for these seas (Map 3 and 4) clearly show that the data distribution is irregular and sparse; some of the areas have no observations at all. This means that any statistical probability of the submarine permafrost prediction needs to be reduced according to the relative density of the basic data. It means also that to make contours with the computer process we have to use interpolation. The areas with a high reliability for grain size data concentration are situated in the southern and central parts of the Chukchi Sea and along the coast of the Beaufort Sea (700-710 N, 144°-155° W). There are gaps in the observations to the north from 71° N in both seas and to the east from 145° W. Some of the areas with reliability of data less than 20% are situated along the Chukchi Sea coast between Cape Lisburne and Point Barrow and in the Beaufort Sea between this point and Smith Bay. The level of reliability for temperature and salinity according to the density of the observation network (Maps 5 and 6) is also variable but mostly higher than 60%, both in the Chukchi Sea and in the Beaufort Sea in the area close to Point Barrow and between Harrison Bay-Camden Bay at the south, and '71°-71030' at the north (Maps 7 and 8). "The space distribution" aspect of the data reliability for sea temperature and salinity is not the



Map 1.—Points of observation for bottom deposit grain size, Chukchi Sea.



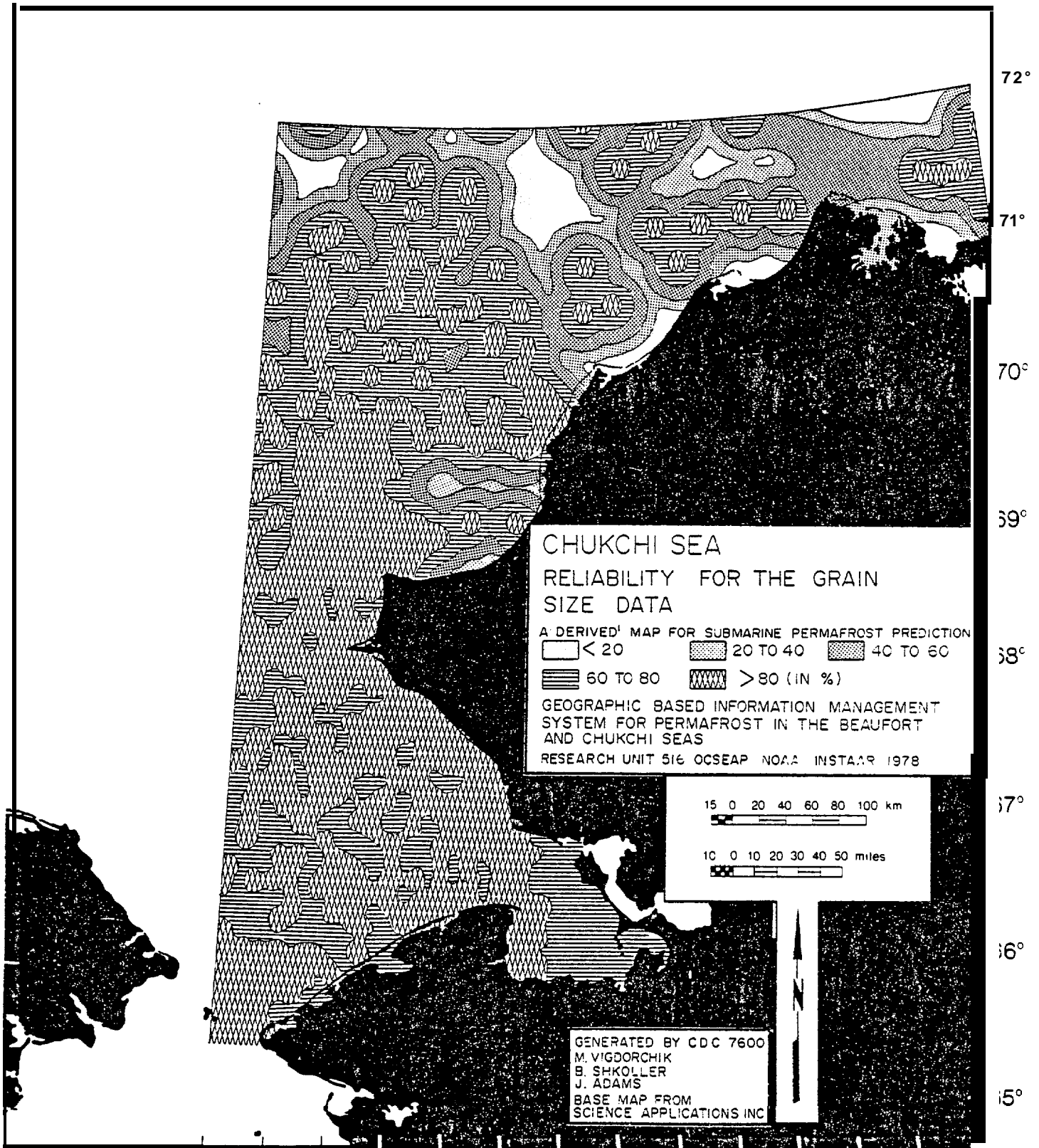
175°

170°

165°

160°

155°



72°

71°

70°

69°

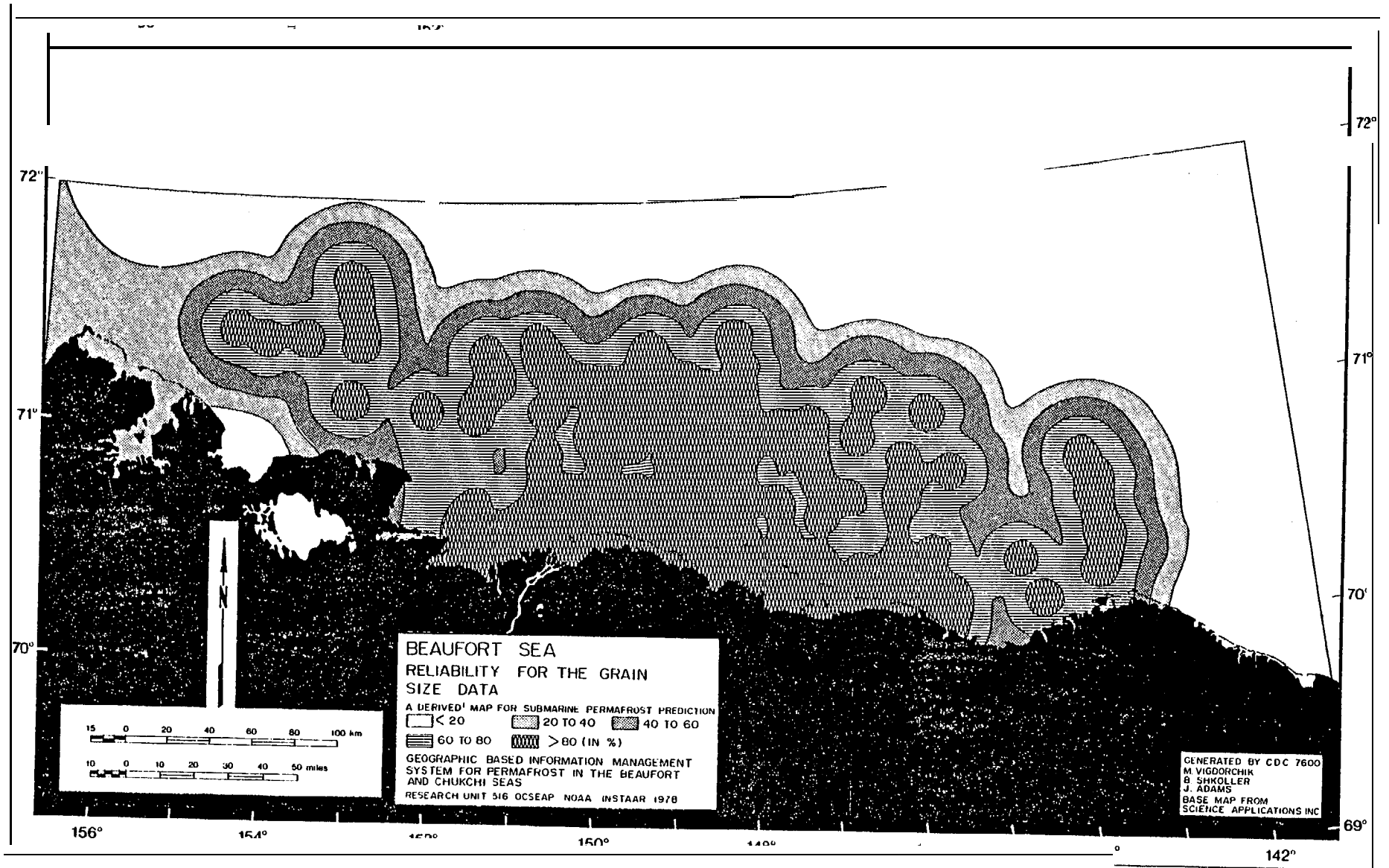
68°

67°

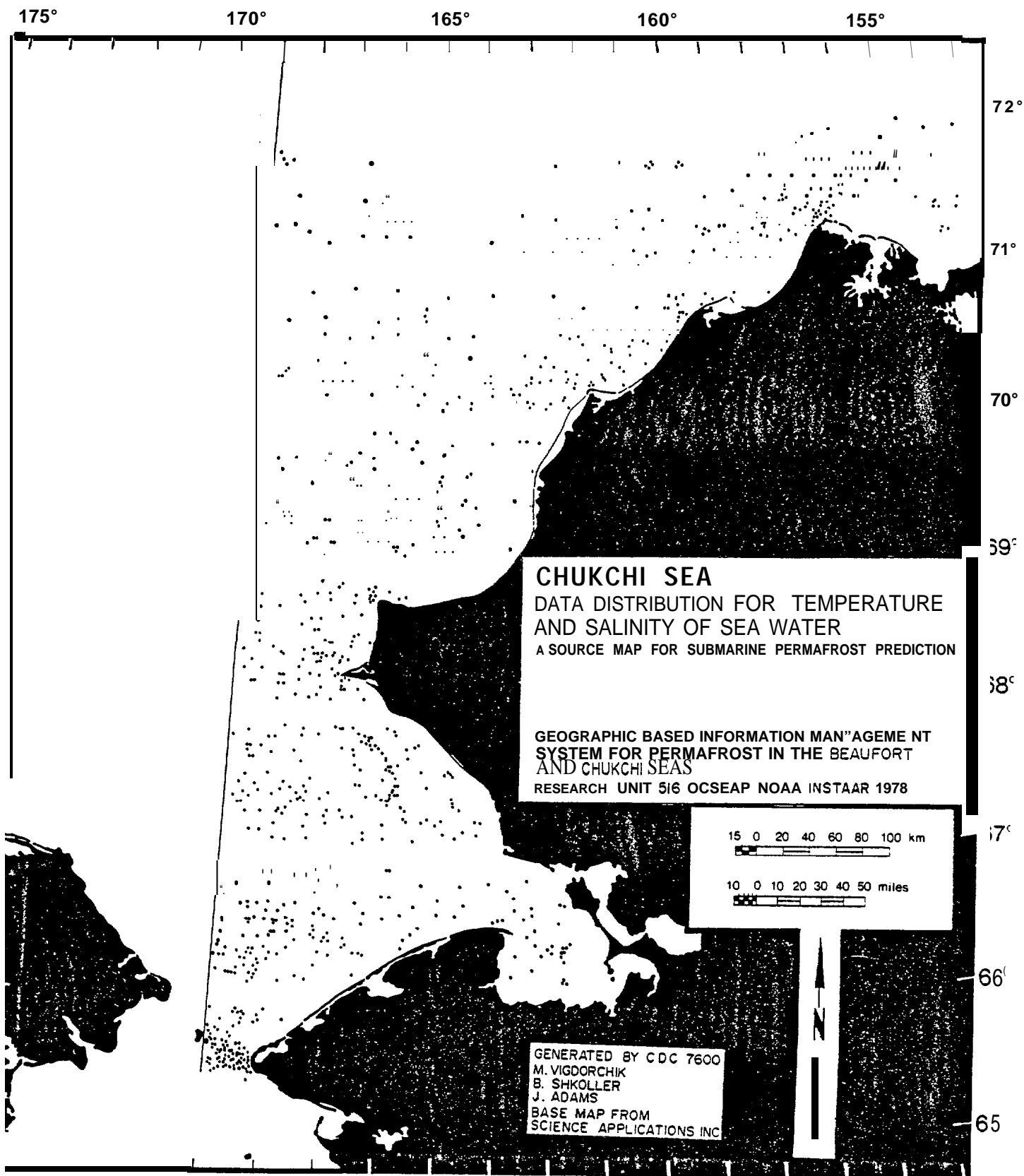
66°

65°

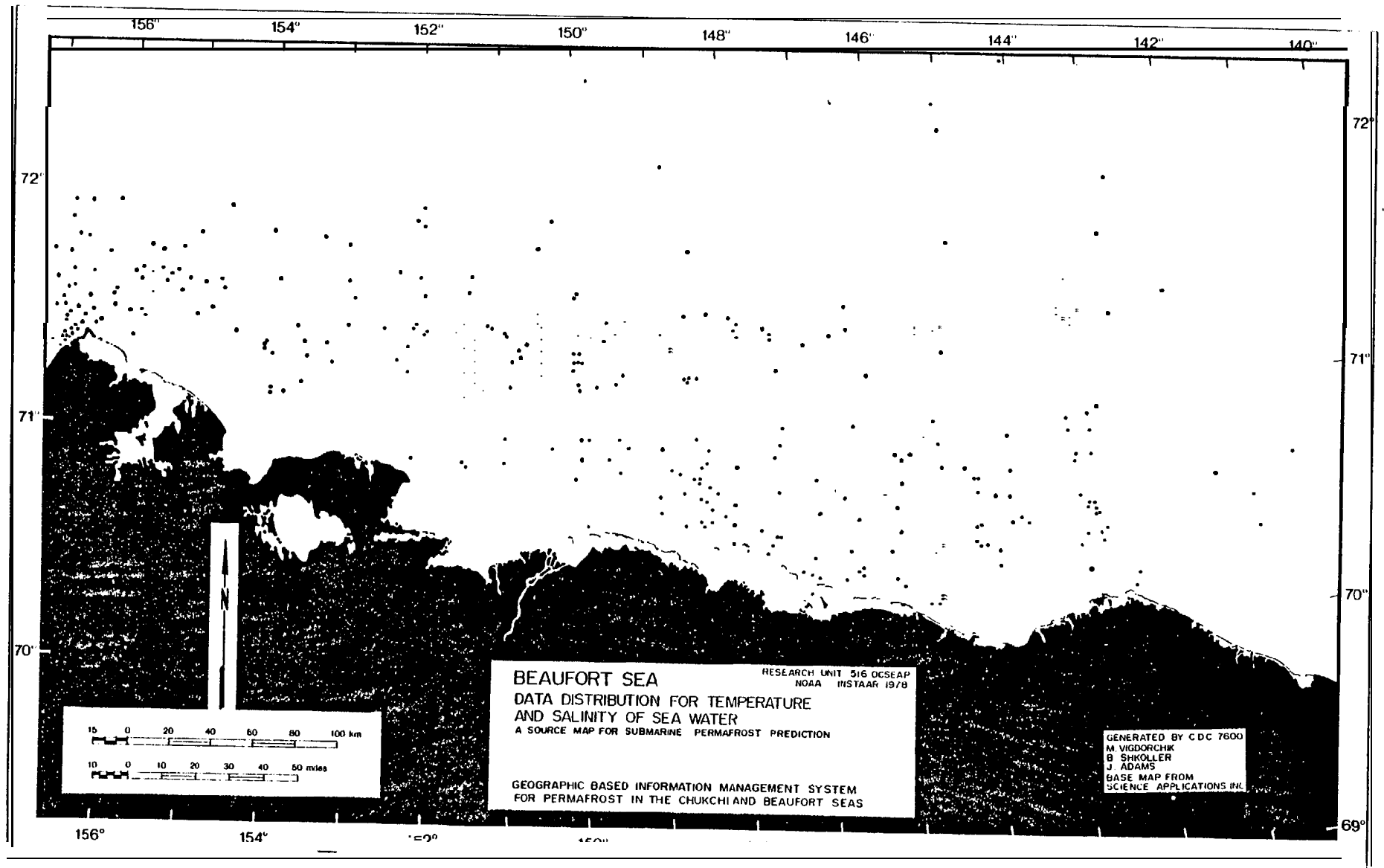
Map 3.—Reliability of the grain size data, Chukchi Sea.



Map 4.—Reliability of the grain size data, Beaufort

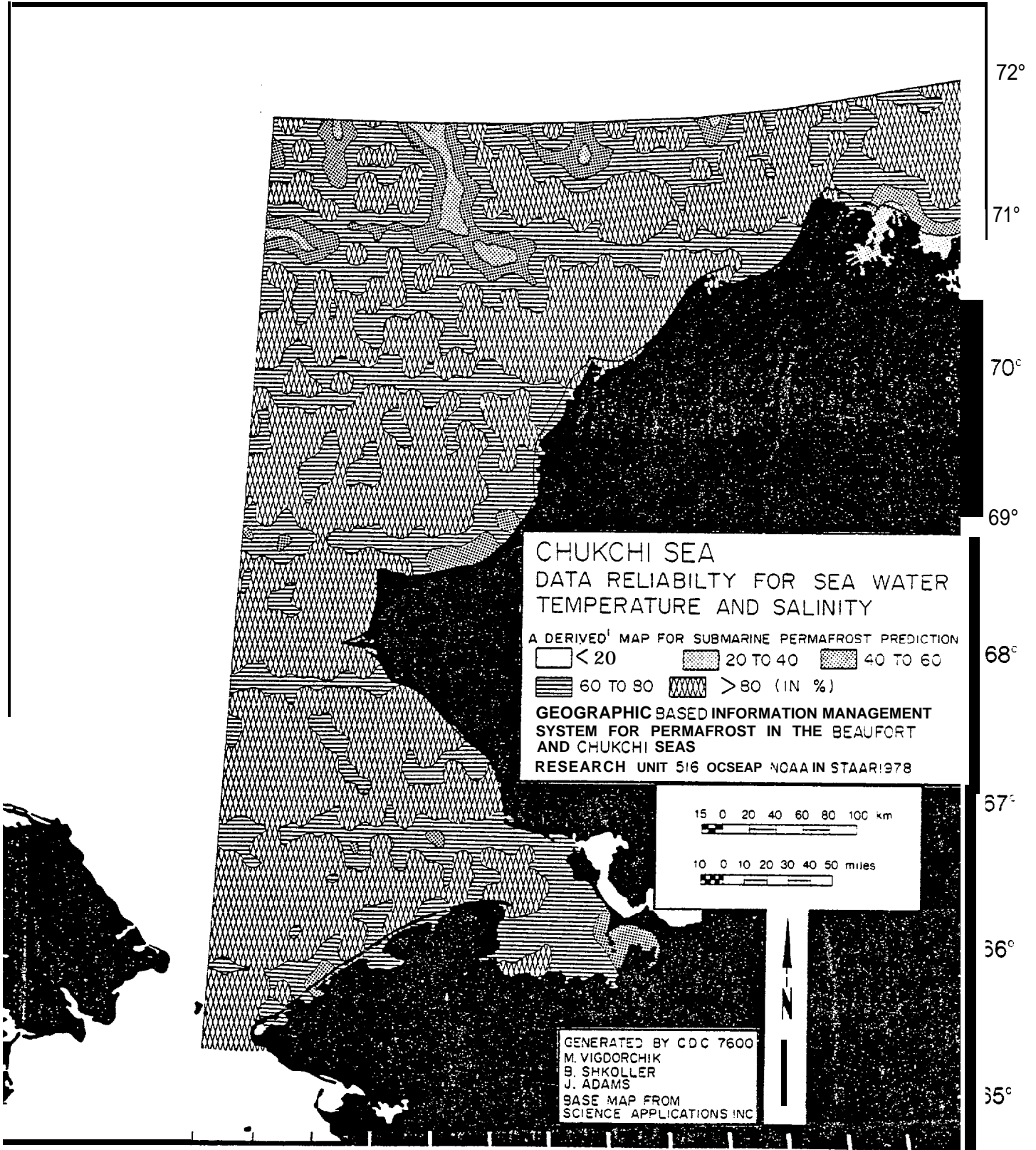


Map 5.—Data distribution for temperature and salinity of seawater at the maximal sampling depth, Chukchi Sea.

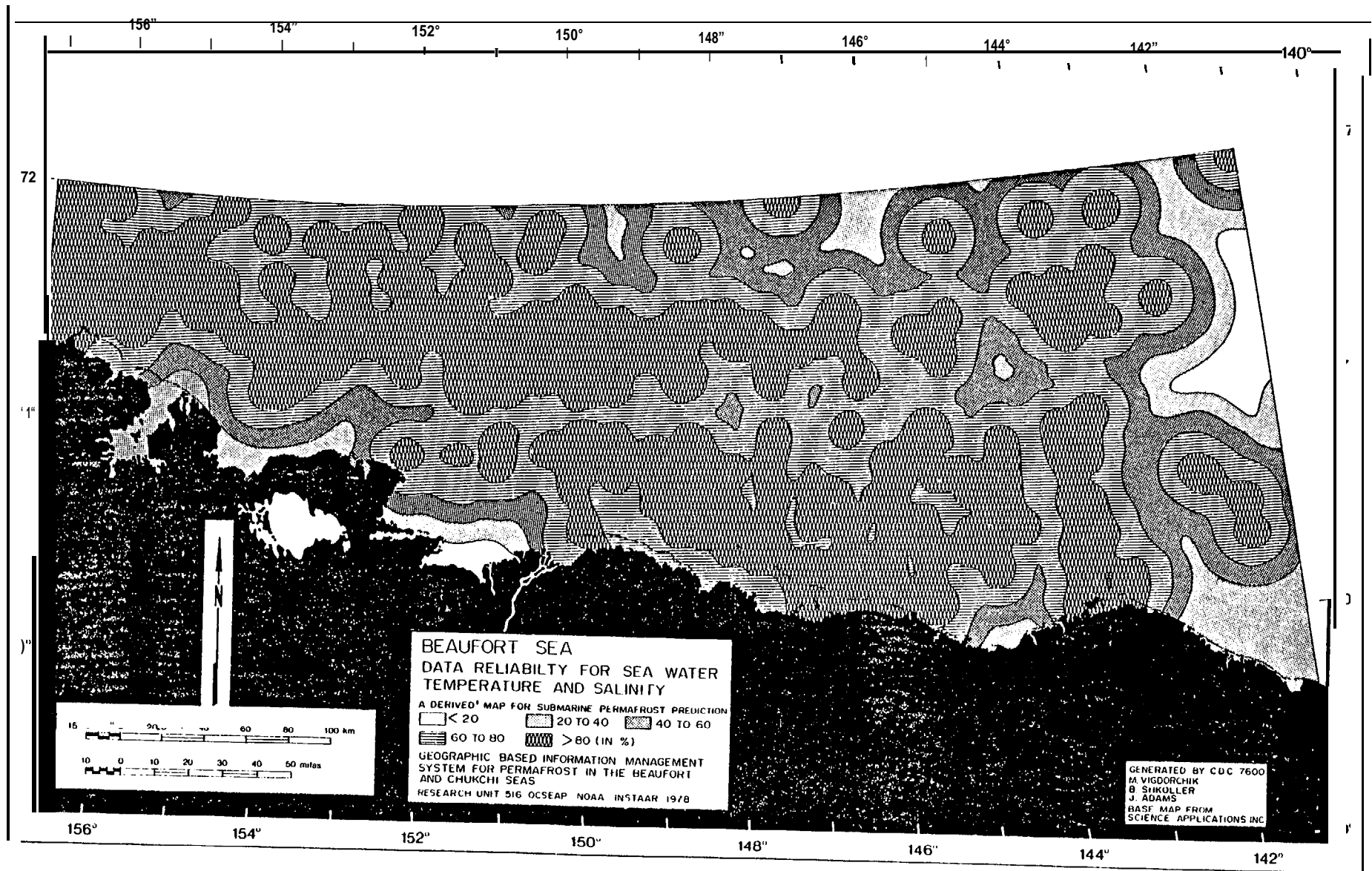


Map 6.—Data distribution for temperature and salinity of seawater at the maximal sampling depth, Beaufort Sea.

175° 170° 165° 160° 155°



Map '7.-Data reliability for temperature and salinity of seawater at the maximal sampling depth, Chukchi Sea.



Map 8.—Data reliability for temperature and salinity of seawater at the maximal sampling depth, Beaufort Sea,

only one. The capability of the seawater to change these parameters yearly, monthly (Tables 4 and 5), and daily is shown very well by Barnes and Reimnitz (1977) for the surface layers at the Colville River delta–Oliktok Point part of the Beaufort sea and it poses another problem. Winter freezing coupled with the exclusion of solutes also affects the salinity and temperature regime of the seawater. But the bottom layers of the seawater, which area our concern, seem to be more stable, and we tried to choose the intervals of contouring according to possible limits of such temperature and salinity changes. Because the seawater sampling depth in the

Table 4.—Distribution of observations by month, Beaufort Sea.

Month	Number	Sampling Depth	Bottom	Temperature	Salinity
1	2	2 "	1	2	2
2	1	1	1	1	1
3	1	1	1	1	1
4					
5	3	3		3	2
6					
7	28	28	18	18	17
8	358	358	351	355	352
9	85	85	81	83	84
10	13	13	13	8	12
11	1	1	1	1	1
12	2	2	2	2	2
Total	491	491	469	472	472

Table 5.—Distribution of observations by month, Chukchi Sea.

Month	Number	Sampling Depth	Bottom	Temperature	Salinity
1	2	2	1	1	2
2	1	1	1	1	1
3	1	1	1	1	1
4	12	12	12	12	12
5	41	41	3	3	14
6	28	28	28	28	26
7	215	215	171	215	206
8	1,957	1,957	1,913	1,957	1,947
9	1,230	1,213	1,196	1,228	1,227
10	213	213	213	209	208
11	26	26	26	18	22
12	2	2	2	2	2
Total	3,718	3,709	3,764	3,764	3,668

Beaufort and Chukchi seas is not always close to the bottom, we need to consider also the relative distance between the deepest interval of sampling and the bottom. The increase of the sampling depth proximity to the bottom (Maps 9 and 10) gives more reliable data on these parameters close to the seabed. The maps of the general reliability (Maps 11 and 12) summarize the picture of the used data reliability (grain size, seawater temperature and salinity) for given areas of the Beaufort and Chukchi seas.

Interpolation Scheme

A 2-dimensional second order polynomial interpolation seems to give the best results. The numerical scheme follows. If we wish to calculate the value of some physical or geological feature at Point M (X_0, Y_0), we first limit our considerations to the domain p' (X_i, Y_i), which satisfies the condition:

$$\sqrt{(X_0 - X_i)^2 + (Y_0 - Y_i)^2} \leq R$$

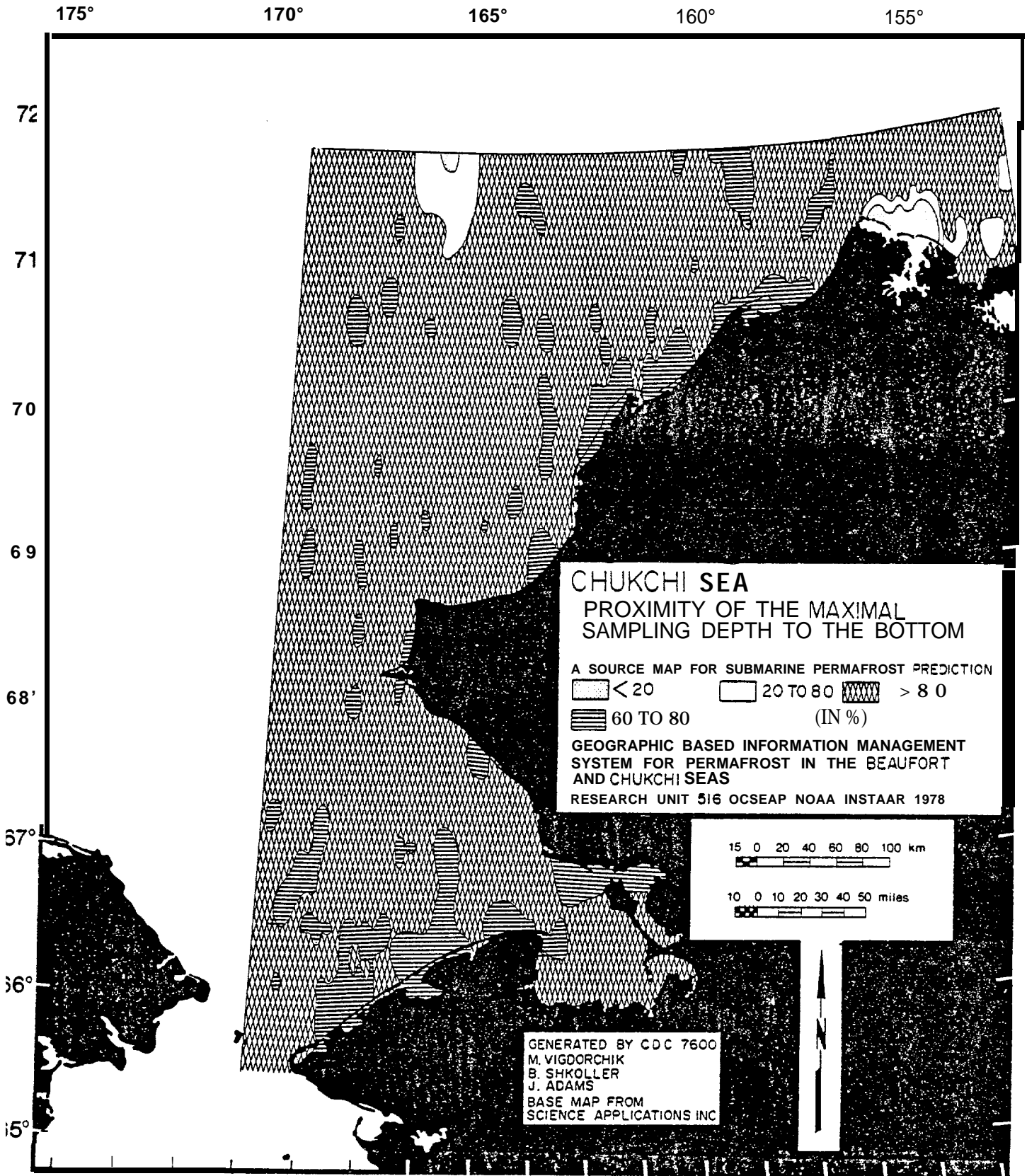
In other words, the point M is inside the circle of the radius R. Each point (X_i, Y_i) has a special weight P_i , which increases when (X_i, Y_i) is near (X_0, Y_0) and decreases elsewhere. At the point M (X_0, Y_0), the value is equal to 1. We take point M as an origin or coordinates. The value of the function in each point inside our domain can be approximated by a first or second degree polynomial.

$$Q_2(X, Y) = C_0 + C_1X + C_2Y + C_3X^2 + C_4XY + C_5Y^2$$

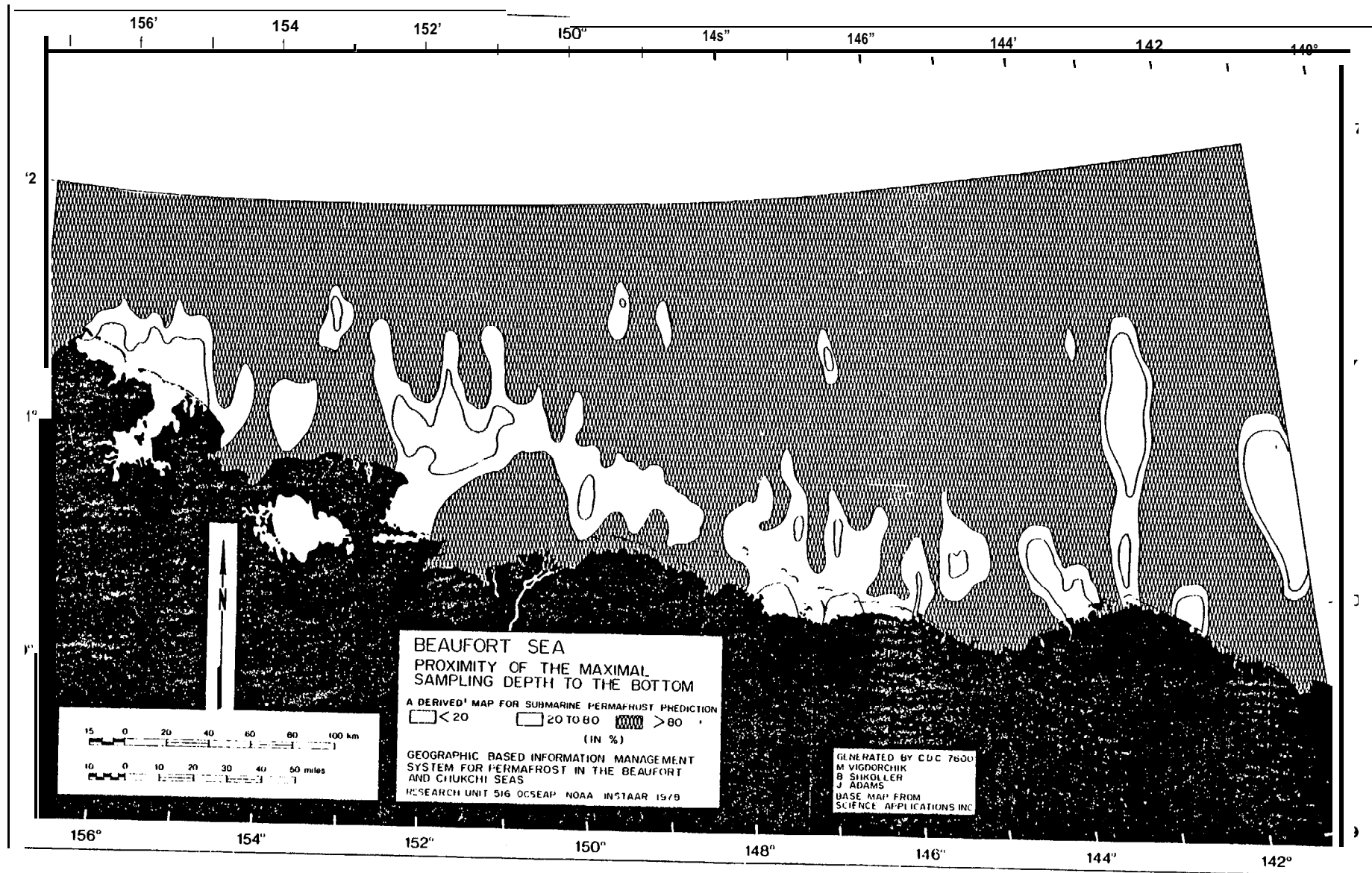
We will now show how to calculate the unknown coefficients $C_0, C_1, C_2, C_3, C_4, C_5$ in the case of the second order polynomial. This is done by using the least squares numerical method. We find such coefficients that will give the minimum to the sum

$$S = \sum_{i=1}^N P_i (C_0 + C_1X_i + C_2Y_i + C_3X_i^2 + C_4X_iY_i + C_5Y_i^2 - Q_i)^2$$

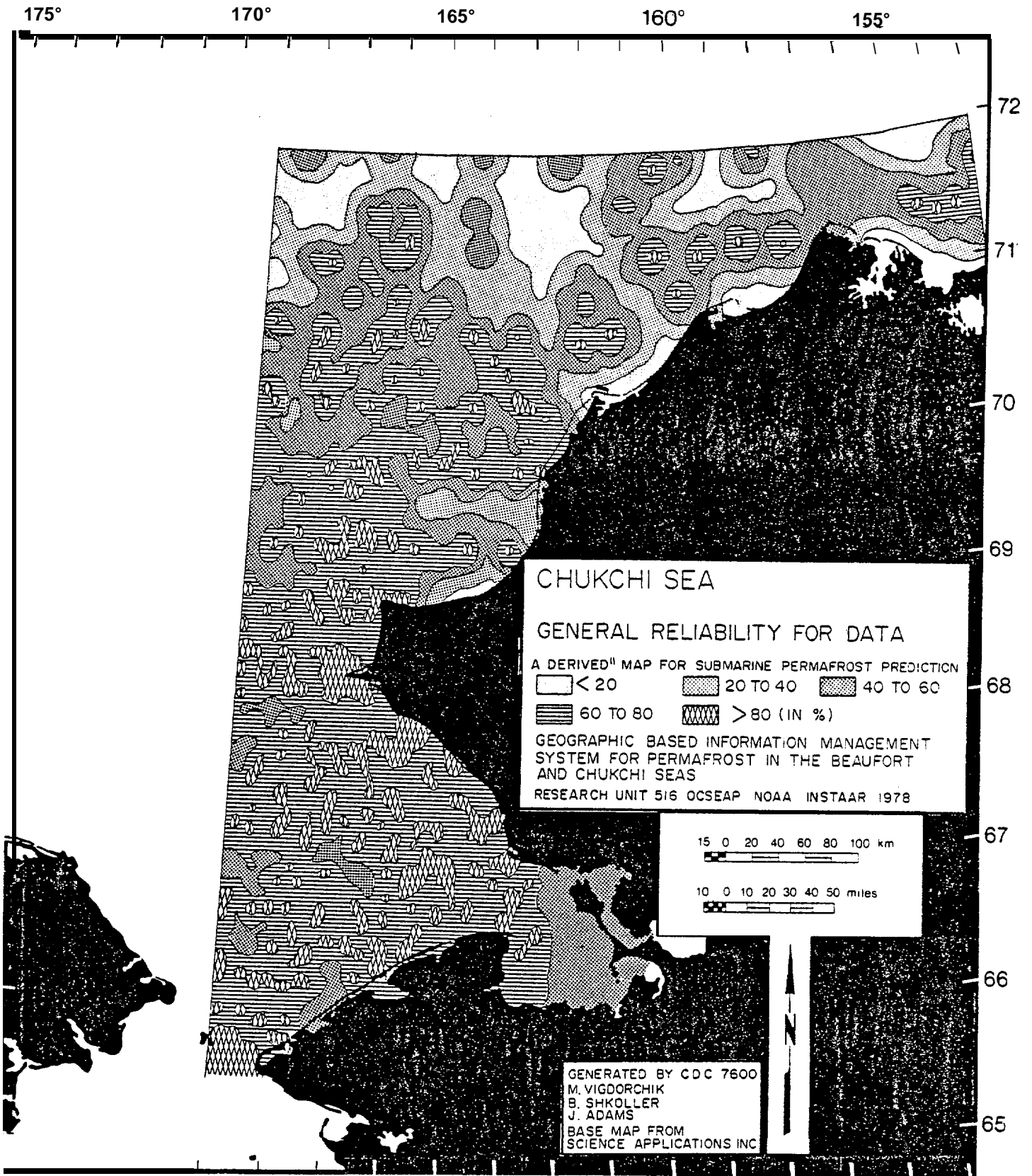
where N is number of observations inside the circle of radius R; X_i, Y_i are coordinates of the given observations inside the circle; and Q_i are the values of the function (salinity, temperature, depth) at these points. In order to obtain a minimum of S we must take the derivatives of this expression with regard to $C_0, C_1, C_2, C_3, C_4, C_5$ and obtain six linear equations, which are called normal equations:



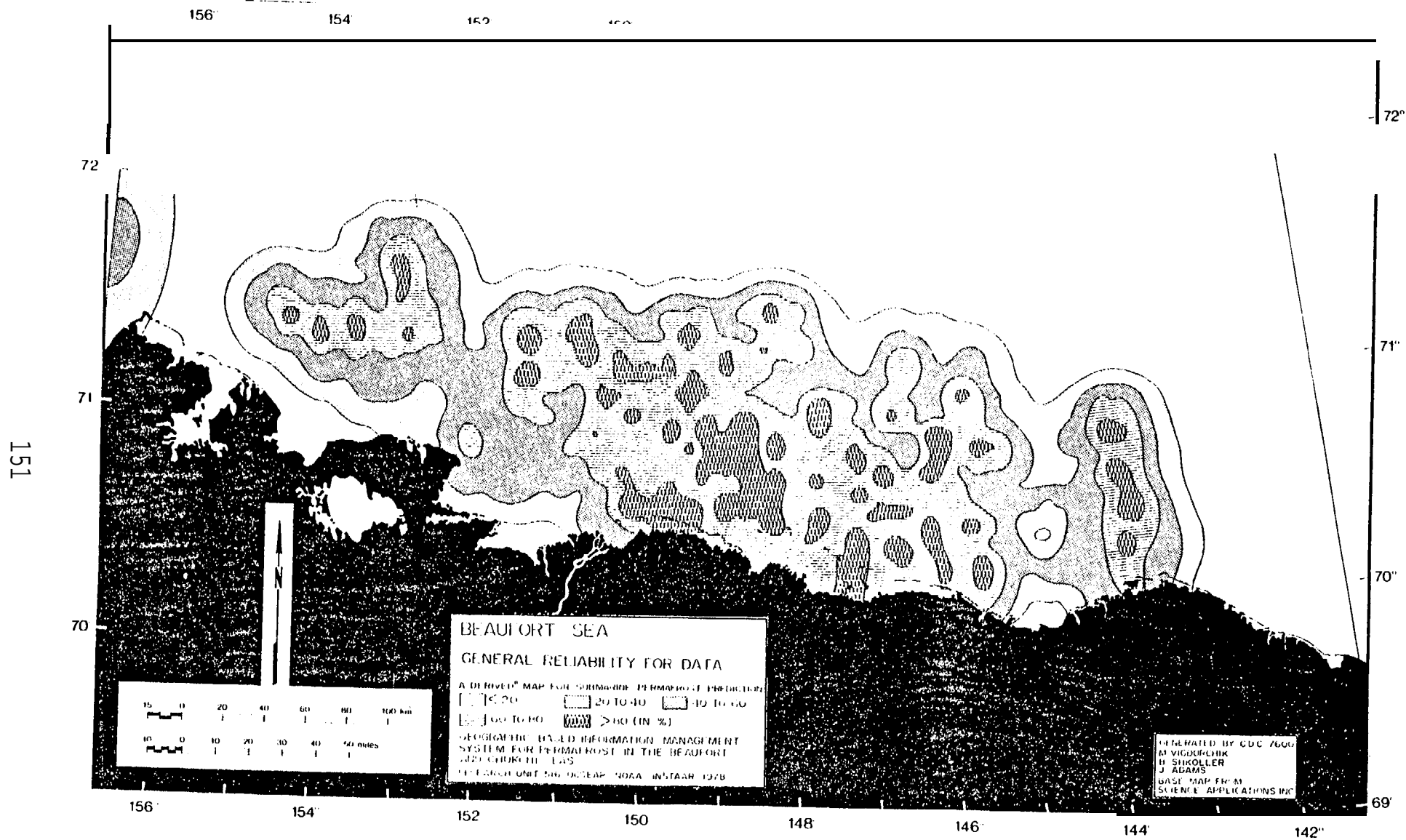
Map 9.—Proximity of the maximal sampling depth to the bottom, Chukchi Sea.



Map 10.—Proximity of the maximal sampling depth to the bottom, Beaufort Sea.



Map II.-General reliability of the data, Chukchi Sea.



Map 12. reliability of the data, Beaufort

$$\bar{X}_i = X_i - X_0 ; \quad \bar{Y}_i = Y_i - Y_0$$

$$C_0 \sum \tilde{P}_i + C_1 \sum \tilde{P}_i \bar{X}_i + C_2 \sum \tilde{P}_i \bar{Y}_i + C_3 \sum \tilde{P}_i \bar{X}_i^2 + C_4 \sum \tilde{P}_i \bar{X}_i \bar{Y}_i + C_5 \sum \tilde{P}_i \bar{Y}_i^2 = \sum \tilde{P}_i Q_i$$

$$C_0 \sum \tilde{P}_i \bar{X}_i + C_1 \sum \tilde{P}_i \bar{X}_i^2 + C_2 \sum \tilde{P}_i \bar{X}_i \bar{Y}_i + C_3 \sum \tilde{P}_i \bar{X}_i^3 + C_4 \sum \tilde{P}_i \bar{X}_i^2 \bar{Y}_i + C_5 \sum \tilde{P}_i \bar{X}_i \bar{Y}_i^2 = \sum \tilde{P}_i \bar{X}_i Q_i$$

$$C_0 \sum \tilde{P}_i \bar{Y}_i + C_1 \sum \tilde{P}_i \bar{X}_i \bar{Y}_i + C_2 \sum \tilde{P}_i \bar{Y}_i^2 + C_3 \sum \tilde{P}_i \bar{X}_i^2 \bar{Y}_i + C_4 \sum \tilde{P}_i \bar{X}_i \bar{Y}_i^2 + C_5 \sum \tilde{P}_i \bar{Y}_i^3 = \sum \tilde{P}_i \bar{Y}_i Q_i$$

$$C_0 \sum \tilde{P}_i \bar{X}_i^2 + C_1 \sum \tilde{P}_i \bar{X}_i^3 + C_2 \sum \tilde{P}_i \bar{X}_i^2 \bar{Y}_i + C_3 \sum \tilde{P}_i \bar{X}_i^4 + C_4 \sum \tilde{P}_i \bar{X}_i^3 \bar{Y}_i + C_5 \sum \tilde{P}_i \bar{X}_i^2 \bar{Y}_i^2 = \sum \tilde{P}_i \bar{X}_i^2 Q_i$$

$$C_0 \sum \tilde{P}_i \bar{X}_i \bar{Y}_i + C_1 \sum \tilde{P}_i \bar{X}_i^2 \bar{Y}_i + C_2 \sum \tilde{P}_i \bar{X}_i \bar{Y}_i^2 + C_3 \sum \tilde{P}_i \bar{X}_i^3 \bar{Y}_i + C_4 \sum \tilde{P}_i \bar{X}_i^2 \bar{Y}_i^2 + C_5 \sum \tilde{P}_i \bar{X}_i \bar{Y}_i^3 = \sum \tilde{P}_i \bar{X}_i \bar{Y}_i Q_i$$

$$C_0 \sum \tilde{P}_i \bar{Y}_i^2 + C_1 \sum \tilde{P}_i \bar{X}_i \bar{Y}_i^2 + C_2 \sum \tilde{P}_i \bar{Y}_i^3 + C_3 \sum \tilde{P}_i \bar{X}_i^2 \bar{Y}_i^2 + C_4 \sum \tilde{P}_i \bar{X}_i \bar{Y}_i^3 + C_5 \sum \tilde{P}_i \bar{Y}_i^4 = \sum \tilde{P}_i \bar{Y}_i^2 Q_i$$

Remembering that $M(X_0, Y_0)$ is the origin of the coordinates $\bar{X}_i = 0, \bar{Y}_i = 0$, we have only to find C_0 ; then $Q(m) = C_0$. When calculating the value of the needed function at point M , we have only to move to the next point and repeat the above calculations. The value of Piisa function of the distance

$$\zeta_i = \sqrt{(X_i - X_0)^2 + (Y_i - Y_0)^2}$$

and must equal zero when $di=R$. In our calculations we have chosen the expression

$$P_i = ((R^2 - \zeta_i^2)/\zeta_i^2)^2$$

The radius R was chosen as $R = 2.5\Delta X$; however, it is important to be sure that at least six observations are inside the circle when using a second order interpolation. Generally all calculations were made with second order polynomials. As a test, we also used the first order, and usually the results were almost the same. However, the second order as a rule gives the smoother contours.

Data Structuring

Data Structure Diagram (Figure 22) represents and organizes data requirements, the stages of mapping, and the production of information resulting from the study. This diagram differs from the Data Structure Diagram of the first reports in that some changes were made after studying the available source data in this area, including such parameters as: sea bottom temperatures and salinities, grain size of the Holocene sediments, and bathymetry.

This Data Structure Diagram illustrates the relationships among the data information used in the study, and it can be viewed as describing the flow of mappable information. The layout and content of the diagram are developed in response to the relevant issues. The diagram is organized both horizontally and vertically, with the vertical organization arranged by the type of map analysis. The source *data* column contains 'nonvalue-oriented' data from maps. The next few columns, *derived data* maps, contain the results of the two or three stages of the usage of the data management. Then, the composite map displays information developed from source data and derived maps. This map is defined by interdisciplinary knowledge and the relationships between source data topics. All these maps serve as a basis for further subjective analysis.

We have used computer methods as the mechanisms for identifying and organizing the multiplicity of the values of the data into a form useful in the composite analysis stages. Composite mapping records and illustrates our opinion about the major problem—the tracing of areas with potential for the existence of permafrost in the Beaufort and Chukchi seas offshore.

Four basic techniques are used for interpreting and analyzing the data: (1) the Translation technique for converting a single source data map into a secondary data map; (2) the Comparison technique for comparing two or more maps in order to produce a third derived map showing the results of the comparison; (3) the Overlay technique for combining two or more maps in order to produce a composite map showing the results of the overlay process; and (4) the Distance technique which is used for calculating the distance of all geographical areas from a given point, line, or area.

We have six blocks in our system: seawater, bathymetry, geology, sea ice, direct data on permafrost, and reliability of data. Three generations of derived maps and one of composite map have been produced.

COMPUTERIZED MAPPING

The computerized mapping involves the following phases:

- 1.) a) Data digitation and preparation for computer use.
 - b) Preparation of *source* maps (one map—one characteristic).

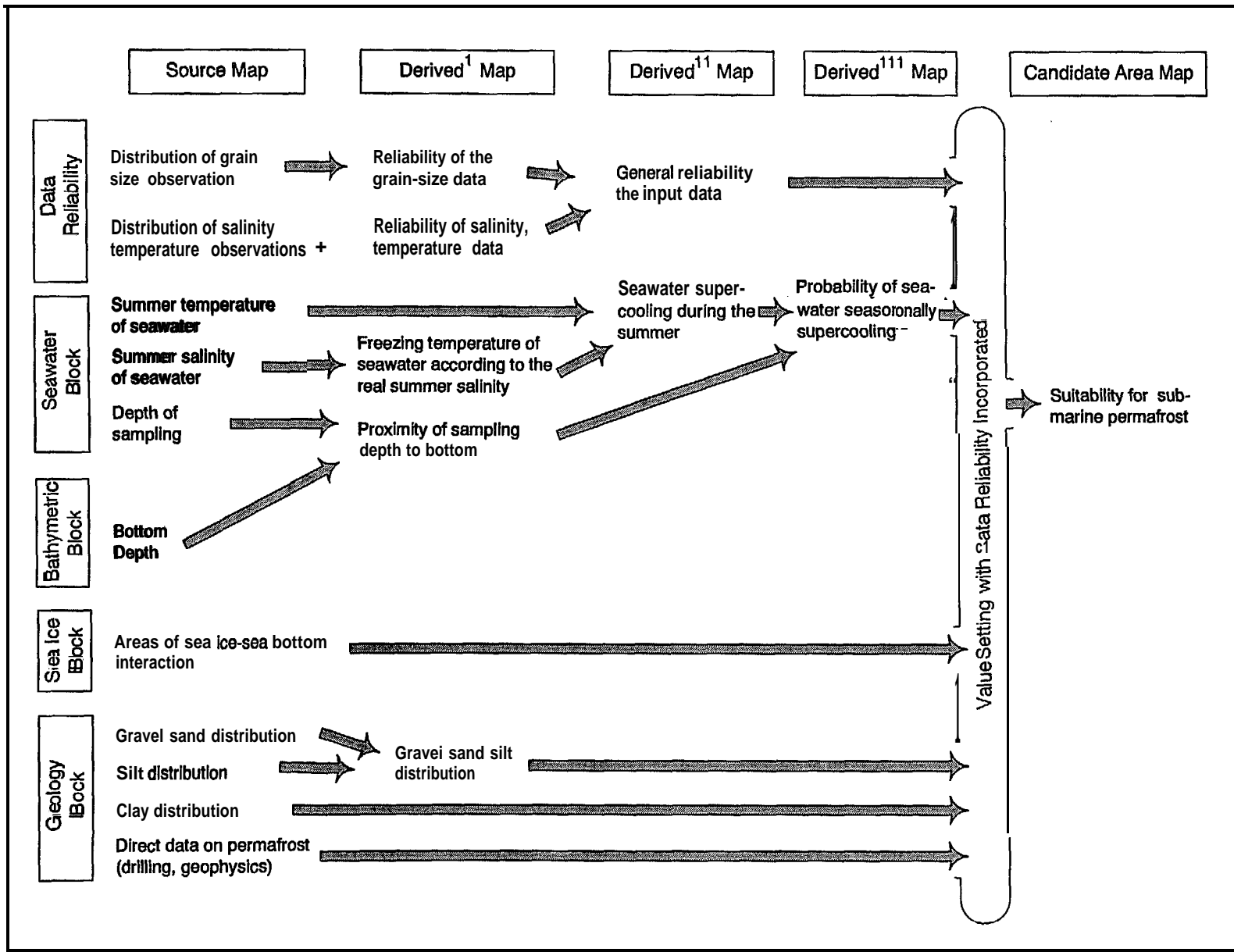


Figure 22.—Structure diagram of the data management system for submarine permafrost prediction in the Beaufort and Chukchi seas.

- 2.) Generation of *derived* maps, based on source maps and/or on the physical and statistical relations between different characteristics, belonging to one discipline (first generation of the derived maps) or several disciplines (second or third generations).
- 3.) Compilation of composite maps based on the assessment value setting obtained from all previous maps. A composite map is produced as a result of the overlay process for combining several maps in order to reach the ultimate goal of the work. In terms of probability it has to specify the candidate areas suitable for submarine permafrost in the Beaufort and Chukchi seas according to the paleoenvironmental and environmental data. To compile the composite map we used the source data on bathymetry, grain size, sea ice, and seawater.

Source Maps

The grain size source maps are based on the grade scale most commonly used for sediments-Wentworth Size Classes (Wentworth 1922). The materials of Barnes and Reimnitz (1976), Naidu and Mowat (1974), and Creager and McManus (1967) have been used for computerized source mapping of the distribution percent of clay, silt, silt plus sand plus gravel at the Beaufort and Chukchi seas. It is known that the grain size of the sediments is an important factor in ice segregation during the freezing process. According to the empirical data, ice segregation is very active in the silty deposits, The impermeable clay is not suitable for ice segregation. In pure sands, ice segregation is possible in the course of water freezing, usually if there is a piezometric head. In Figure 23 and in Table 6 (after Tsythovich 1973) we see that the finer (more clayey) the soil, the larger the amount of unfrozen water it contains at a given subzero temperature. This is understandable when we realize that finer soils have larger specific surface mineral-particle areas and, consequently, have a greater capacity for the binding of pore water. Another factor in ice segregation is the heterogenic structure of the sediments, with changes of grain size mostly in the vertical direction. That is why the areas with silt and silty sands (sometimes with gravel) could be considered as more suitable for ice bonding (if the temperature and other conditions are favorable) and subsea permafrost development. Areas of clay domination usually have low potential for ice-bonded permafrost. The aerial distribution of these grain size classes is shown in source maps 13-18.

Temperatures of the seawater (Aagard 1977, 1978; Aagard and Haygen 1978; Coachman and Aagard 1974; Hufford 1973; Hufford, Fortier et al. 1974; Hugget et al. 1977) at the maximal sampling depth during the summer (Maps 19 and 20) in the southern Chukchi Sea and close to Point Barrow are above 0°C. The main boundary of this "warm" deep water and the cold deep water (0 °C to -30 C) could be traced along latitudes 70 °40'-71020'. In the Beaufort Sea deep water layers, negative temperatures dominate but there are several spots of "warm" water

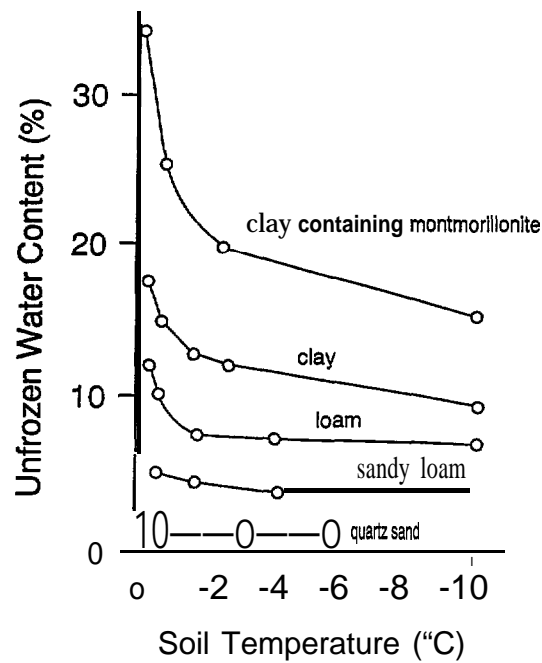


Figure 23.—Graph of unfrozen water content in frozen soils. After Tsytoovich (197'3).

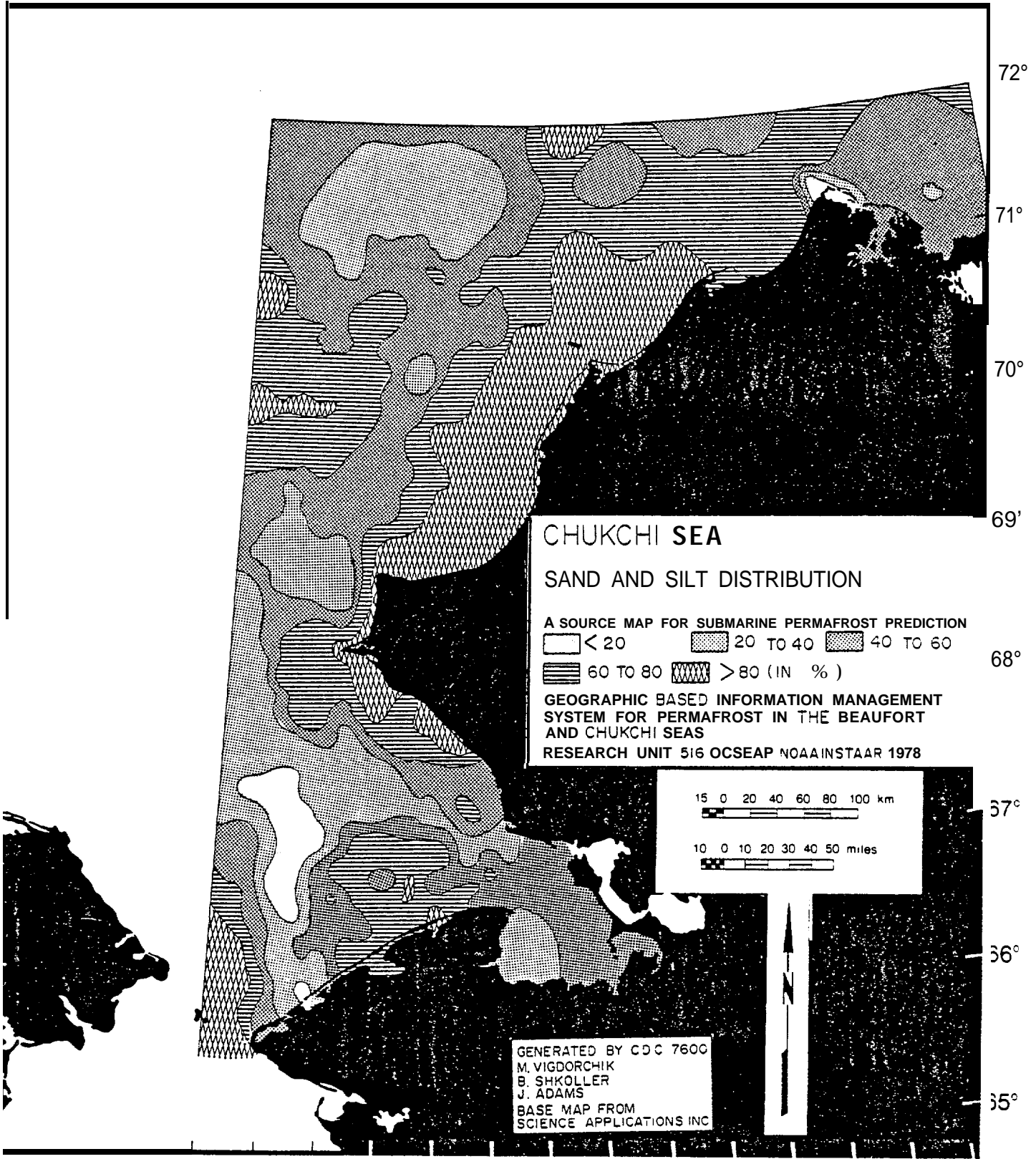
close to the coast and river deltas, which is normal. But the specific of some of these spots seemed to be their meridional shapes oriented to the north (seen in the case of the very detailed intervals of mapping). There is a possibility that some of them could be related to the meridional **geomorphological** and structural **lineaments** of the shelf. We can distinguish these meridional **lineaments** in the river systems (see above), lakes, and topography of the coastal area, the former sea bottom continuing toward the shelf. The “meridional type” of these **morphostructural** elements could be easily reflected in the distribution of other natural conditions, including the temperature of the deep water layers. On the **Eurasian** shelf of the Arctic basin the alternation of the relatively cool and warm belts, sometimes considered in connection with the **hydrogeological** peculiarities of the areas and the discharge of the underground and artesian water through the fractures (see Part 11). Salinity of the deep seawater layers during the summer (Maps 21 and 22) in the **Chukchi** Sea is usually between the 27-31 ppt along the coast and 31-35 ppt for the rest of the sea. In the Beaufort Sea close to Point Barrow, **Elson** Lagoon, Cape **Halkett**, the **Colville** Delta, and Prudhoe Bay, the salinity is usually low, less than 27 ppt, sometimes even less. The more saline deep water extends to the northern parts of the shelf (31-35 ppt and greater).

Table 6.—Unfrozen-water contents of salt free soils vs. degrees of negative temperature, After Tsytoich (1973).

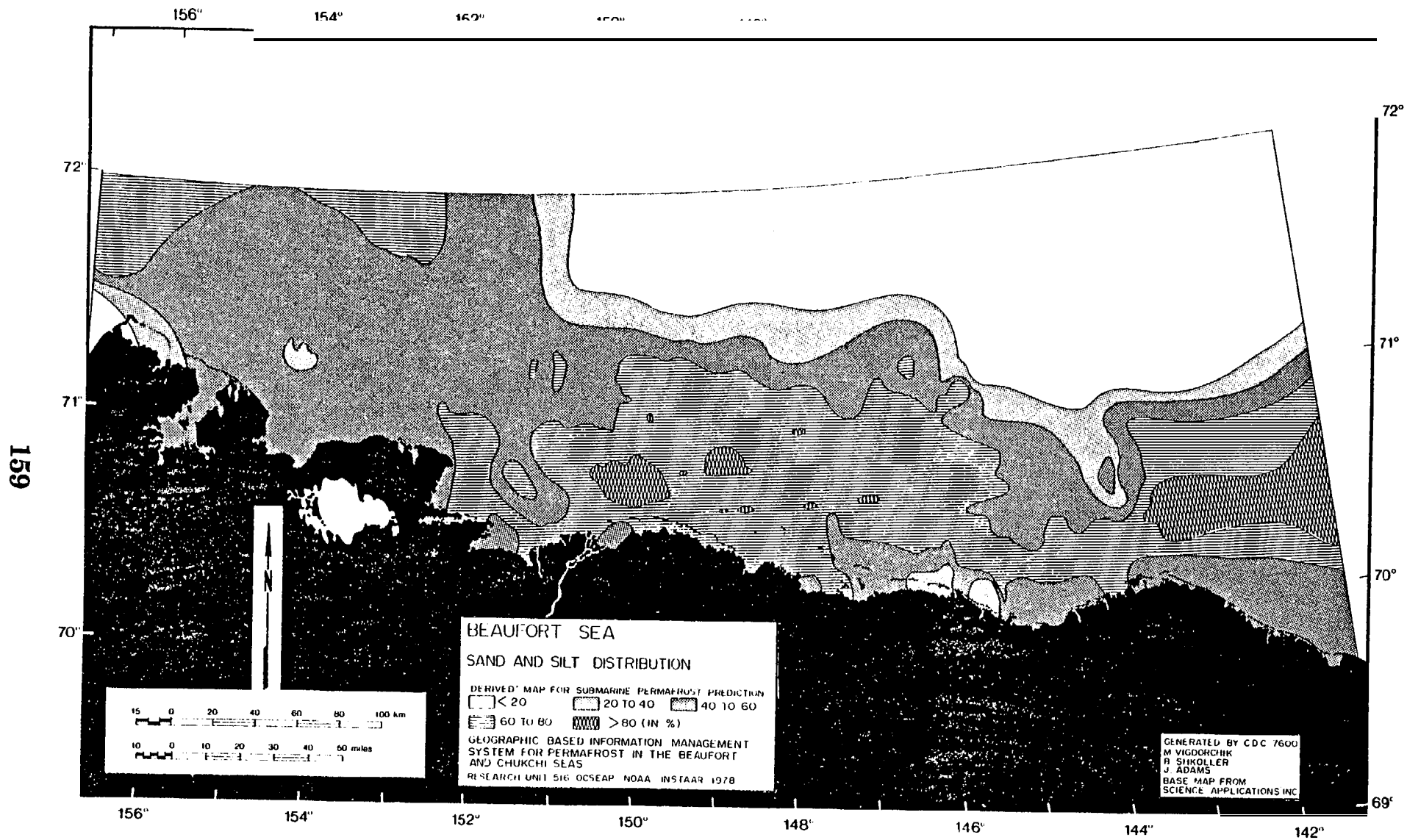
Designation of Soil	Amount of unfrozen water, in percent of weight of dry soil, as a function of temperature in 'C					
	-0.2 to -0.5	-0.5 to -0.5	-1.0 to -1.5	-2.0 to -2.5	-4.0 to -4.5	-10.0 to -11.0
Sand	0.2	0.2			0.0	0.0
Sandy loam		5.0	4.5		4.0	3.5
Loam	12.0	10.0	7.8		7.0	6.5
Clay	17.5	15.0	13.0	12.5		9.3
Clay containing montmorillonite	34.3	25.9		19.8	-	15.3

* (continuing montmorillonite)

175° 170° 165° 160° 155°



Map 13.—Sand and silt distribution, Chukchi Sea.



14.—Sand and silt distribution, Beaufort

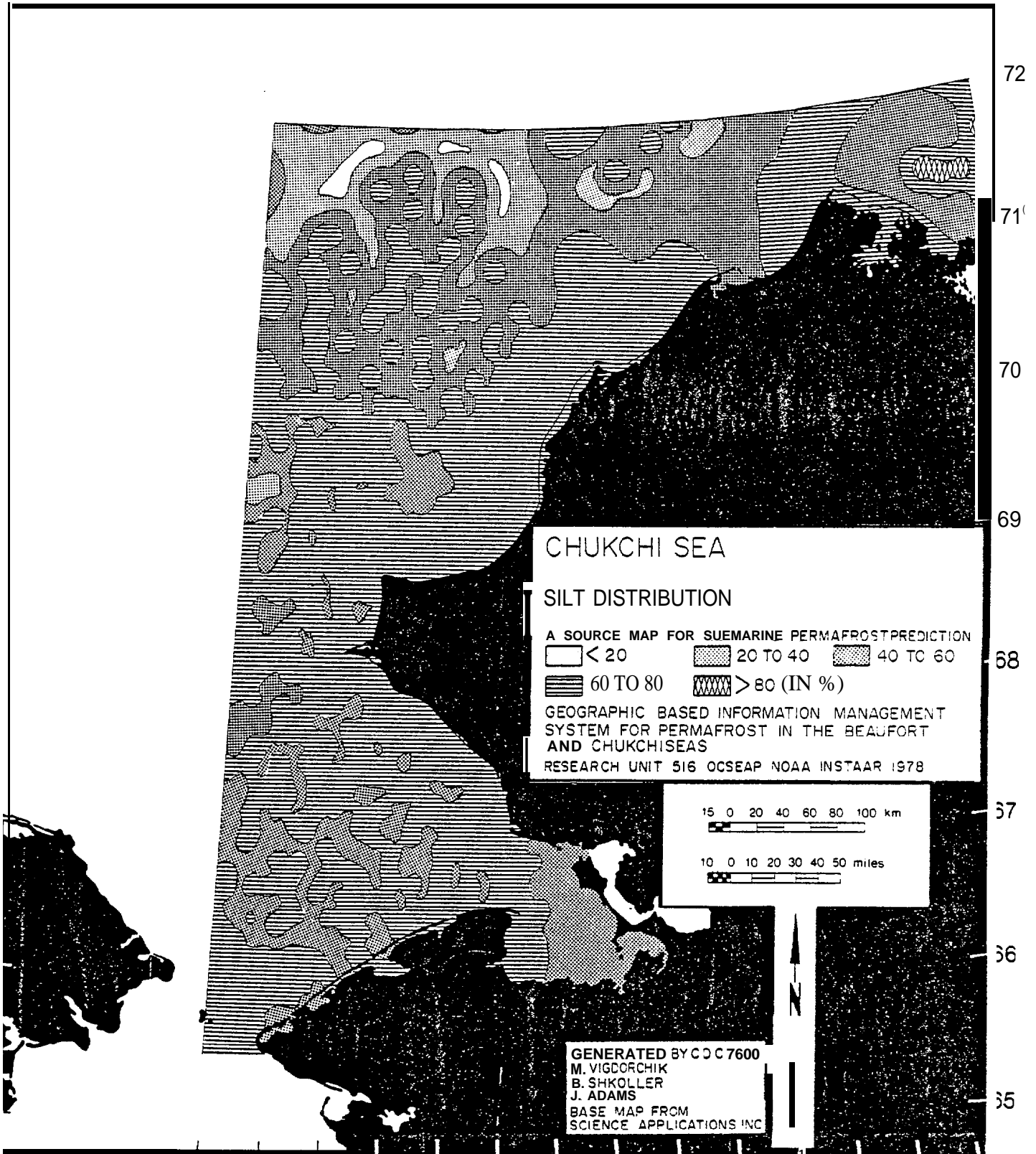
175°

170°

165°

160°

155°



72

71

70

69

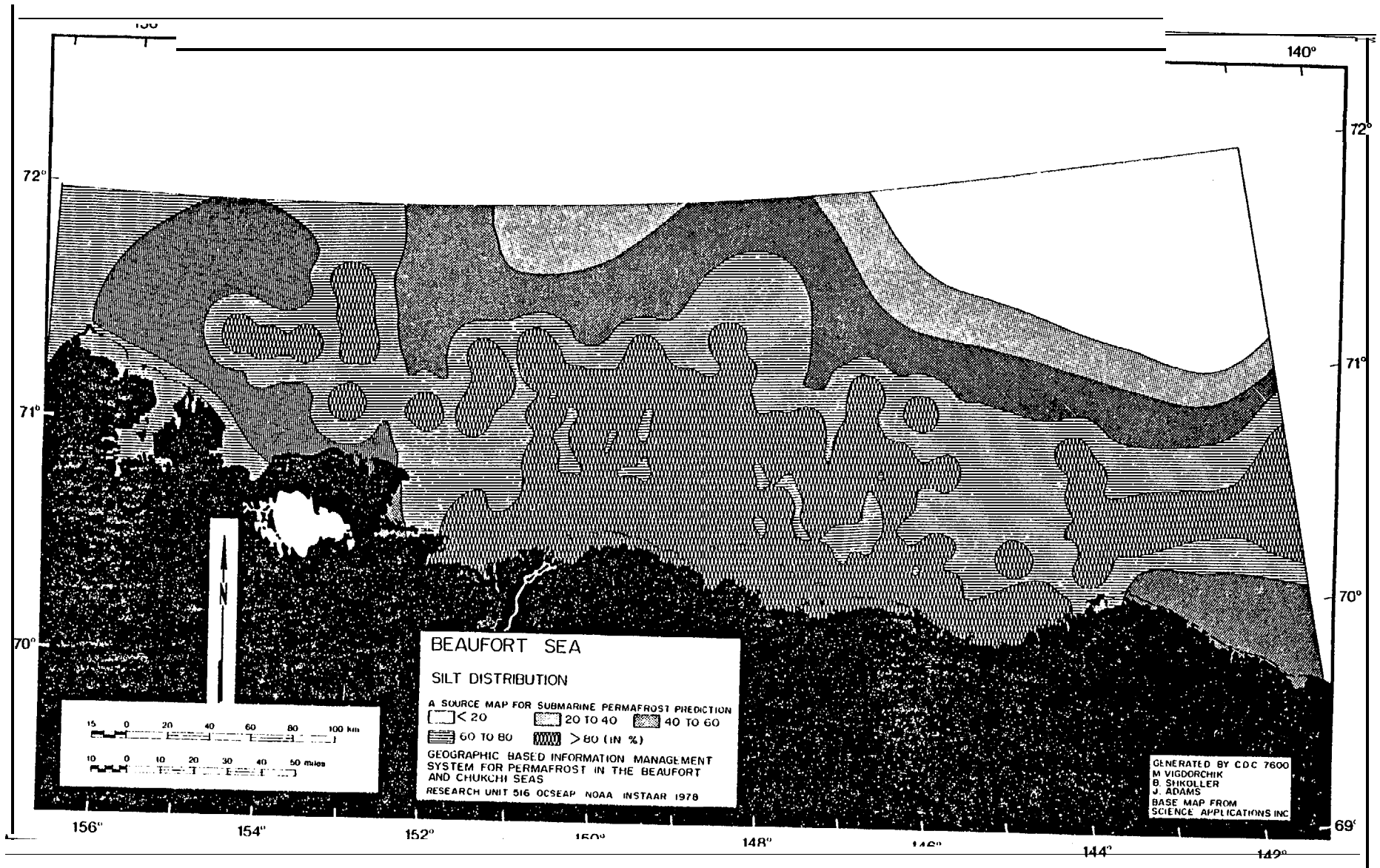
68

67

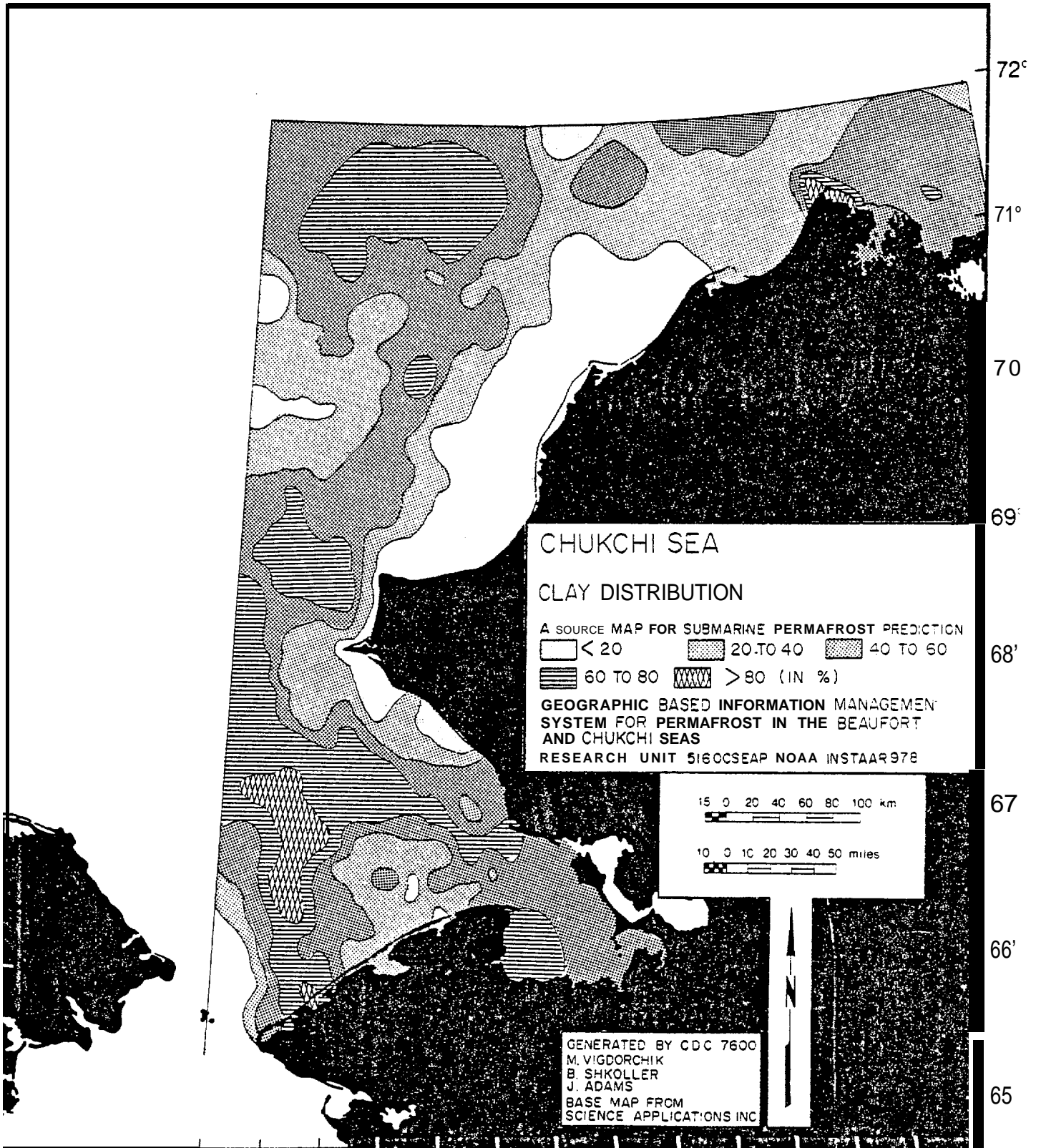
66

65

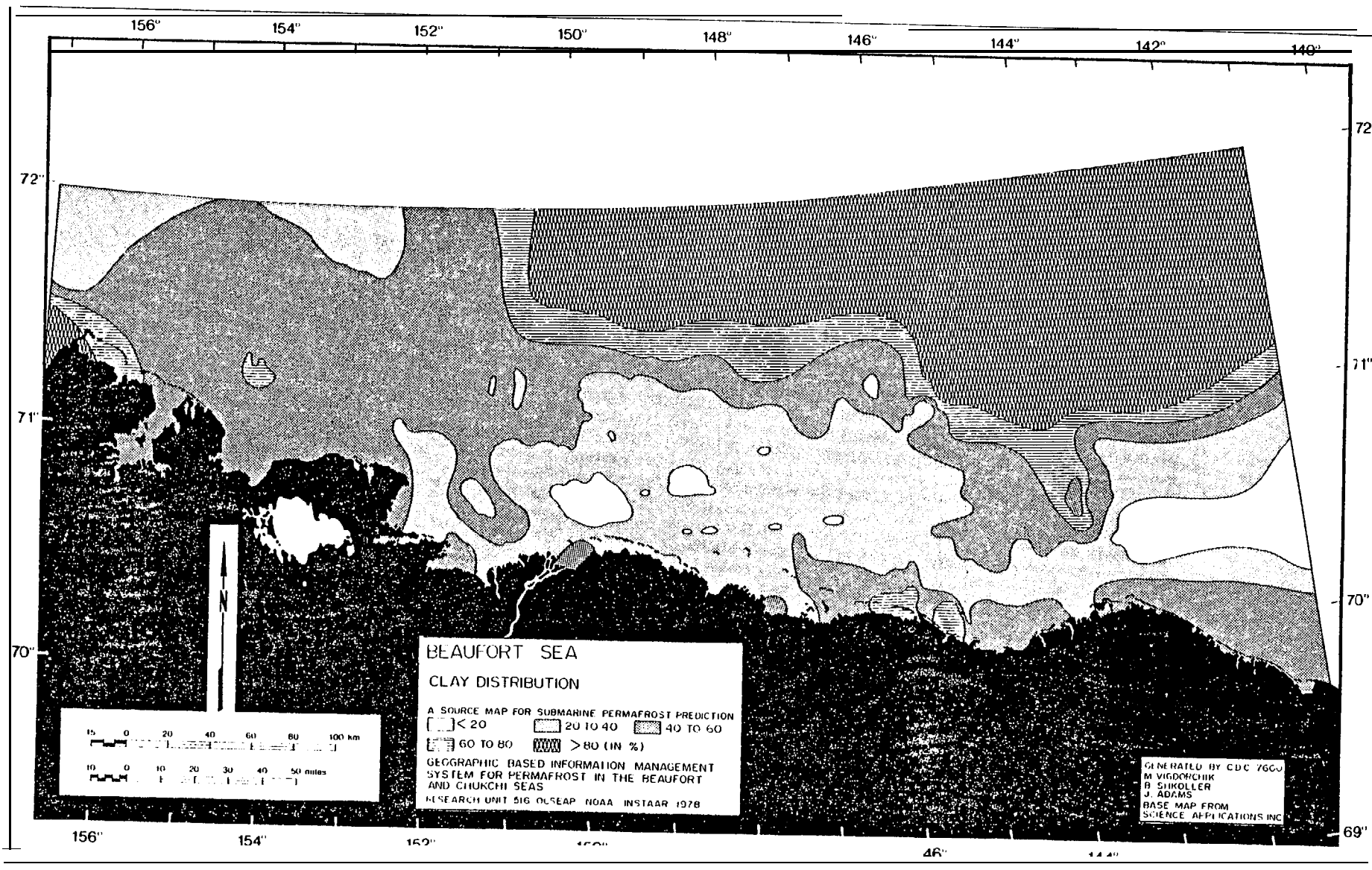
Map 15.—Silt distribution, Chukchi Sea.



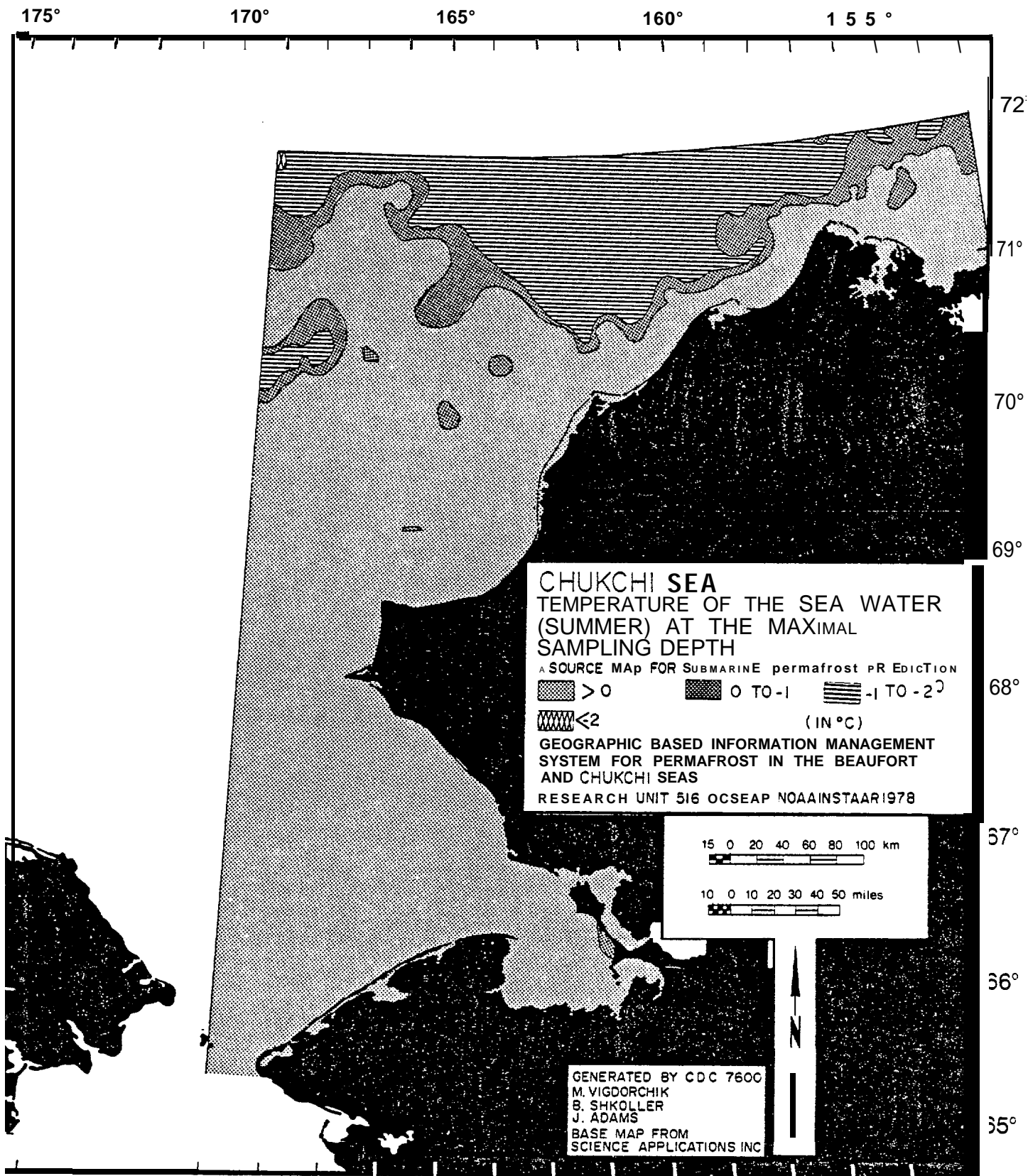
Map 16.—Silt distribution, Beaufort Sea.



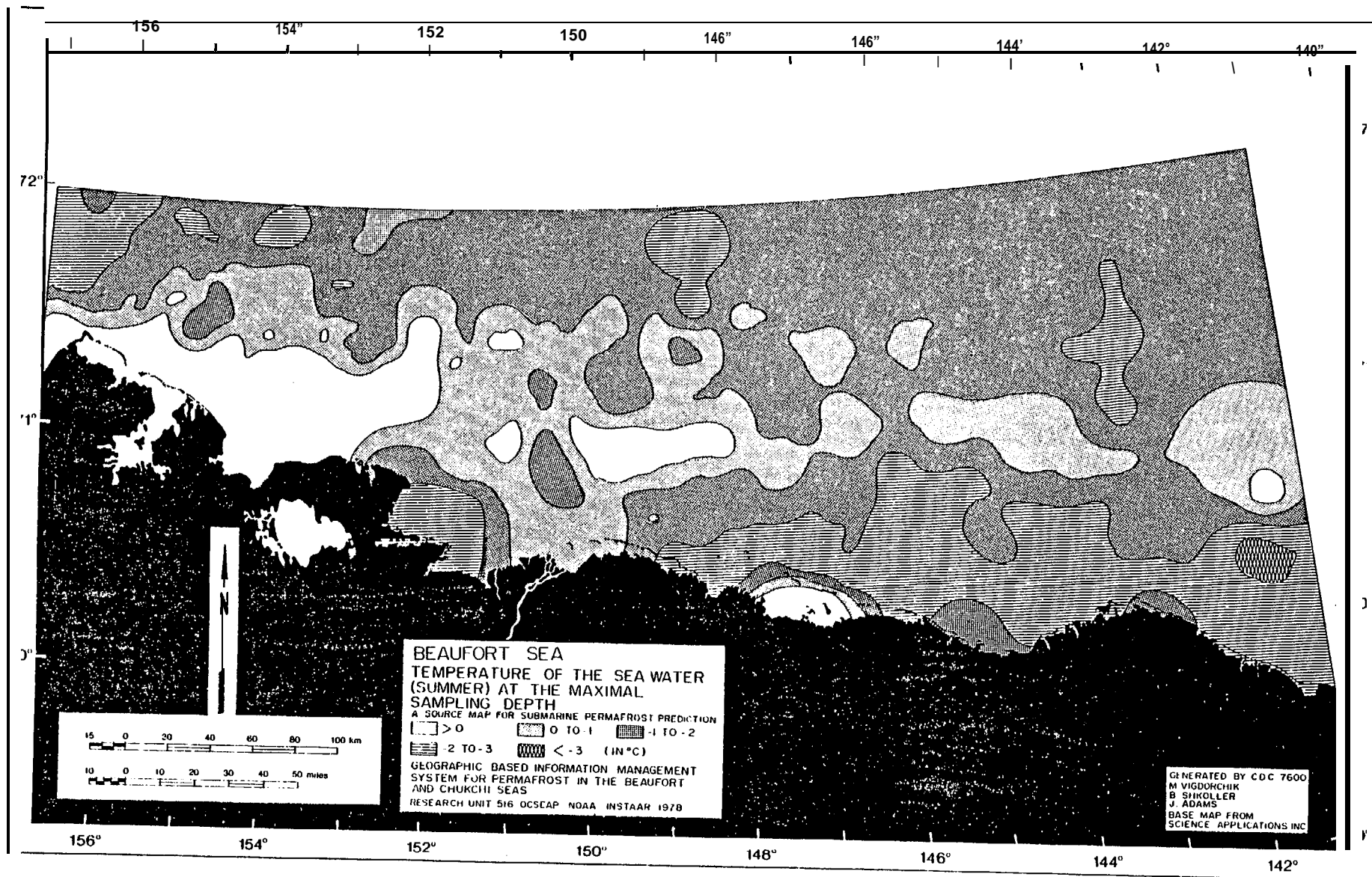
Map 17.—Clay distribution, Chukchi Sea.



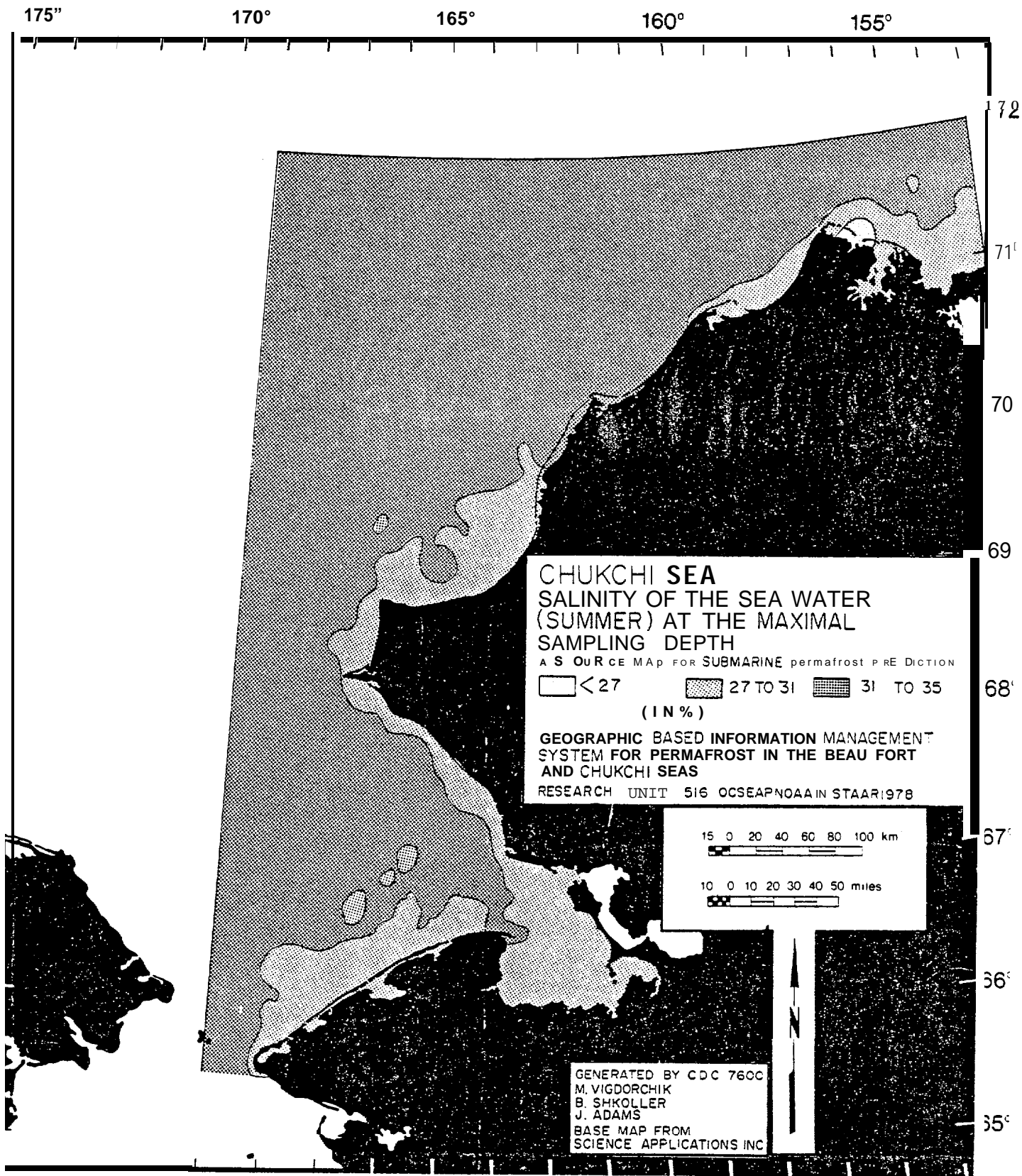
Map 18. Clay distribution, Beaufort



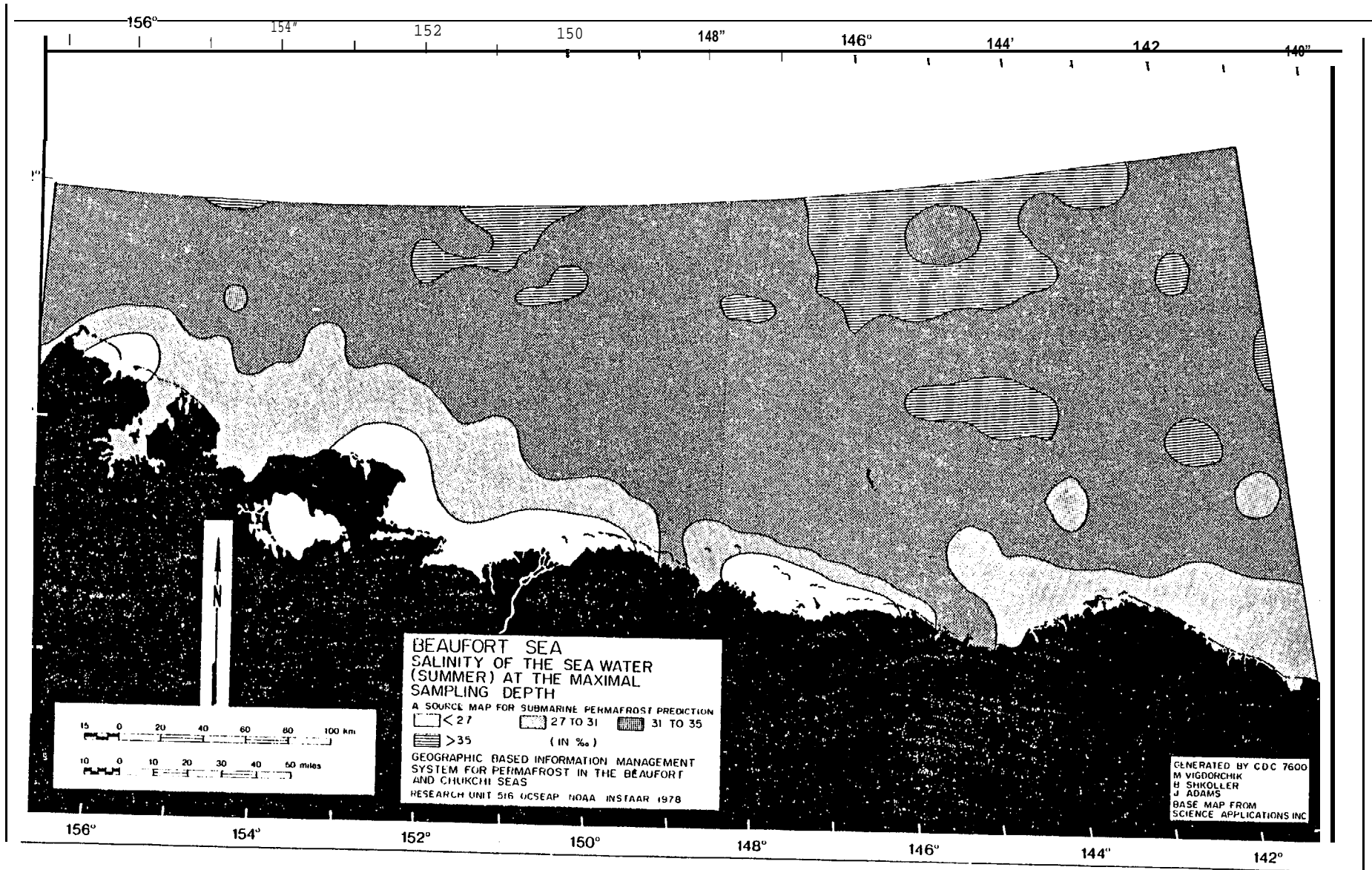
Map 19.—Temperature of seawater in summer at the maximal sampling depth, Chukchi Sea.



Map 20.—Temperature of seawater in summer at the maximal sampling depth, Beaufort Sea.



Map 21.—Salinity of seawater in summer at the maximal sampling depth, Chukchi Sea.



Map 22.—Salinity of seawater in summer at the maximal sampling depth, Beaufort Sea.

Compilation of Derived Maps

Derived Map of Freezing Temperature of Seawater according to Real Summer Salinity (F_{ij})

This can be produced using Savel'ev's formula (1963)*

$$F_{ij} = 2.6 \cdot 10^{-3} - 5.265 \cdot 10^{-2}S - 2.89 \cdot 10^{-6}S^2 - 3.6 \cdot 10^{-7}S^3 - 1.2 \cdot 10^{-9}S^3,$$

or according to Krummel's formula:

$$F_{ij} = 0.003 - 0.0527S - 0.4 \cdot 10^{-4}S^2 - 0.4 \cdot 10^{-6}S^3$$

To generate the map of this characteristic (Maps 23 and 24) we have used the second equation according to the real summer salinity (S_{ij}).

Seawater Supercooling in Summer (C_{ij})

This map (Maps 25 and 26) gives the difference between real summer water temperature (T_{ij}) and freezing temperature (F_{ij}).

$$C_{ij} = T_{ij} - F_{ij}$$

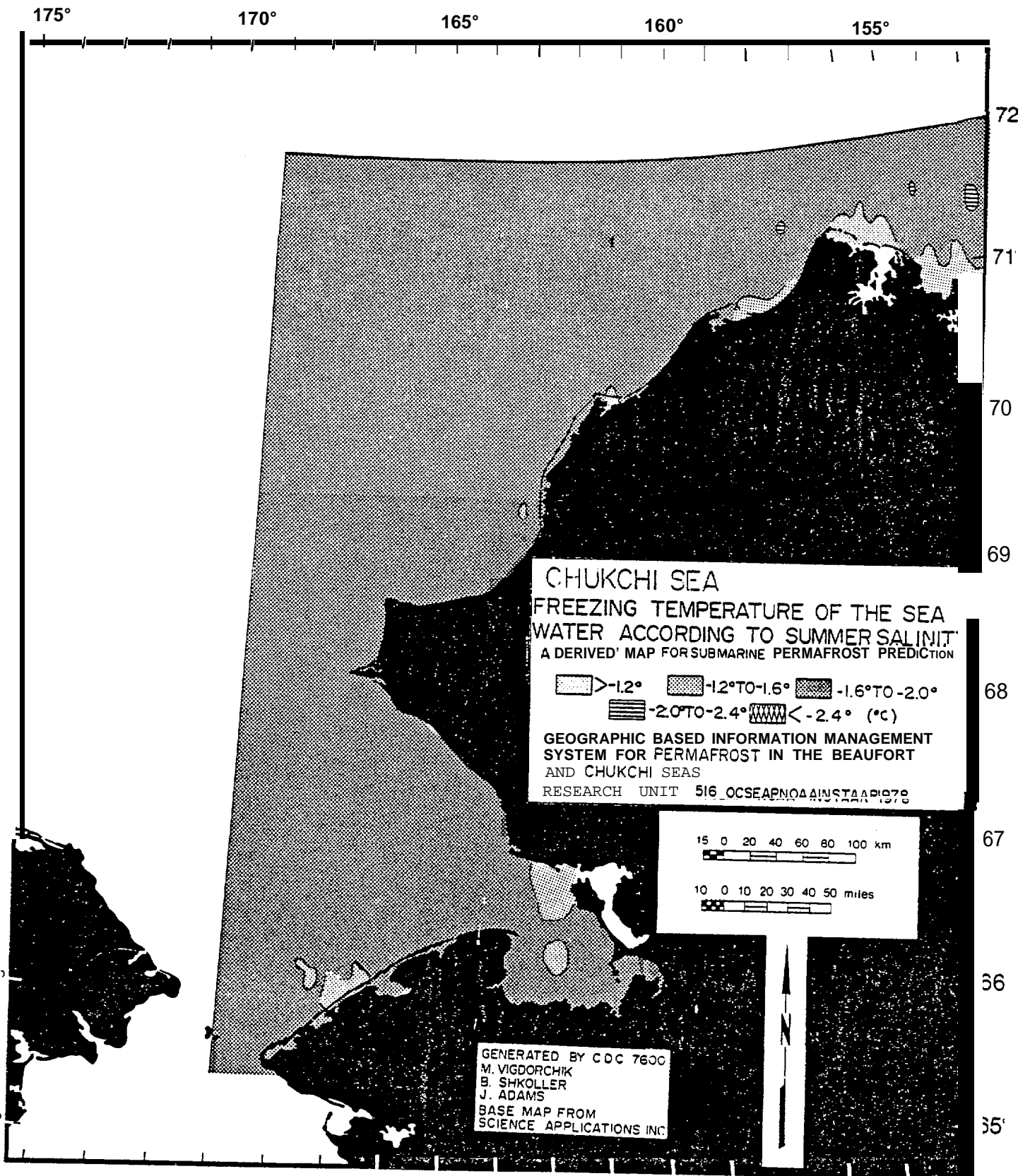
Probability of Seawater Seasonal Supercooling (Maps 27 and 28)

Coachman (1966)* * used the observations from more than 300 oceanographic stations in the Arctic basin to determine the deviations of water temperature in the upper 50 m layer from the freezing temperature for the given salinity (Figure 24). The results of the calculations for depth levels of 5 m and 25 m were grouped according to months. They show that the supercooling of water in the Arctic Ocean is quite well-defined throughout the whole year and that it is most pronounced from October to April. The greatest supercooling (0.130) was observed at the end of February at a depth of 60 m.

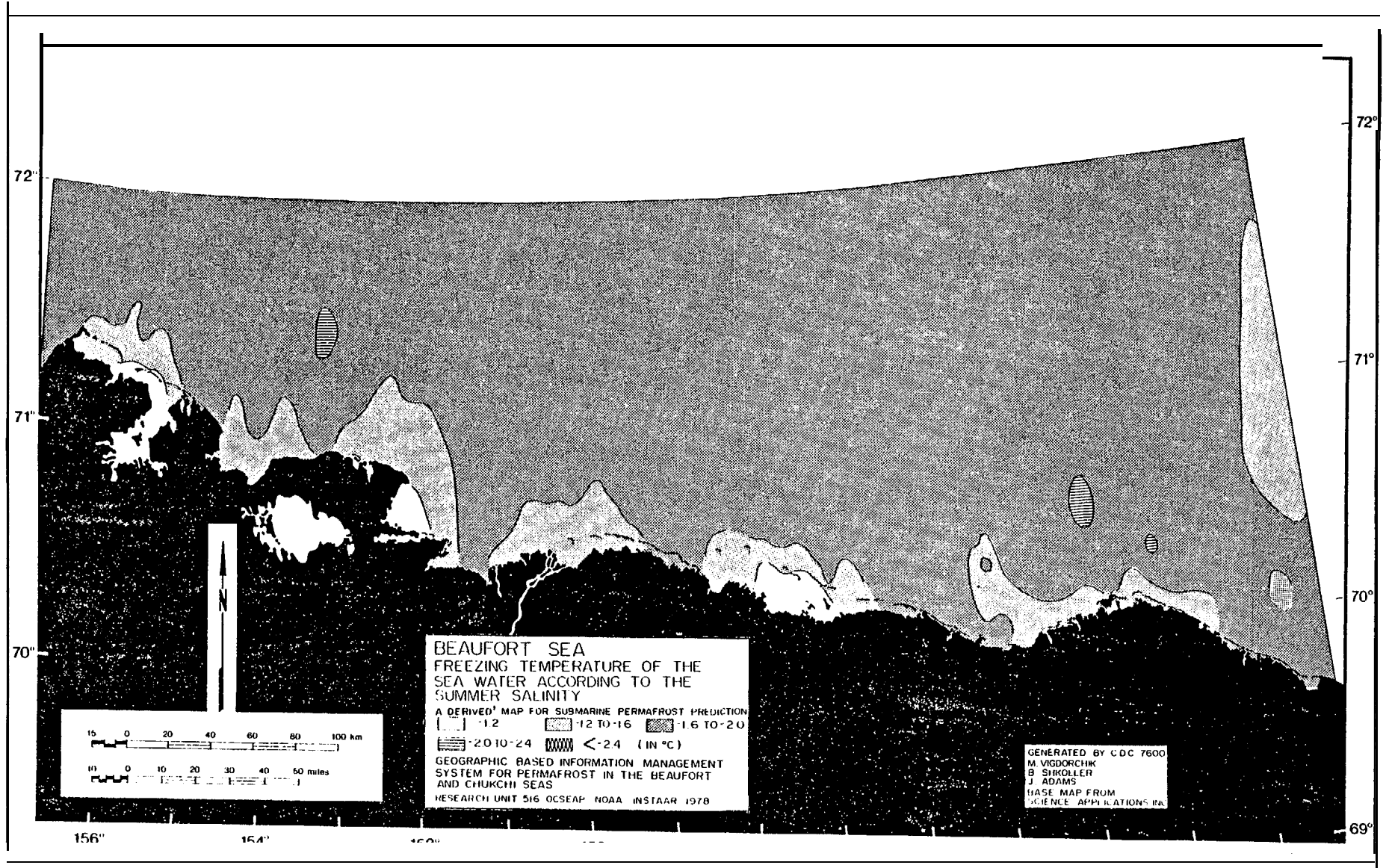
In the Beaufort Sea 0.07° supercooling of the water was recorded during the drift of ice island T-3 (Coachman 1966). Coachman also processed bathymetric data for a 10-m water layer, obtained during the drift of the *Maud* along the land side of the eastern Siberian Sea from April to June 1924. He established that the greatest supercooling (close to 0.1°) were recorded at the surface of the sea from October to December; that is, from the time when low air temperatures began to be observed.

* Savel'ev, B. A. *Stroenie, sostav i svoistva ledyanogo pokrova morshikh i presnykh vodoemov* (The Structure, Composition, and Properties of Ice Covers of Marine and Freshwater Bodies), Moskva, Izdatel'stvo Mosk. Gos. Universiteta, 1963.

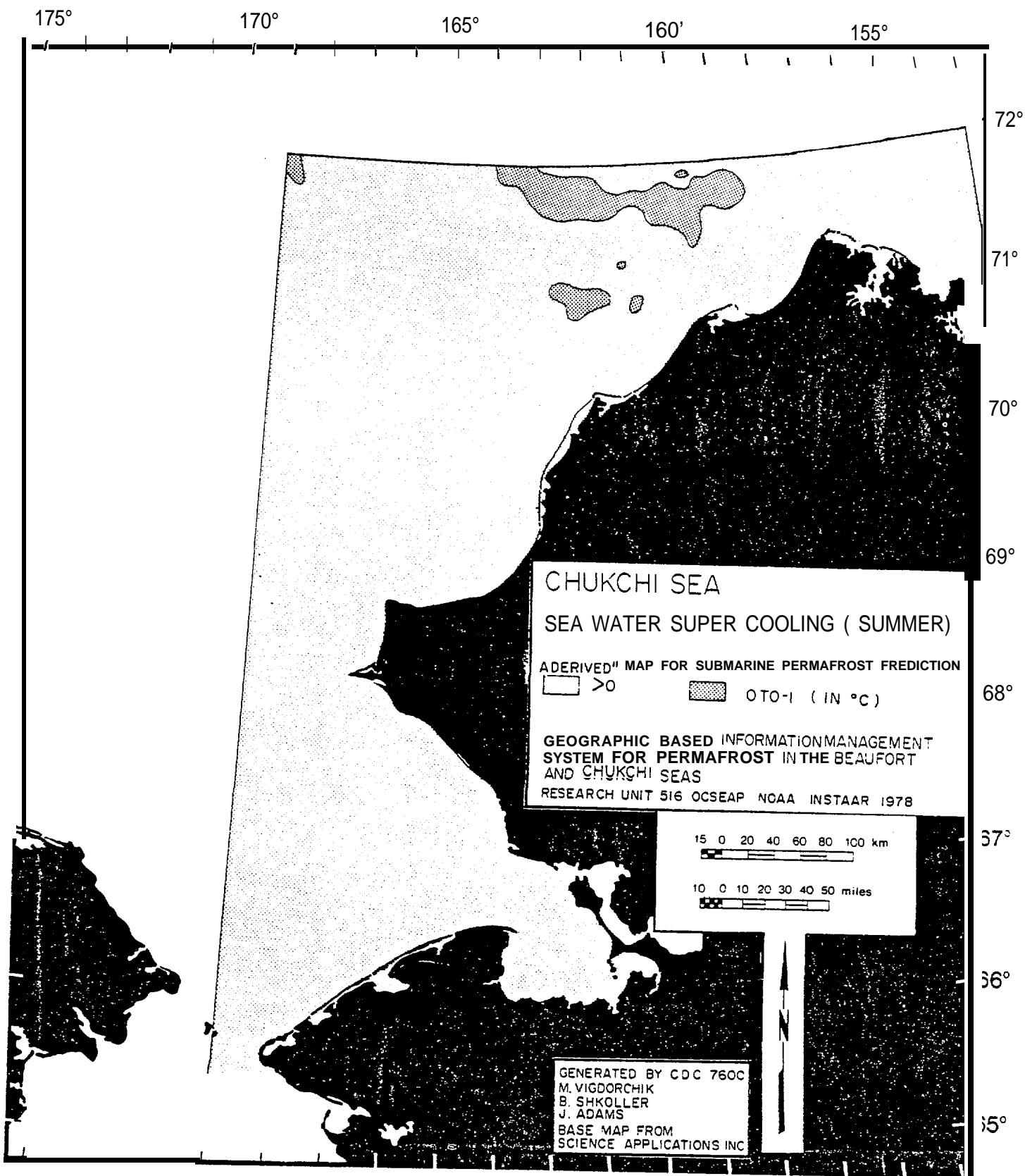
* * L K Coachman. production of Supercooled Water during Sea Ice Formation. Contribution number 383, Dept. Oceanography, Univ. Washington, 1966.



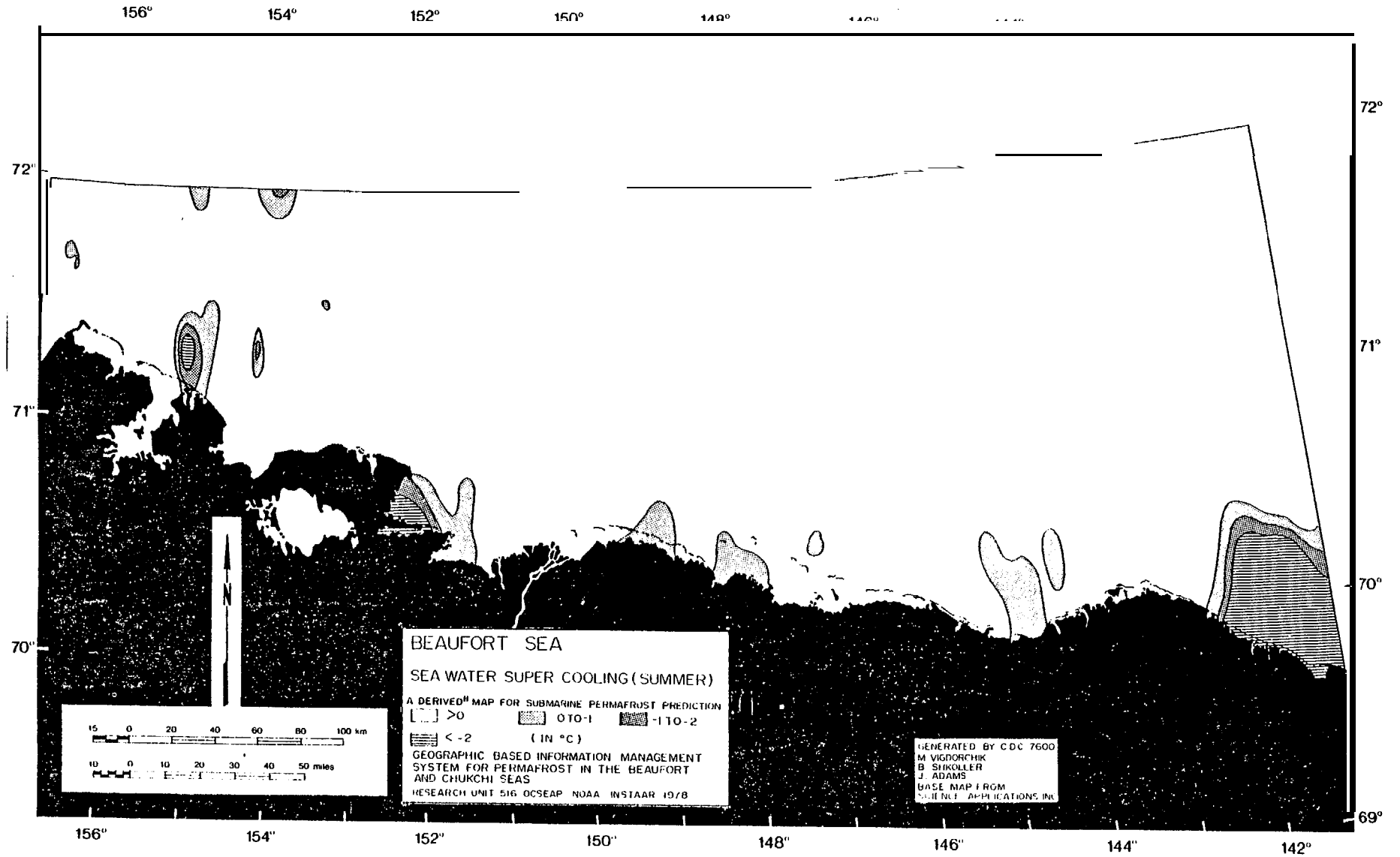
Map 23.—Freezing temperatures of seawater at summer salinities, Chukchi Sea.



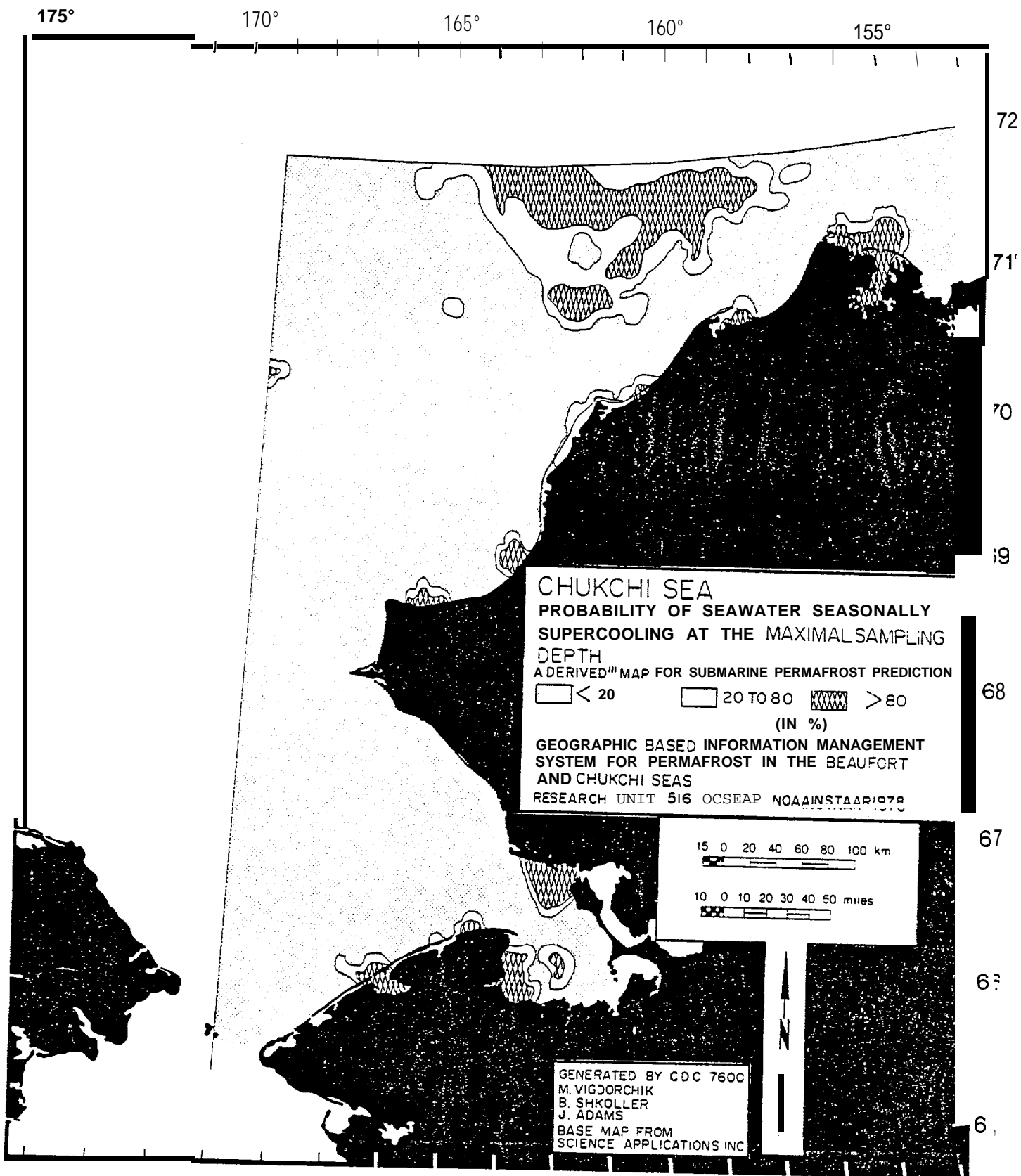
Map 24.—Freezing temperature of seawater at summer salinities, Beaufort Sea.



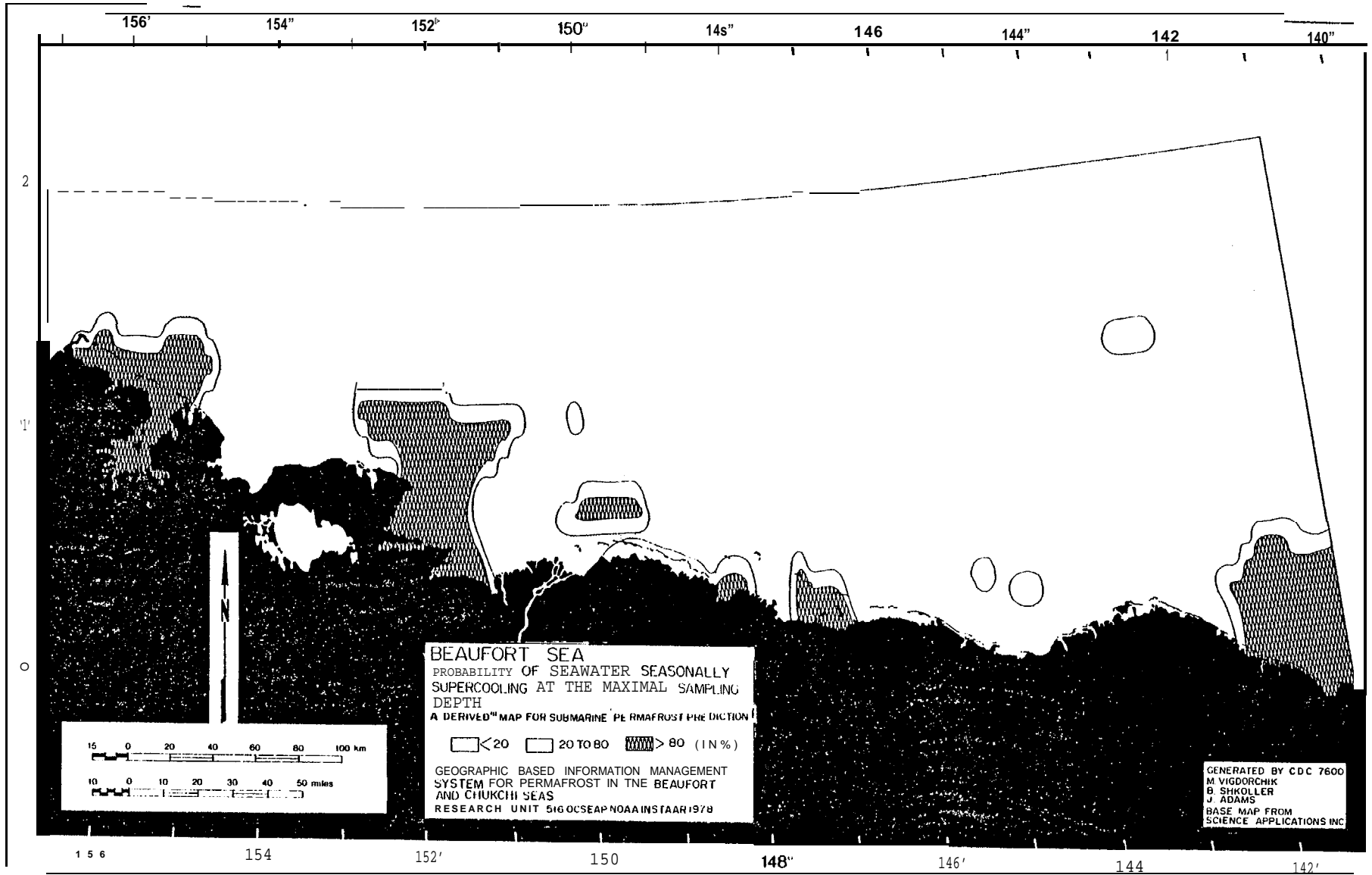
Map 25.—Supercooling of seawater in summer, Chukchi Sea.



Map 26.—Supercooling of in summer, Sea.



Map 27.—Probability of seasonal supercooling of seawater, Chukchi Sea.



Map 28.—Probability of seasonal supercooling of seawater, Beaufort Sea.

possibility of supercooling. The increase of the *sampling depth proximity to the bottom also increase* this possibility. Thus, taking this characteristic into account, we may do the following:

$$\text{if } E_{ij} = D_{ij}/B_{ij} \quad (\text{proximity in } \%), \text{ then } P_{ij}^* = P_{ij} \cdot E_{ij}, \text{ in } \%$$

where P_{ij}^* is the probability decreased according to the proximity data.

Composite Mapping Algorithm

The Composite Mapping Algorithm is used for combining a number of individual maps in order to produce a single map showing the combined influence of each of the individual maps relative to a particular evaluation. In our case it will be the candidate area map showing the suitability of the environmental data for the ice-bonded permafrost in the upper layers of the seabed (in %). It is understandable that the environmental source data today provide us only with the information related to the upper layers of the sea bottom. In addition to the notations mentioned above, the following are used:

- R - General reliability of data, in %
- R_1 - Reliability of the grain size data, in %
- R_2 - Reliability of the seawater data, in %
- r_1 - Distance between grid point and the nearest observational point (grain size data), in miles
- r_2 - Distance between grid point and the nearest observational point (seawater data), in miles
- A_x - Horizontal distance (W-E) between adjacent grid points changing from latitude to latitude, in miles
- Δy - Vertical distance (S-N) between two adjacent grid points, in miles
- G - Percentage of silt-sand classes appropriate for active ice segregation
- A - Probability of ice-bonded permafrost distribution, in %
- W - Suitability for ice-bonded permafrost in the upper layers of the seabed

The algorithm to find W is described by

$$\begin{aligned} W &= A \cdot R, \\ A &= p_{ij}^* \cdot G \quad \text{and} \\ R &= R_1 R_2 \\ R_1 &= 100\% (1 - (r_1/5\Delta y)) \\ R_2 &= 100\% (1 - (r_2/\Delta y)) \end{aligned}$$

It means: $W = P_{ij}^* \cdot G R_1 R_2$, or $W = (P_{ij} \cdot D_{ij} \cdot G \cdot R_1 R_2) / B_{ij}$ (in %)

Candidate Areas for Submarine Permafrost Related to BLM Lease Nomination

The candidate areas for ice-bonded submarine permafrost in the upper layers of the seabed in the **Chukchi** and Beaufort seas (Maps 29 and 30) might be characterized the following way:

On the Beaufort Sea shelf the probability of ice-bonded permafrost is not very high (20%). At the western part of the shelf there are three major areas of higher probability. Area 1, about 60 square miles, is situated in the northern part of Cape Simpson. The probability here is 20–40%. Area 2, about 2,100 square miles, is situated at the northeastern part of Harrison Bay and at the open sea to 50 miles from the shore. The probability here is 20–40% and 40–60%. Area 3, about 350 square miles, is situated to the N-NE from the Colville River delta, close to the northern edges of the barrier islands and far to the north. The probability here reaches 60–80%. The small area with probability of 20–40% could be defined to the north from Area 3.

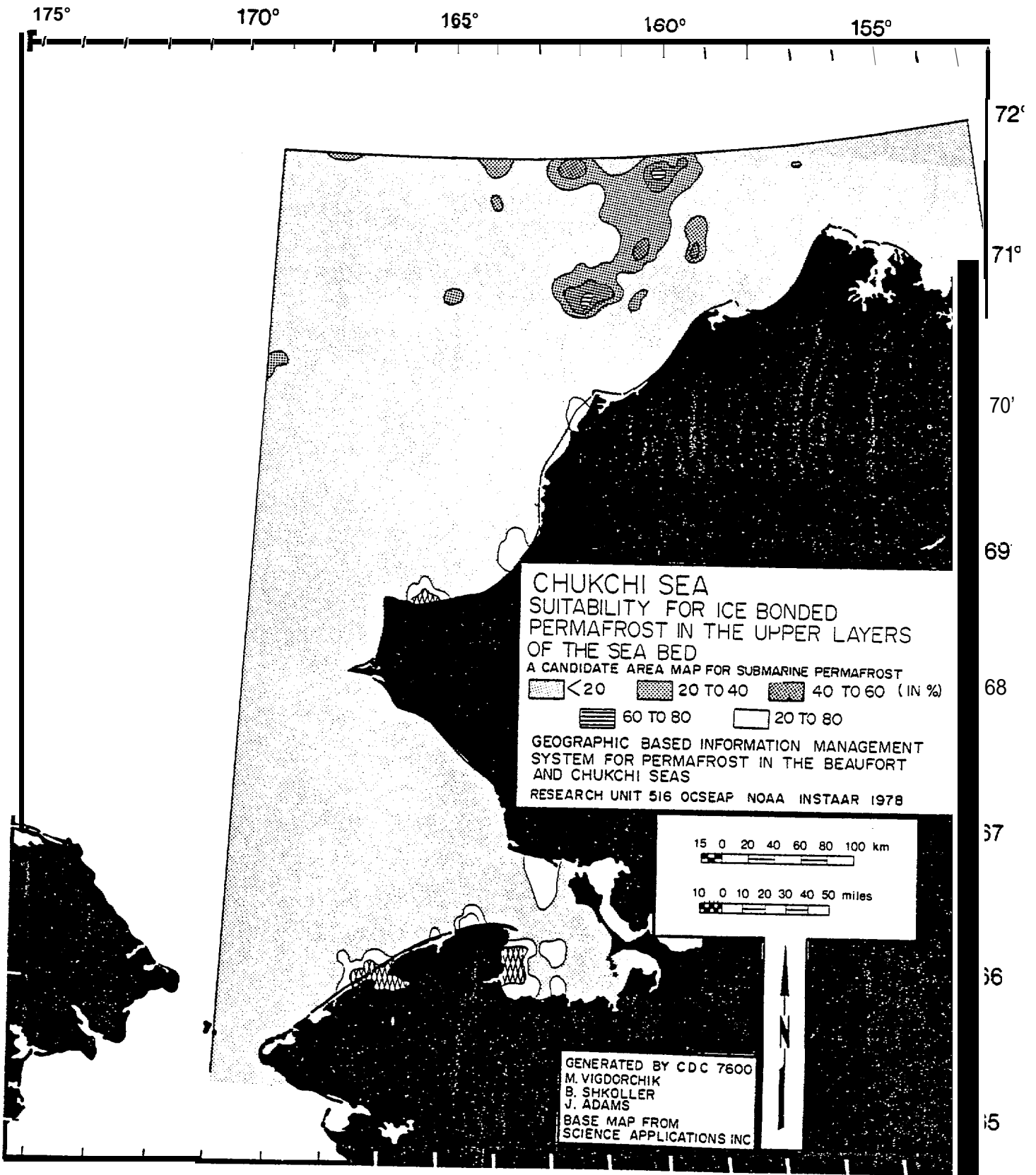
In the central part of the Beaufort Sea shelf the prospective permafrost areas are situated much closer to the shore mostly between the shore and barrier islands, or at the shallow areas a little north from the islands. Area 4 is such an area, about 780 square miles, with the probability in its inner part (closer to the shoreline) about 60–80%. Two very small spots with probability more than 20% are defined at Camden Bay (Area 5). Table 7 characterizes the level of probability for submarine ice-bonded permafrost in the upper layers of the seabed (limited to 5 m) for each unit of the lease areas.

We also need to specify the suitability for submarine relic permafrost within the boundaries of the same three areas of the Beaufort Sea (Map 31).

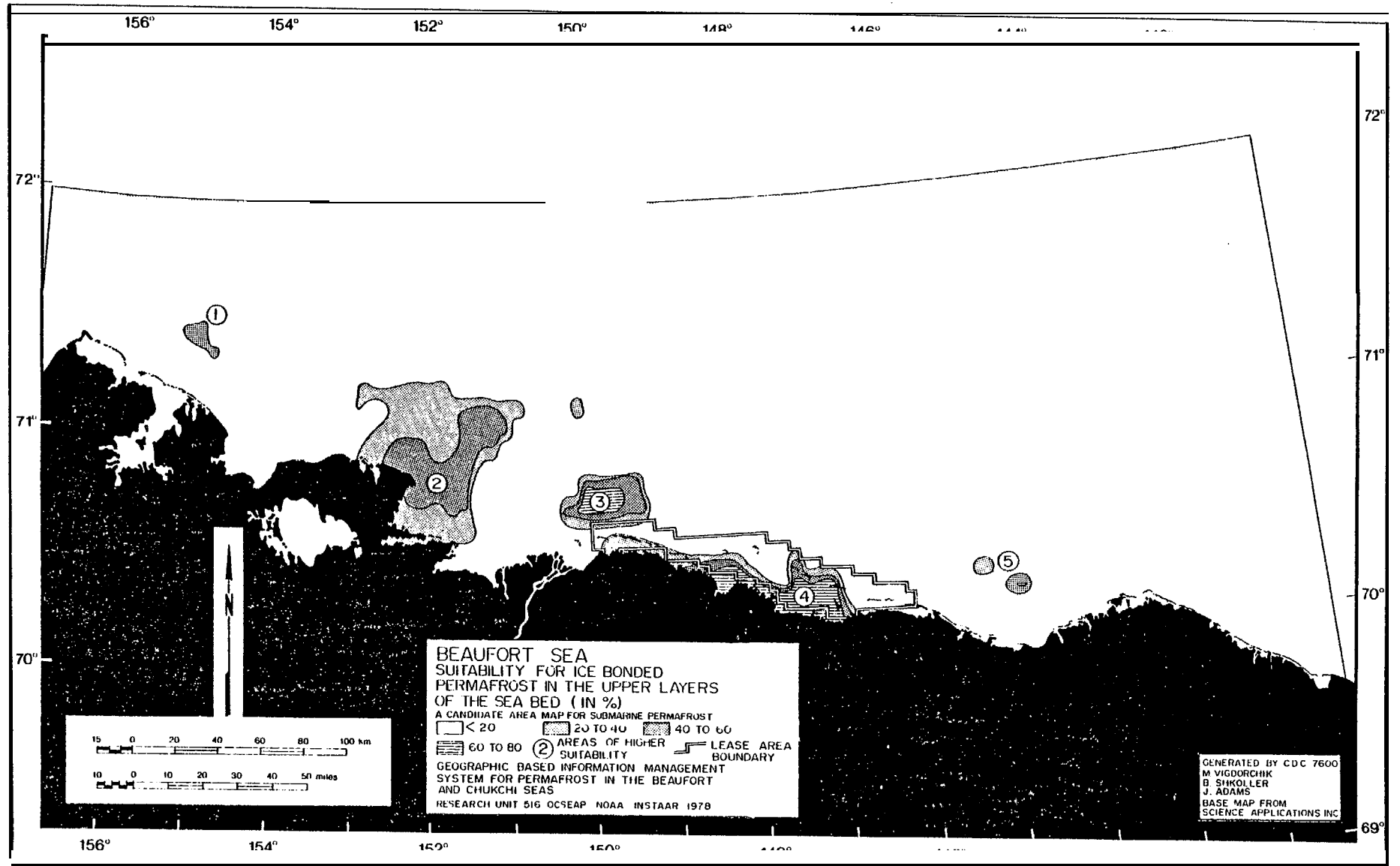
The western part of the Beaufort Sea can be considered as suitable for relic permafrost. Average thickness could reach 100–120 m. Permafrost might be met at the first 50–100 m from the seabed where the seawater depth is 0–60 ± 20 m. ‘Taliks’ are typical for such kinds of relic permafrost extension according to studies of the **Eurasian** shelf. The relic permafrost body could be separated from the upper ice-bonded permafrost spots on the seabed, by taliks, and this connection in each case could be clear only from site specific investigations.

The second, or central, area of the Beaufort Sea can be characterized by low potential for relic permafrost, possible only at the boundary with the western area. A body of deep permafrost could be a continuation of a thick (about 600 m) coastal cryogenic zone and limited to 18–22 km offshore. General thickness would be about 150–200 m; seaward this is less—30–50 m. **Taliks** are also typical for such submarine permafrost and sometimes give the impression of a multilayered structure of permafrost.

No relic permafrost can be considered to exist in the third, or eastern, part of the sea. The coastal permafrost could not extend farther than 2–5 km offshore. Permafrost depth here could be 50–100 m. Lack of data on coastal permafrost thickness prohibits speculation on



Map 29.—Suitability for ice-bonded permafrost at the upper layers of the seabed, Chukchi Sea.



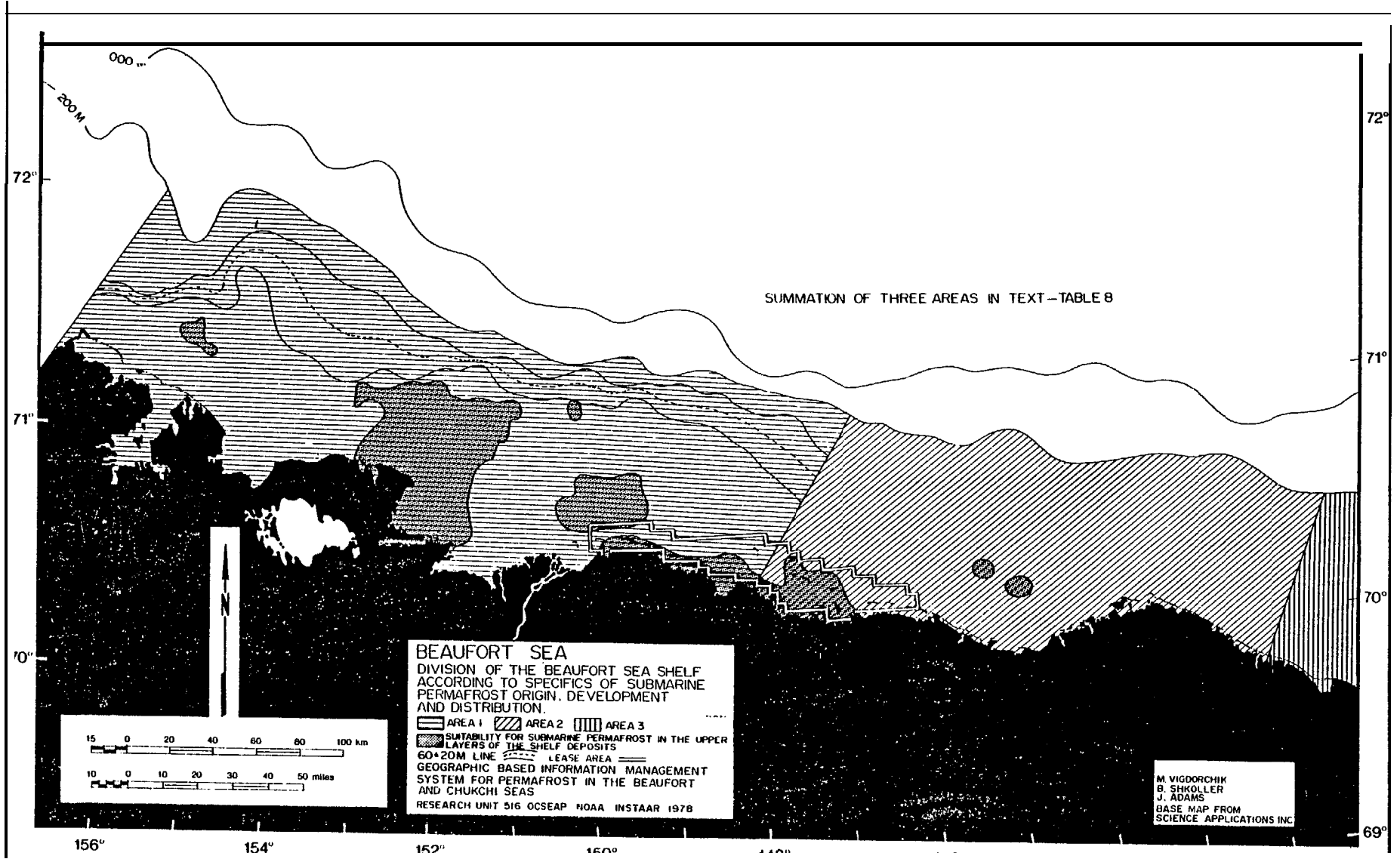
Map 30.—Suitability for ice-bonded permafrost at the upper layers of the seabed, Beaufort Sea.

Table 7.—Probability of submarine permafrost in the lease areas
(by lease unit numbers).

< 20%0	20-40%	40-60%	60-80%'
1-22	23-29	95-101	57
30	32-40	110	50
31	59-61	114-116	111-113
41-56	77-90	129-131	126-128
62-76	102	135	139
91-94	103	140	158
104-108	109	153	171-175
119-121	117	157	182-189
125	118	145-148	201-208
132	122-124	159-162	220-221
133	130	168-170	233
143	131	176	234
151	134	190	
152	136-138	209	
163-167	141	222	
178-181	142	235	
192-200	144		
211-219	149		
224-232	150		
	154-156		
	177		
	191		
	210		
	223		
	236		

the thickness of the permafrost offshore. Depending on the coastal permafrost thickness, it must be 2-3 times less. Seasonally frozen layers might be met on any part of the Beaufort Sea coast within the limits of the sea ice-sea bottom interaction (isobath -2 m),

In the **Chukchi** Sea the areas with relatively high potential for the development of ice-bonded permafrost in the upper layers of the shelf deposits are situated to the west-northwest from the Barrow Canyon and at the east-southeastern slope of **Hanna** Shoal. Some relatively small spots could be traced along the coast close to Icy Cape, Cape Beaufort, Cape Lisburne, between Cape Thompson and **Kivalina** at Kotzebue Sound and **Shishmaref** (Map 30). There are no data available on the relic ice-bonded permafrost in these areas and the relationship between the prospective areas for ice-bonded permafrost at the surface of the seabed and any deeper permafrost body if it exists. Generally speaking, the influence of the relatively warm water of the Bering Sea, lack of thickness of the permafrost in the coastal zone (<300 m), its discontinuous character (Péwé 1976), and possibly a higher thermal flux



Map 31.—Division of the Beaufort Sea shelf according to the specifics of submarine permafrost origin and distribution.

in the zone of convective heat transfer in the southern part of the Chukchi Sea—all these factors are negative for preservation of relic ice-bonded permafrost, if it ever existed. The deep submarine permafrost could exist only extremely close to the coast (usually less than 1.5-2.0 km) and might be connected with the coastal permafrost body or disconnected (lenses). In both cases the thickness of the submarine permafrost could reach nearly 20-30 m. The spots suitable for ice-bonded permafrost in the upper layers of the shelf deposits might represent the area where the intrusion of the coastal permafrost body into the shelf takes place. To answer the question special investigations need to be done.

APPLICATION OF THE SYSTEM TO THE BEAUFORT SEA AREAS WITH KNOWN SUB MARINE PERMAFROST (COMPARISON OF RESULTS)

An opportunity to check the efficiency of our system for permafrost prediction occurred when we compared our maps (computerized variations) with maps made for the Canadian shelf. We will therefore show here the following maps of the Mackenzie Bay and Delta and adjacent areas (after Hunter et al. 1976): bathymetry (Figure 25); summer and winter bottom water temperature in the southern Beaufort Sea (Figure 26); summer and winter bottom water salinities in the southern Beaufort Sea (Figure 27); and an interpretation of the occurrence of subsea bottom ice-bonded permafrost from industry seismic records (Figure 28). Then we compare them with the following maps of our system ("seawater block") made for the Canadian part of the Beaufort Sea according to existing data at the same scale and projection: summer temperature of the seawater at the maximal sampling depth (Figure 29); summer salinity of the seawater at the maximal sampling depth (Figure 30); freezing temperature of seawater according to the summer salinity (Figure 31); seawater supercooling during the summer at the maximal sampling depth (Figure 32); probability of the seawater seasonally supercooling at the maximum sampling depth (Figure 33).

In general, the summer seawater temperature distribution on the Canadian map and our map look similar. The main areas with positive or negative seawater temperatures are the same. The differences may be observed in the size of the northeastern positive spot, which is oriented more to the west on the Canadian map, and also in the discontinuous character of the positive spots in the middle and upper parts of the territory. The temperature contours on the Canadian map are discontinuous also in the western areas. Following the same trend, the summer temperature contours on the computerized map show considerable extension of negative temperature zones during the summer too. Both maps of salinity are also very close but the computerized map shows much more detail, especially for the northern part of the shelf and to the north from the Mackenzie River delta. According to the freezing temperature of the seawater (calculated by using the summer salinity), the areas of seawater

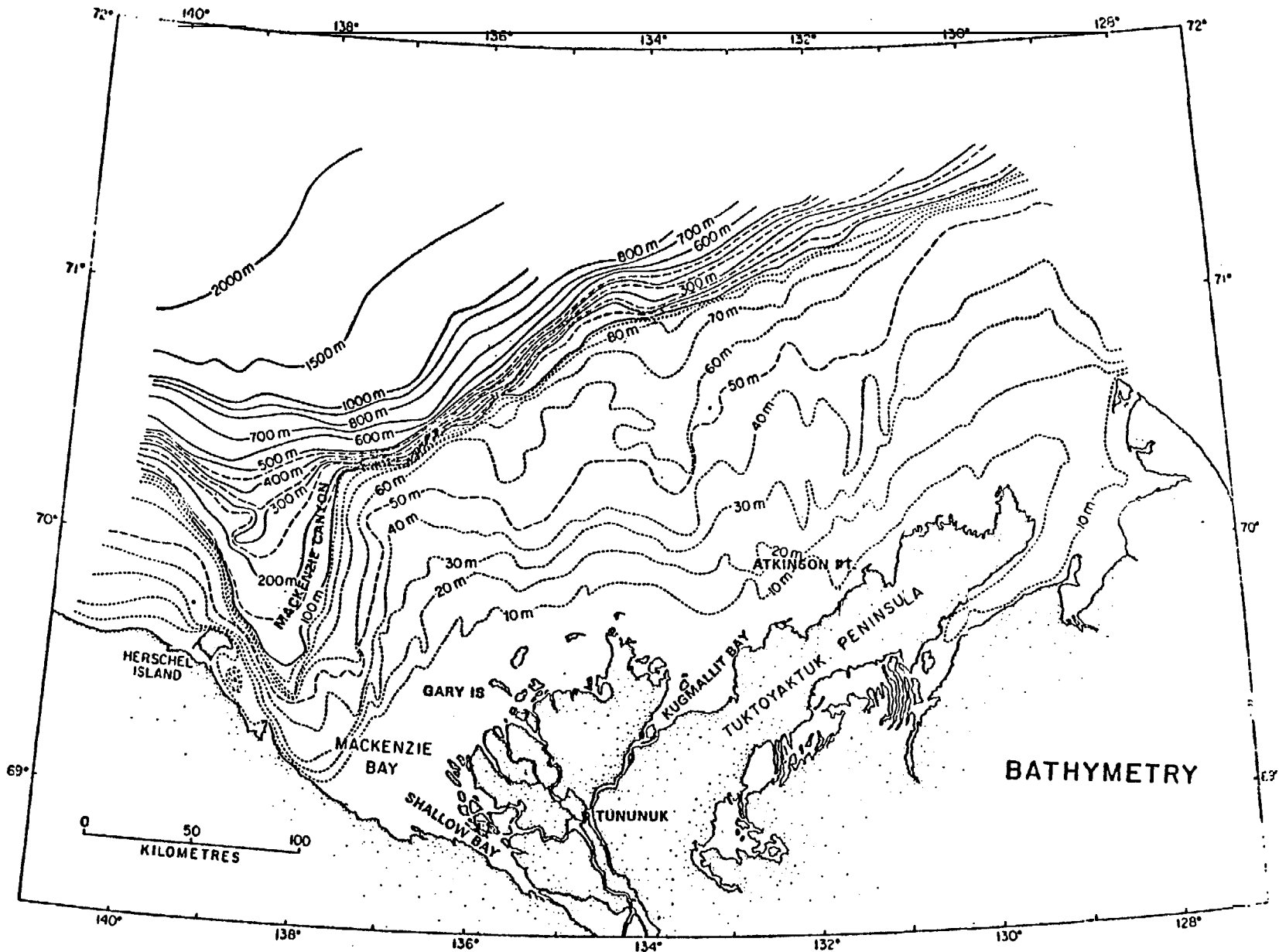


Figure 25.—Bathymetry of the southern Beaufort Sea. After Hunter et al. (1976).

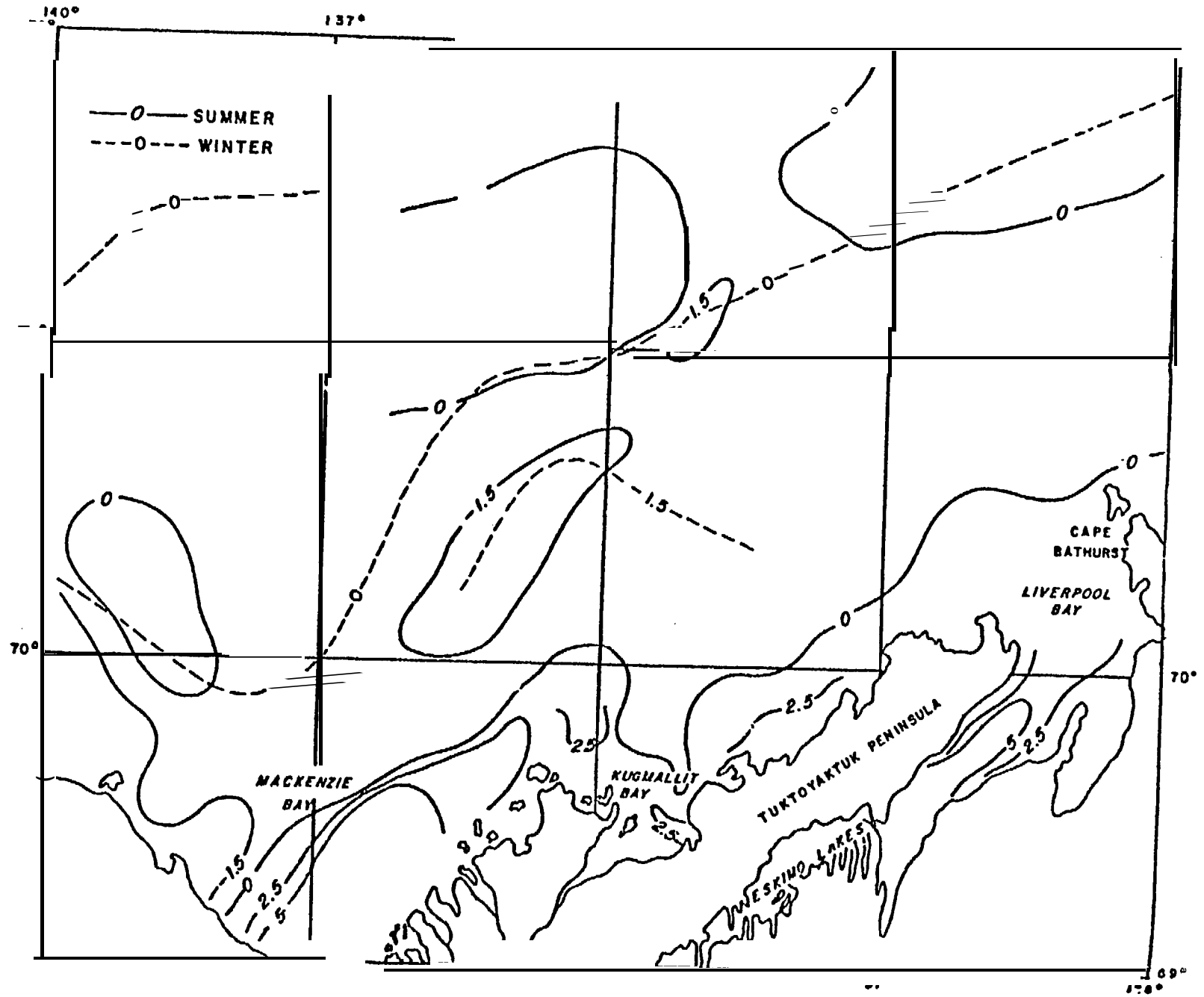


Figure 26.—Summer and winter bottom water temperature in the southern Chukchi Sea. After Hunter et al. (1976).

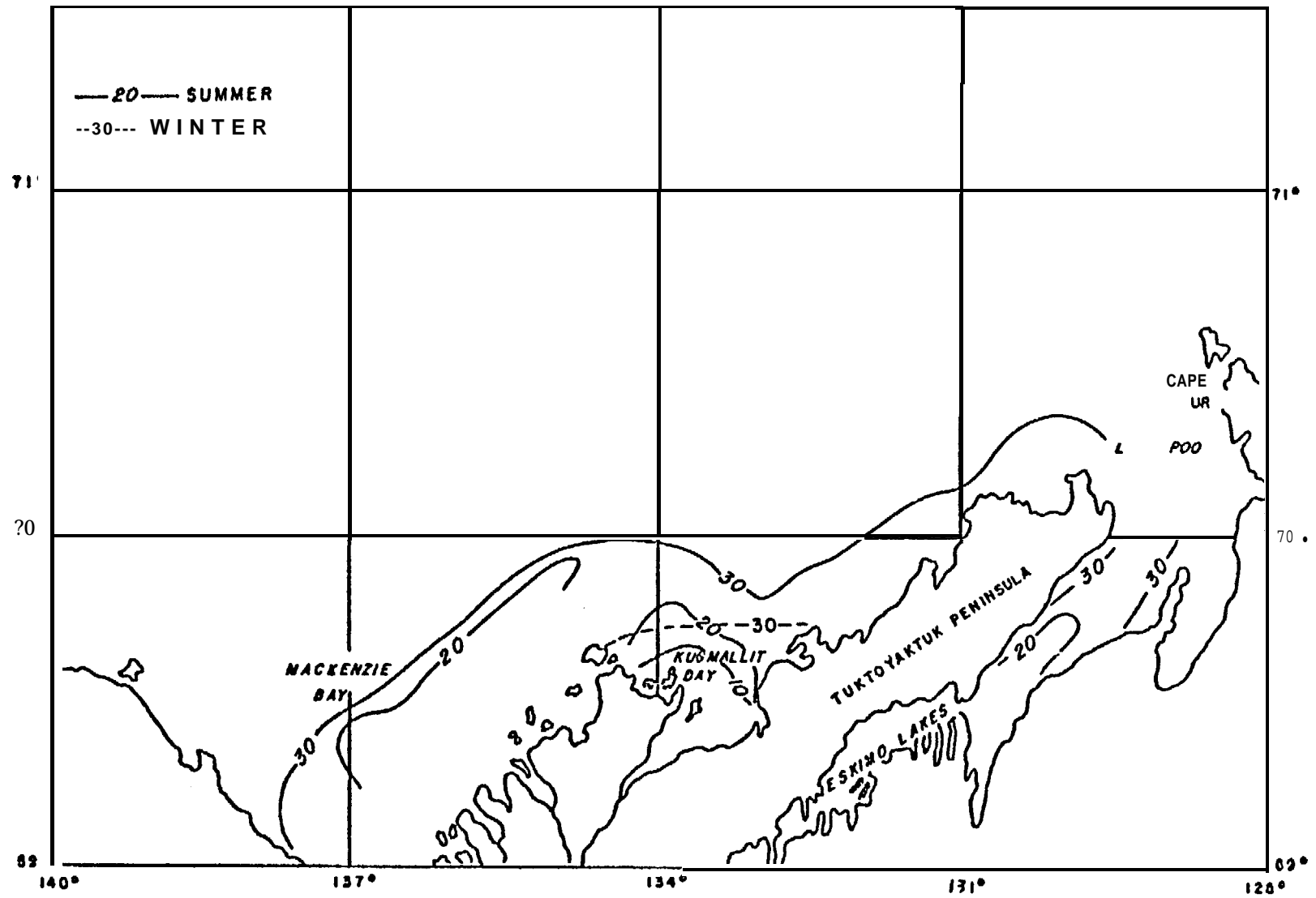


Figure 27.—Summer and winter bottom water salinities in the southern Beaufort Sea. After Hunter et al. (1976).

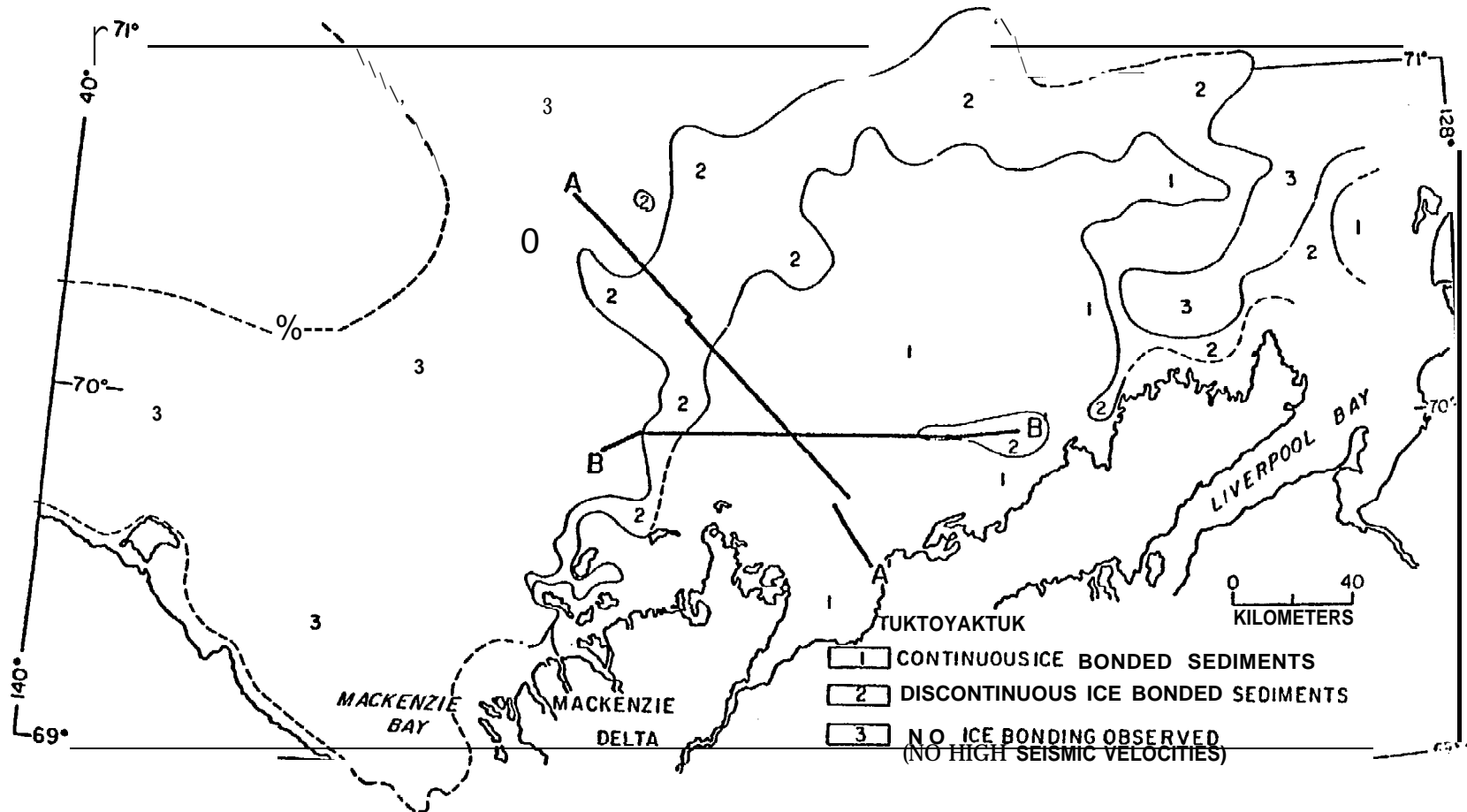


Figure 28.—An interpolation of the occurrence of subsea bottom ice-bonded permafrost. After Hunter et al. (1976).

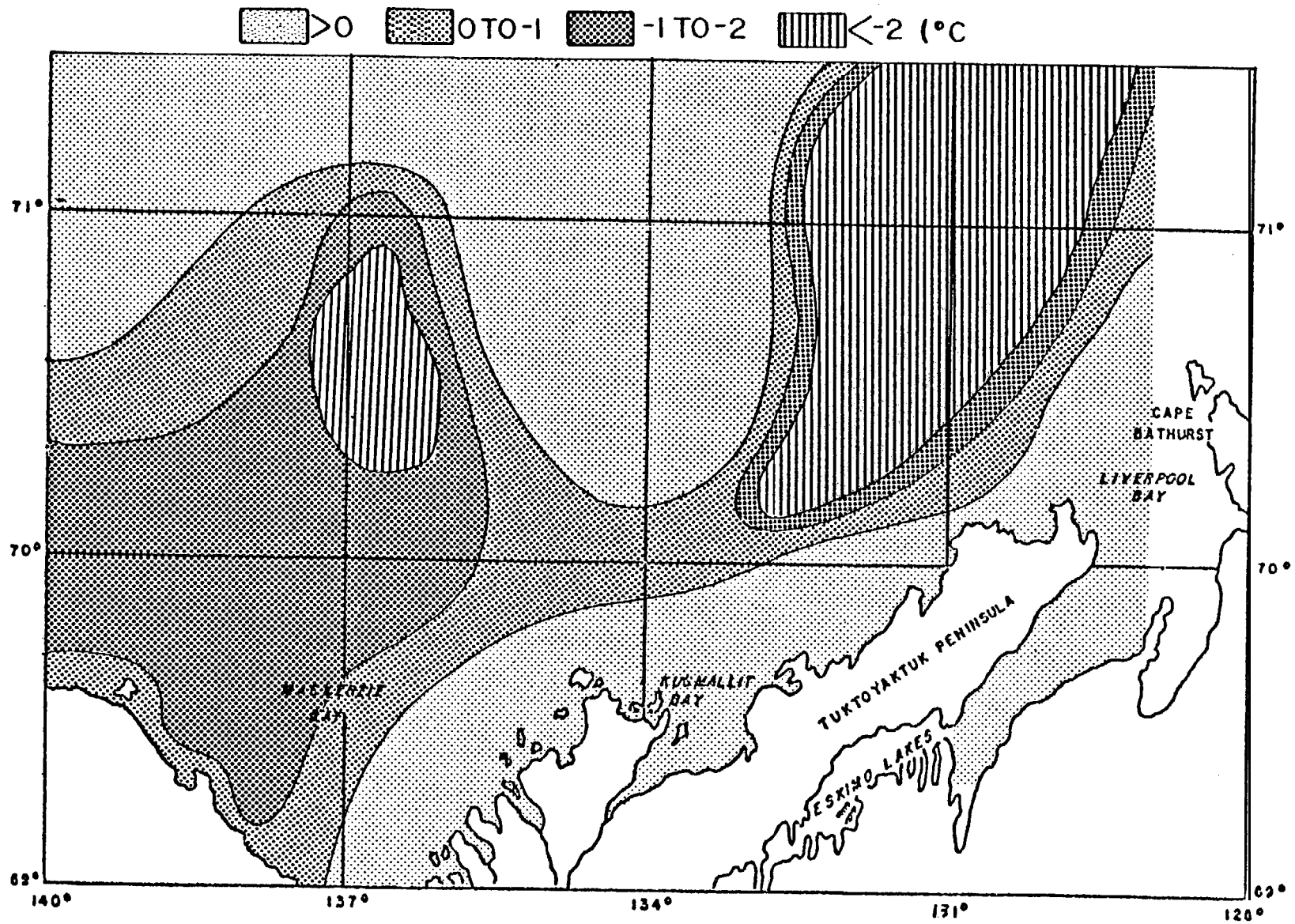


Figure 29.—Summer temperature of seawater at the maximal sampling depth in the southern Beaufort Sea.

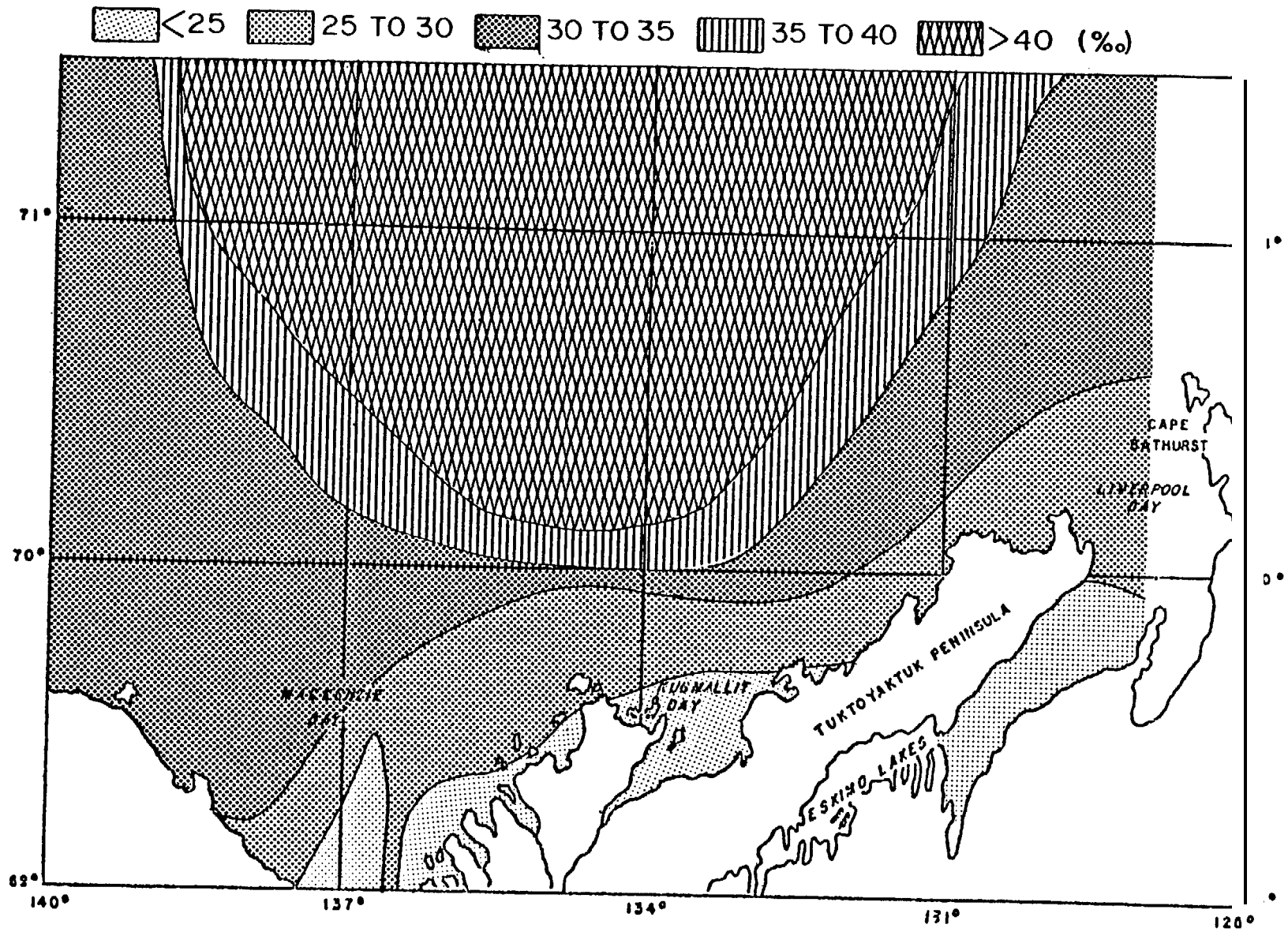


Figure 30.—Summer salinity of seawater at the maximal sampling depth in the southern Beaufort Sea.

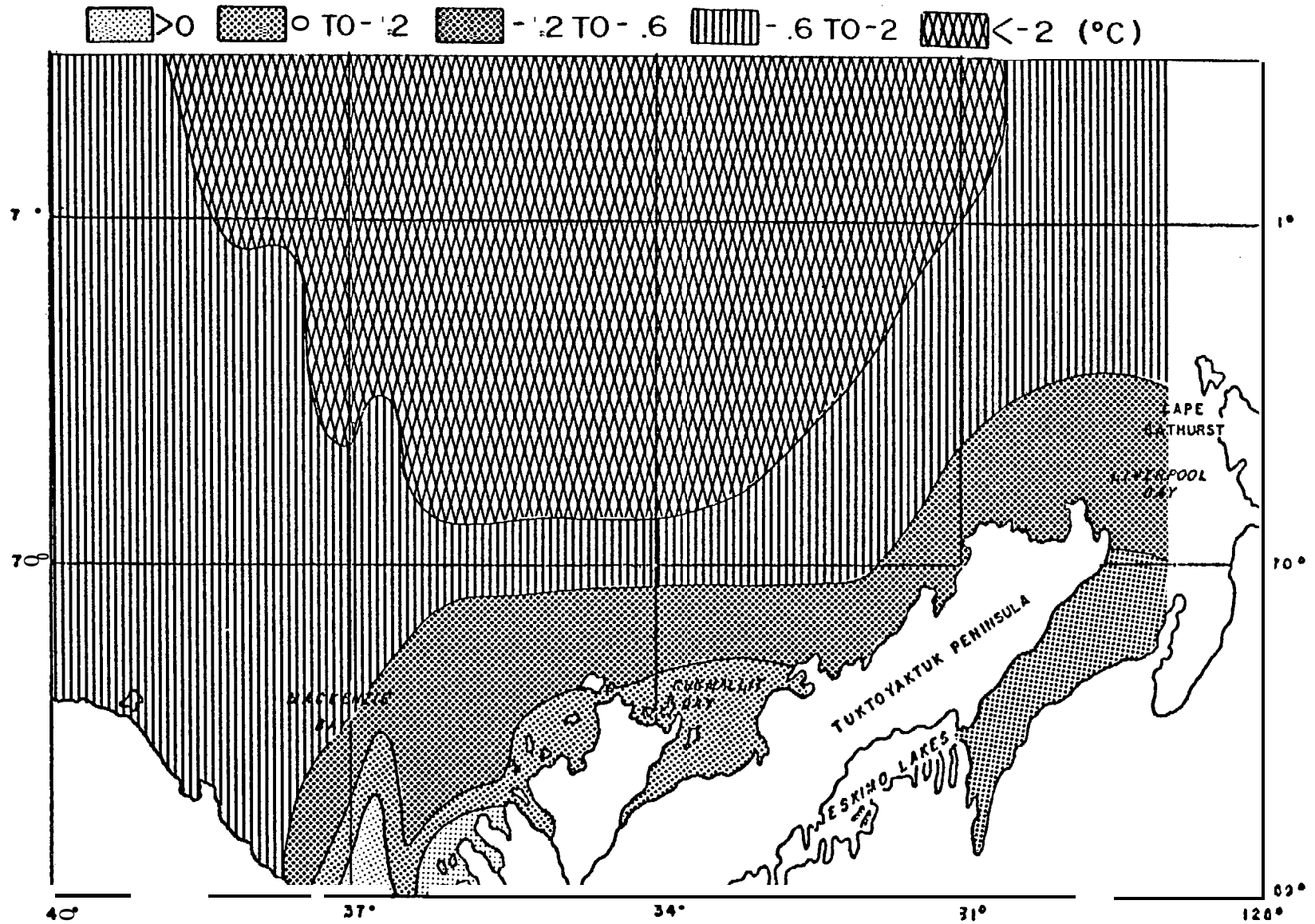


Figure 31.—Freezing temperatures of seawater according to summer salinity in the southern Beaufort Sea.

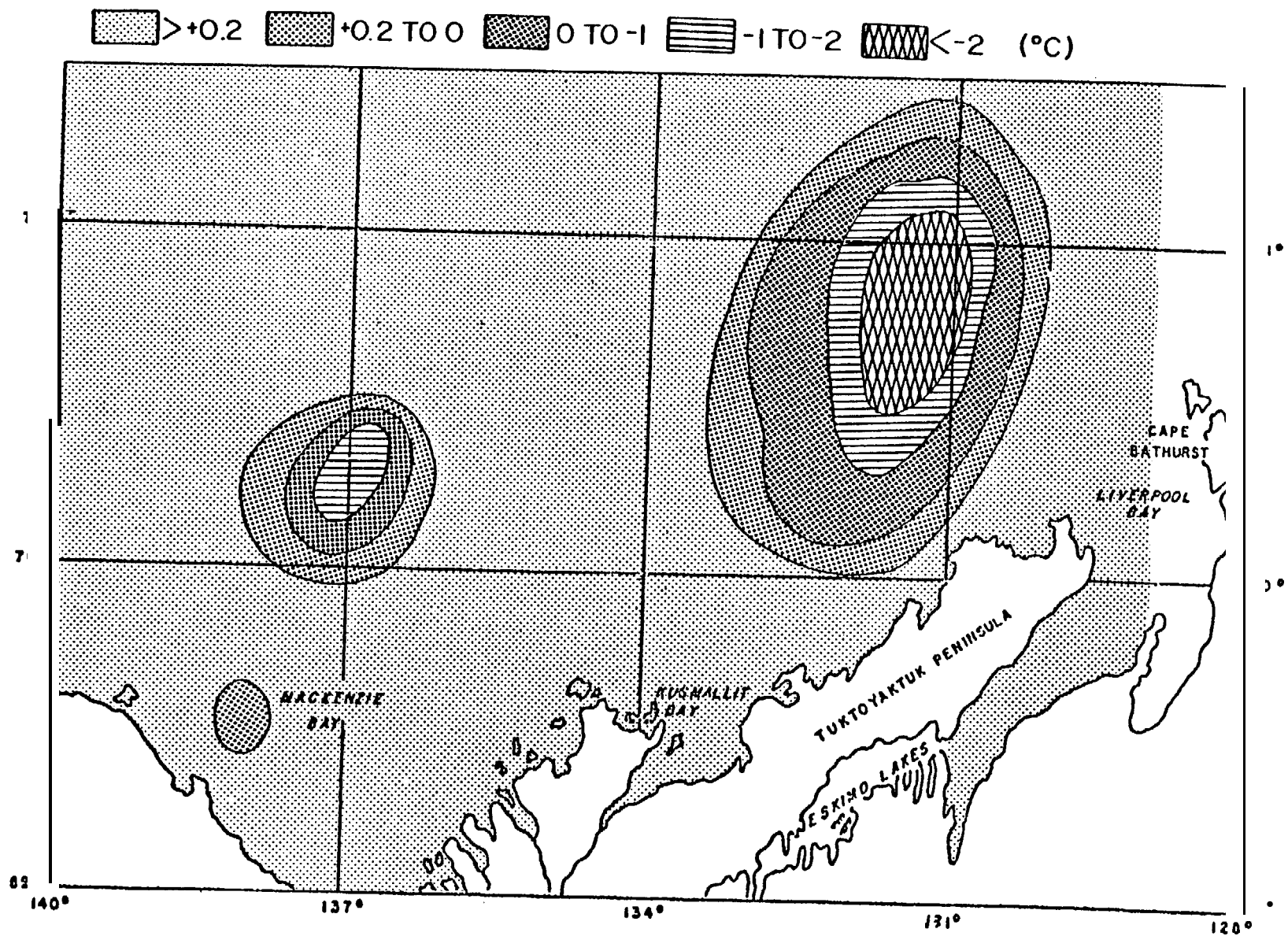


Figure 32.—Seawater supercooling during the summer at the maximal sampling depth in the southern Beaufort Sea.

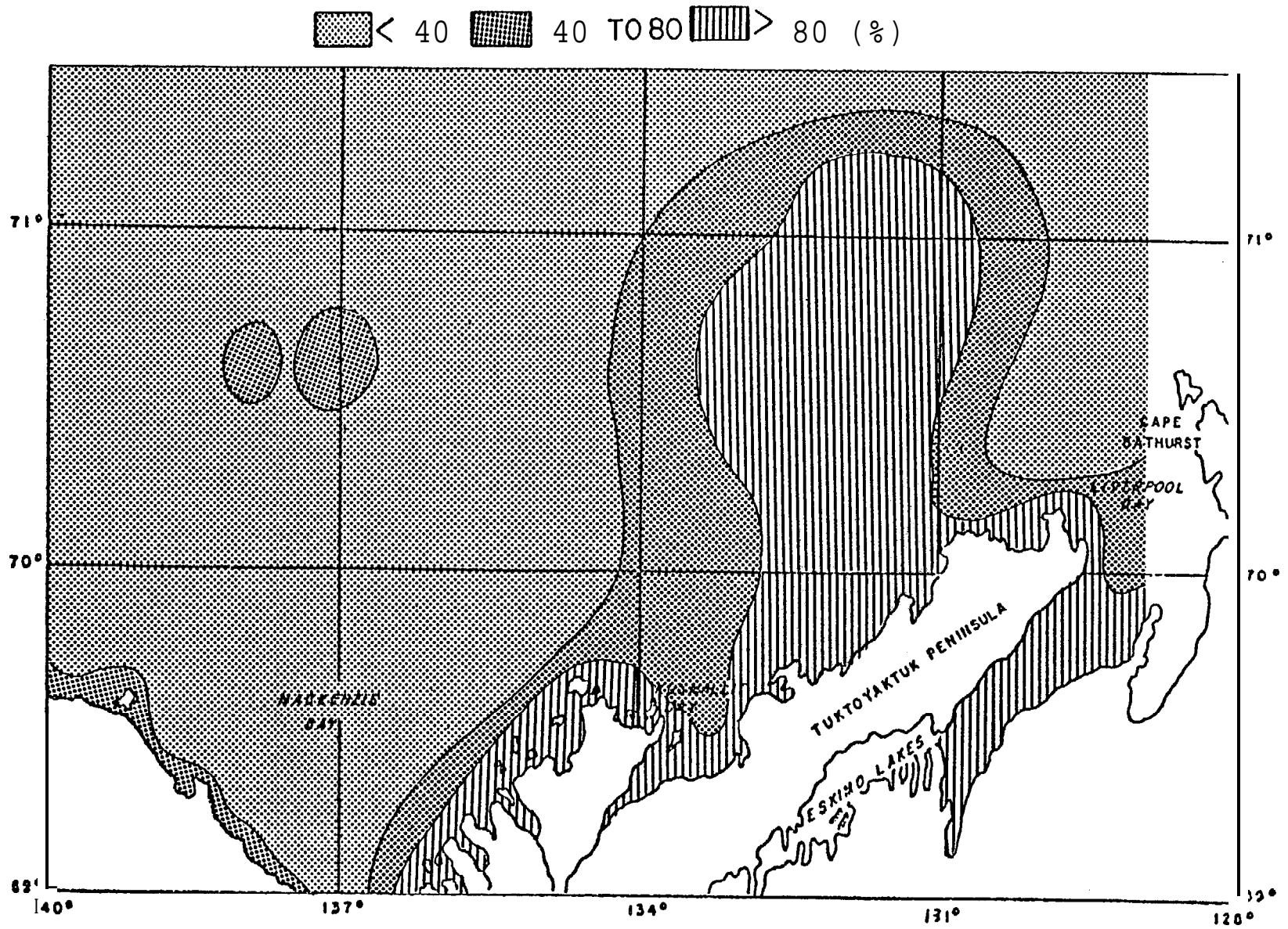


Figure 33.—Probability of seasonal supercooling at the maximal sampling depth in the southern Chukchi Sea.

supercooling during the summer look like three isolated spots on the computerized map. The biggest one is between 700-71015 'N and 130030 '-1330 W. A couple of other spots can be seen in the western part of the territory.

Because of the sparse data the seawater winter temperatures on the Canadian map are shown only by two contours following the general direction of the bathymetry contours.

Most interesting are the results of the comparison of the final map from the Canadian publication and the derived map produced by our system. Hunter et al. (1978) have compiled a map of the subsea bottom ice-bonded permafrost as an interpretation from industry seismic records. The Canadian geologists show continuous ice-bonded permafrost in the area that looks in a bathymetrical and geomorphological sense, like the submarine continuation of the Mackenzie Delta, between 69030'-71°20' N and 130-135° W. The area of continuous ice-bonded sediments is surrounded by a relatively narrow belt of discontinuous ice-bonded permafrost. The probability map for the seawater seasonally supercooling at the maximal sampling depth gives essentially the most probable areas (80-100%O) inside or very close to the zones of continuous ice-bonded sediments at the submarine part of the Mackenzie Delta and 40-80% probability in the limits of discontinuous zones of ice-bonded sediments there. The shape of the territory without ice-bonded permafrost also looks similar in both maps. A small part of the peripheral discontinuous submarine permafrost zone in the center of the territory is indented in an area of low probability y for seasonal supercooling (< 40%), but along the coast this probability is higher (40-80%).

Our impression is that according to the comparison the areas of seawater seasonally supercooling are good indicators of submarine permafrost, lying not only right under the sea bottom, but to a considerable depth below it and at the areas with bathymetry ranging from 7 to 100 m. The absence of ice-bonded permafrost below the sea bottom when it exists at greater depths could be explained by higher concentrations of salt in the pore water in the sediments forming the upper layers of the seabed.

We see that the results of the comparison are positive. This means that the use of the described system could help in tracing the areas with possible submarine permafrost extension. It is also important that the shelf areas with the seawater under summer and seasonal supercooling have an obvious correlation with the subsea permafrost. Perhaps these spots of supercooling water could be the result of cooling effects of the perennially frozen shelf deposits. In such a case, the spots themselves might be indicators of submarine permafrost.

CONCLUSION

The results of the work are summarized in Table 8, in which the division of the Beaufort Sea shelf, according to the specifics of the submarine permafrost's origin and distribution,

Table 8.—Division of the Beaufort Sea shelf according to specifics of submarine permafrost origin and distribution.

Area	Seawater Depth	Geological Structure	Geomorphological Structure	Extension of the Area Seaward
1	2	3	4	5
Western part of the shelf: Point Barrow-148°	0-60 ± 20 m	Colville Syncline	Continuation of the north-Alaskan flat plain. Probability of the “ancient valleys” development buried & half-buried & thermokarst polygonal-tetragonal forms in the different stages of thawing	70-80 km
Central part of the shelf: 148°-1420	0-200 m	Tectonically active transitional zone, possible boundary of Asian & American plates	Gentle plain on the complicated system of the submeridional, meridional, and latitudinal faults, blocks & dome structures	100 km
Eastern part of the shelf: 142° - Mackenzie River	0-200 m	Anticline	Relatively steep slope of the mountain range	85 km

Table 8.—Continued.

Average Rate of Coastal Retreat	Possible Rate of the Recent Vertical Movement	Possibility of Exposure during Last Glaciation and How Long	Time of Submergence
6	7	8	9
(W) 4.7 m/year	2.2 ± 2.0 nun/year	During last glaciation 25-10,000 years ago	10,000 to present
(C) 1.6 m/year	6.6 ± 2.5 mm/year	Low probability of exposure & only for small blocks at the boundary with the western part of the Beaufort shelf for a short time	>25,000 years
(E) 1 m/year	10.34 ± 3.7 mm/year	No possibility	>25,000 years

BIBLIOGRAPHY

- Aagaard, K. 1977, 1978. STD measurements in possible dispersal regions of the Beaufort Sea. Annual Reports, RŪ 151. OCSEAP, Arctic Project.
- Aagaard, K. and D. Haugen. 3.977. Current measurements in possible dispersal regions of the Beaufort Sea. Annual Report, RŪ 91. OCSEAP, Arctic Project.
- Anderson, D. M. 1966. Phase composition of frozen montmorillonite-water mixtures from heat capacity measurements. *Proc. Soil Science Society of America* 30(5): 670-675.
- Anderson, M. and A. R. Tice. 1971. Low temperature phases of interracial water in clay-water systems. *Proc. Soil Science Society of America* 35(1): 47.
- Anderson, D. M. et al. 1973. The unfrozen water and the apparent specific heat capacity of frozen soils. *Permafrost*, National Academy of Sciences, Washington, D.C.
- Barnes, P. W., and E. Reimnitz. 1974. Sedimentary processes on Arctic shelf off the northern coast of Alaska. *In* J. C. Reed and J. E. Sater, eds., *The Coast and Shelf of the Beaufort Sea*, Arctic Institute of North America, Arlington, Virginia, pp. 439-476.
- Barnes, P. W. 1974. Preliminary results of marine geologic studies off the coast of Alaska. U.S. Coast Guard, Oceanographic Report Series, pp. 373-464,
- Barnes, P. and E. Reimnitz. 1977. Marine environmental problems in the ice covered Beaufort Sea shelf and coastal regions. Annual Report, RŪ 205. OCSEAP, Arctic Project.
- Barnett, D. M. 1966. A reexamination and reinterpretation of tide gauge data for Churchill, Manitoba. *Canadian J. Earth Sci.* 3(1).
- Baskokov, G. and A. O. Shpaikher. 1970. Recent vertical movements of the Arctic seaboard. *Problems of Polar Geography*.
- Bird, B. 1954. Postglacial marine submergence in central Arctic Canada. *Bull. Geol. Soc. Am.* 65(5).
- Biswas, N. N., L. Gedney and P. Huang. 1977. Seismicity studies in northeast Alaska by a localized seismographic network. Univ. Alaska Geophysical Inst. Report, UAG R-241, 22 pp.
- Black, R. F. 1964. Gubic formation of Quaternary age in northern Alaska, U.S. Geol. Survey Prof. Paper 302-C, 91 pp.
- Budanov, V. I., A. S. Monin, P. A. Kaplan and V. S. Medvedev. 1960. Soveremennye vertikal'nye dvizheniya beregov morei Sovetskogo Soyuza (Recent Vertical Movements along USSR Sea Coasts). *Doklady sovetskikh geologov na XXI sessii Mezhdunarodnogo geologicheskogo kongressa, Moskva, Izd. AN SSR.*
- Chebanenko, I. N. 1957. Geotektonicheskoe znachenie vraschatel'nogo dvizheniya Zemli (Geotectonic Importance of the Rotational Movement of the Earth). *Doklady AN UkrSSR*, No. 5.
- Chebanenko, I. 1966. Osnovnye Zakonomernosti razlomnoi tektoniki zamonoi kory (Basic rules of fault-tectonics of the Earth's crust). *Trudy Instituta geologicheskikh nauk AN UkrSSR*, Kiev.

- Chikovskii, S. S. 1970. Studies on ice physics and ice engineering. *Arkticheskie i Antarkticheskie Instit.*, Trudy, Vol. 300, p. 132.
- Coachman, L. K. 1966. Production of supercooled water during sea ice formation. Contribution No. 383, Dep. Oceanography, Univ. Washington.
- Coachman, L. K. and K. Aagaard. 1974. Physical oceanography of arctic and subarctic seas. *In Marine Geology and Oceanography of the Arctic Seas*, Y. Herman, ed., Springer Verlag, New York, pp. 1-72.
- Creager, J. S. and D. A. McManus. 1967. Geology of the Bering and Chukchi seas. *American Studies in D. M. Hopkins, cd.*, The Bering Land Bridge, Stanford University Press, Stanford, pp. 7-31.
- Dillon, Howard B. and O. B. Andersland. 1966. Predicting unfrozen water contents in frozen soils. *Canadian Geotech. J.* 3(2): 53-60.
- Drake, D. E. 1976. Suspended sediment transport and mud deposition on continental shelves. *In D. J. Stanley and D. J. P. Swift, eds.*, Marine Sediment Transport and Environmental Management, John Wiley and Sons, Inc., New York, pp. 137-158.
- Eitrem and Grantz. 1977. Seismic and tectonic hazards in the Hope Basin and Beaufort Shelf. Report No. RN 432.
- Environmental Assessment of the Alaskan Shelf Interim Synthesis: Beaufort/Chukchi, August 1978. NOAA-BLM.
- Grantz, A., W. F. Hanna and S. D. Wolf. 1970. Chukchi Sea seismic reflection and magnetic profiles 1969, between northern Alaska and international date line: U.S. Geol. Survey Open-File Report 70-139, 1 sheet magnetic profiles, 25 sheets seismic profiles.
- Grantz, A., W. F. Hanna and S. L. Wallace. 1971. Chukchi Sea seismic reflection profiles and magnetic data, 1970, between northern Alaska and Herald Island: U.S. Geol. Survey Open-File Report 71-125, 32 sheets seismic profiles, 2 sheets magnetic data, 1 location map.
- Grantz, A., W. F. Hanna and S. L. Wallace. 1972a. Chukchi Sea seismic reflection and magnetic profiles, 1971, between northern Alaska and Herald Island. U.S. Geol. Survey Open-File Report 72-137, 38 sheets seismic profiles, 2 sheets magnetic profiles, 2 location maps, and index map, 1969-71.
- Grantz, A., M. L. Holmes, D. C. Riley and S. L. Wallace. 1972b. Seismic reflection profiles, Part I of Seismic, magnetic, and gravity profiles—Chukchi Sea and adjacent Arctic Ocean, 1972. U.S. Geol. Survey Open-File Report 72-138, 19 sheets seismic reflection profiles, 2 maps.
- Grantz, A., A. G. MacHendrie, T. H. Nilson and C. J. Yorath. 1974. Seismic reflection profiles 1973 on the continental shelf and slope between Bering Strait and Barrow, Alaska, and Mackenzie Bay, Canada. U.S. Geol. Survey Open-File Report '74-42, 49 sheets seismic reflection profiles, 2 index maps, scale 1:1,000,000.
- Grantz, A., M. L. Holmes and B. A. Kososki. 1975. Geologic framework of the Alaskan Continental Terrace in the Chukchi and Beaufort seas. *In C. J. Yorath, E. R. Parker and D. J. Glass, eds.*, Canada's Continental Margins and Offshore Petroleum Exploration. Canadian Soc. Petroleum Geologists Mere. 4, pp. 669-700.

- Gold, L. W., and A. H. Lachenbruch. 1973. Thermal conditions in permafrost—a view of North American literature. *In* Permafrost - North American Contributions, 2nd International Conf., Yakutsk, USSR, July 1973: Natl. Acad. Sci., Washington, D.C., pp. 3-25.
- Gutenberg, B. 1941.. Changes in Sea Level, Postglacial Uplift and Mobility of the Earth's Interior. *Bull. Geol. Soc. America*, Vol. 52(5).
- Hopkins, D. M. 1967. The Cenozoic history of Beringia: a synthesis. *In* D. M. Hopkins, cd., *The Bering Land Bridge*, Stanford University Press, pp. 451-484.
- Hopkins, D. M. 1973. Sea level history in Beringia during the past 250,000 years. *Quaternary Research*, 3: 520-540.
- Hopkins, D. M. et al. 1976. Offshore permafrost studies, Beaufort Sea, Research Unit 204, U.S. Geol. Survey Quarterly Report, July-September, 8 pp.
- Hopkins, D. M. 1977. Coastal processes and coastal erosional hazards to the Cape Krusenstern archaeological site. U.S. Geol. Survey Open-File Report 77-32, 15 pp.
- Hufford, G. L. 1973. Warm water advection in the southern Beaufort Sea, August-September, 1971. *J. Geophys. Res.* 78:2702-2707.
- Hufford, G. L. 1974. On apparent upwelling in the southern Beaufort Sea. *J. Geophys. Res.* 79: 1305-1306.
- Hufford, G. L., S. H. Fortier, D. E. Wolfe, J. G. Doster and D. L. Noble. Physical oceanography of the western Beaufort Sea. *In* Websec 71-72, An ecological survey in the Beaufort Sea, U.S. Coast Guard, Oceanographic Report No. 373-64.
- Hufford, G. L. and R. D. Bowman. 1974. Airborne temperature survey in Harrison Bay, Arctic 27: 69-70.
- Hunter, J. A. M., A. S. Judge, H. A. MacAuley, and others. 1976. Permafrost and frozen subseabottom materials in the southern Beaufort Sea. Canada Dep. Environ., Beaufort Sea Tech. Report No. 22, 174 pp.
- Jahns, H. O. et al. 1973. Permafrost protection for pipelines. Permafrost, National Academy of Sciences, Washington, D.C.
- Ives, J. D. and R. G. Barry, eds. 1974. *Arctic and Alpine Environments*, Methuen, London.
- Klyev, S. B. 1966. Proyavleniye termokarsta ka dne morya Laptevih (Thermokarst evidences at the Laptev Sea bottom) *In* "Problemy Arktiki i Antarktiki" (Problems of Arctic and Antarctic), Leningrad.
- Kovacs, A. 1976. Grounded ice in the fast ice zone along the Beaufort Sea coast of Alaska, USA. CRREL Report 76-32, 21 pp.
- Kudryavtsev, N. A. 1963. Glubinnye razlomy i neftnyanye mestorzhdeniya (Deep-seated Faults and Oil Deposits). *Trudy Vsesoyuznogo nauchno-issledovatel'skogo geologo-razvedochnogo instituta*, No. 215, Moskva.

- Lachenbruch, A. H. 1957. A probe for the measurement of thermal conductivity of frozen soils in place. *Trans. Am. Geophys. Union* 38: 691-697 and 730-732.
- Lachenbruch, A. H. 1957. Thermal effects of the ocean on permafrost. *Geol. Soc. Am. Bull.* 68: 1515-1529.
- Lachenbruch, A. H. and M. C. Brewer. 1959. Dissipation of the temperature effects of drilling a well in Arctic Alaska. *U.S. Geol. Survey Bull.* 1083-C: 73-109.
- Lachenbruch, A. H. 1968. Permafrost. *In Encyclopedia of Geomorphology*, R. W. Fairbridge, ed., 3: 833-839.
- Lewellen, R. I. 1970. Permafrost erosion along the Beaufort Sea coast: Pub. by the author, Denver, Colorado, 25 pp.
- Lewellen, R. I. 1973. The occurrence and characteristics of nearshore permafrost, northern Alaska. *In Permafrost-North American Contributions*, 2nd International Conf., Yakutsk, USSR, July 1973, *Natl. Acad. Sci., Washington, D. C.*, pp. 3-25.
- Markov, K. K. and I. A. Suetova. 1964. Evstatische kolebaniya urovnya okeana (Eustatic Fluctuations of Sea Level). *In Sbornik 'Sovremennye problemy geografii,' Moskva, 'Nauka.'*
- Metodicheskie ukazaniya Gosudarstvennogo okeanograficheskogo instituta (Methodic instructions from the State Oceanographic Institute), No. 18, 1960. *Compilations of the Catalogue of Level Observations on Seas washing the coasts of the USSR. Moskva, Gidrometeoizdat.*
- Meshcheryakov, Yu. A. 1964. Sovremennye tektonicheskie dvizheniya i zadachi ikh izucheniya v pribaltike (Recent tectonic movements and locations for their study in the Baltic region). *In Sbornik 'Sovremennye i noveishie dvizheniya samnoi kory v Pribaltike,' Vil'nyus, Izd. Litovskoi AN USSR.*
- Meyers, H. 1976. A historical summary of earthquake epicenters in and near Alaska, NOAA Technical Memorandum EDS NGSDC-1, p. 47,
- Miscellaneous Hydrologic and Geologic Observations on the Inner Beaufort Sea Shelf, Alaska. 1977. U.S. Geological Survey, Menlo Park.
- Mountain, D. G. 1974. Preliminary analysis of Beaufort Shelf circulation in summer. *In J. C. Reed and J. E. Sater, eds., The Coast and Shelf of the Beaufort Sea, Arctic Institute of North America, Arlington, Virginia, pp. 27-42.*
- Naidu, A. S. 1974. Sedimentation in the Beaufort Sea: A synthesis. *In Y. Herman, ed., Marine Geology and Oceanography of the Arctic Seas, Springer-Verlag, New York, pp. 173-190.*
- Naidu, A. S. and T. C. Mowatt. 1974. Clay mineralogy and geochemistry of continental shelf sediments of the Beaufort Sea. *In J. C. Reed and J. E. Sater, eds., The Coast and Shelf of the Beaufort Sea, Arctic Institute of North America, Arlington, Virginia, pp. 493-510.*
- Osterkamp, T. E. and W. Harrison. 1978. Subsea Permafrost. Annual Report, OCS.
- Osterkamp, T. E. and W. D. Harrison. 1976. Subsea Permafrost at Prudhoe Bay, Alaska, Drilling Report and Analysis. Univ. Alaska, Geophysical Inst., Rep. UAG-R-245.

- Pelletier, B. R. and J. M. Shearer. 1972. Sea bottom scouring in the Beaufort Sea of the Arctic Ocean, 24th International Geol. Cong., Montreal, Sec. 8: Marine Geol. and Geophys., pp. 251-261.
- Péwé, T. L. and P. V. Sellman. 1973. Geochemistry of permafrost and Quaternary stratigraphy. Permafrost, National Academy of Sciences, Washington, D.C.
- Péwé, T. 1976. Quaternary Geology of Alaska. U.S. Geol. Survey Prof. Paper 835,
- Pierce, C. 1960. Is sea level falling, or the land rising in S.E. Alaska? Surveying and Mapping 20(1).
- Reimnitz, E., P. Barnes, T. Forgatsch and C. Rodeick. 1972a. Influence of grounding ice on the Arctic shelf of Alaska. Marine Geology 13: 323-334.
- Reimnitz, E. and P. W. Barnes. 1974. Sea ice as a geologic agent on the Beaufort Sea shelf of Alaska. *In* J. Reed and J. Sater, eds., The Coast and Shelf of the Beaufort Sea, Arctic Institute of North America, Arlington, Va., pp. 301-351.
- Reimnitz, E. 1976. High resolution seismic profiles, Beaufort Sea. U.S. Geol. Survey Open-File Report 76-848.
- Rodeick, C. A. 1975. The origin, distribution, and depositional history of gravel deposits on the Beaufort Sea continental shelf, Alaska. San Jose State University, M.S. Thesis, 76 pp.
- Savel'ev, B. A. 1963. Stroenie, sostav i svoistva ledyanogo pokrova morshikh i presnykh vodoemov (The structure, composition, and properties of ice covers of marine and fresh water bodies). Moskva, Izadatel'stvo Mosk. Gos. Universiteta.
- Sellman, P. V., R. I. Lewellen, H. T. Ueda, E. Chamberlain and S. E. Blouin. 1976. Operational Report: 1976 USACRREL-USGS Subsea Permafrost Program, Beaufort Sea, Alaska, CRREL Special Report 76-12.
- Sellman, P. V., J. Brown, R. I. Lewellen, H. McKim and C. Merry. 1976. The classification and geomorphic implication of thaw lakes on the Arctic coastal plain, Alaska. CRREL Research Report No. 344.
- Shapiro, L. H., W. D. Harrison and H. R. Bates. 1977. Mechanics of origin of pressure ridges, shear ridges, and hummock fields in landfast ice. Annual Report, RU 250. OCSEAP. Arctic Project.
- Short, A. D., and L. D. Wright. 1974. Lineaments and coastal geomorphic patterns in the Alaskan Arctic. GSA Bull. 85:934-936.
- Short, A. D., J. M. Coleman and L. D. Wright. 1974. Beach dynamics and nearshore morphology of the Beaufort Sea coast, Alaska. *In* J. C. Reed and J. E. Sater, eds., The Coast and Shelf of the Beaufort Sea, Arctic Institute of North America, Arlington, Vs., pp. 477-488.
- Shpaikher, A. O. 1957. Novye dannye o vertikal'nom dvizhenii Fennoskandii (New data on the vertical movement of Fennoscandia). Irv. Vsesoyuznogo geograficheskogo obshchestva. Vol. 89, No. 8.
- Sisco, R. L. 1970. Geomorphology of Stobovoi Island in the Novosibirskie Islands. Problems of Polar Geography, Jerusalem.

- Sovremennye vertikal'nye dvizheniya zemnoi kory na territorii zapadnoi poloviny evropeiskoi chasti SSSR (po geodezicheskim, okeanograficheskim i geomorfologicheskim dannym) (Recent vertical movements of the Earth's crust in the western half of the European part of the USSR—Geodetic, Oceanographic, and Geomorphologic data). 1958. Trudy Tsentral'nogo nauchno-issledo-vatel'skogo instituta geodezii, aeros 'emki i kartografii, No. 123. Moskva. Geodezizdat.
- Stovas, M. V. 1959. Neravnomernost' vrashcheniya Zemli kak geotektonicheskii factor (Irregularities in the revolution of the Earth as a Geotectonic factor). Irv. Vsesoyuznogo geograficheskogo obshchestva No. 4.
- Stovas, M. V. 1962. O roli neravnomernosti vrashcheniya Zemli v obrazovanii planetarnykh gluminykh razlomov zemnoi kory (The role of the irregularity of the Earth's revolution in the formation of deep-seated planetary faults). Geograficheskii Sbornik No. 15, Astrogeologiya, Moskva-Leningrad, Izd. AN SSSR.
- Stovas, M. V. 1963. Nekotorye voprosy tektogeneza (Problems in tectogenesis) *In* Sbornik 'Problemy planitarnoi geologii' Moskva Gosgeoltekhizdat.
- Stovas, M. V. 1964. Sovremennoe tektonicheskoe podnyatie poberezh'ya Belogo i Barentseva morei (Recent tectonic uplift of the coasts of the White and Barents Seas). Informatsionnyi byulleten'. Materialy mezhdunarodnogo geofizicheskogo goda, No. 6, Kiev.
- Stovas, M. V. 1965. Molodoe tektonicheskoe podnyatie poberezh'ya morei Karskogo, Laptevykh, Bostochno-Sibirskogo (Young tectonic uplift of the coasts of the Kara, Laptev, East Siberian, and Chukchi seas). DAN SSSR, Vol. 161, No. 1.
- Stringer, W. 1977, 1978. Nearshore ice conditions by means of satellite aerial remote sensing. Annual Reports, RU 257. OCSEAP, Arctic Project.
- Vakar, V. A., P. S. Voronov and R. M. Demenitskaya. 1958. K voprosu o regional'nykh razlomakh severa Srednei Sibiri (The problem of regional faults in the northern part of central Siberia). Trudy Nauchno-issledovatel'skogo instituta geologii Arktiki, Vol. 64, No. 7, Leningrad.
- Volchanskaya, J. K. 1973. Skvoznaya zona Encoridg-Prudo-bay (Transitional active tectonic zone Anchorage-Prudhoe Bay as the boundary of the plates). *In* 'Metallogenics and New Global Tectonics;' Leningrad.
- Voronov, P. S. et al. 1970. Orientation and origin of lineaments. Problems of Polar Geography, Jerusalem.
- Walker, H. J. 1974. The Colville River and the Beaufort Sea: some interactions. *In* The Coast and Shelf of the Beaufort Sea, Arctic Institute of North America, pp. 513-540.
- Washburn, A. J. 1973. Periglacial Processes and Environments. New York.
- Weeks, W. F., and A. Kovacs. 1977. Dynamics of nearshore ice. Annual Report, Research Unit 88. OCSEAP, Arctic Project.
- Weeks, W. F., A. Kovacs, S. J. Mock, W. D. Hibler and A. J. Gow. 1977. Studies of the movement of coastal sea ice near Prudhoe Bay, Alaska. *J. Glaciology*, 19(81): 533-546.

- Weeks, W. F., W. B. Tucker, M. Frank and S. Fungcharoen. 1978. Characterization of the surface roughness and floe geometry of the sea ice over the continental shelves of the Beaufort and Chukchi seas. ICSI/AIDJEX Conf. on Sea Ice Processes and Models, Univ. Washington Press, Seattle, Washington.
- Wiseman, W. J., Jr., J. M. Coleman, A. Gregory, S. A. Hsu, A. D. Short, J. N. Suhayda, D. C. Walters, Jr., and L. D. Wright. 1973. Alaskan Arctic Coastal Processes and Morphology. Louisiana State University.
- Wiseman, W. J., Jr., J. N. Suhayda, S. A. Hsu and C. D. Walters, Jr. 1974. Characteristics of nearshore oceanographic environment of Arctic Alaska. *In* J. C. Reed and J. E. Sater, eds., *The Coast and Shelf of the Beaufort Sea*, Arctic Institute of North America, Arlington, Vs., pp. 49-64.
- Yeend, W. 1977. Surficial geology of the foothills and mountains of NPRA, Alaska. Circular 772-B.